NORTHWEST GEOLOGY

The Journal of The Tobacco Root Geological Society

Volume 39, August 2009

35th Annual Field Conference

The Anaconda Area, Montana

July 29—August 1, 2010

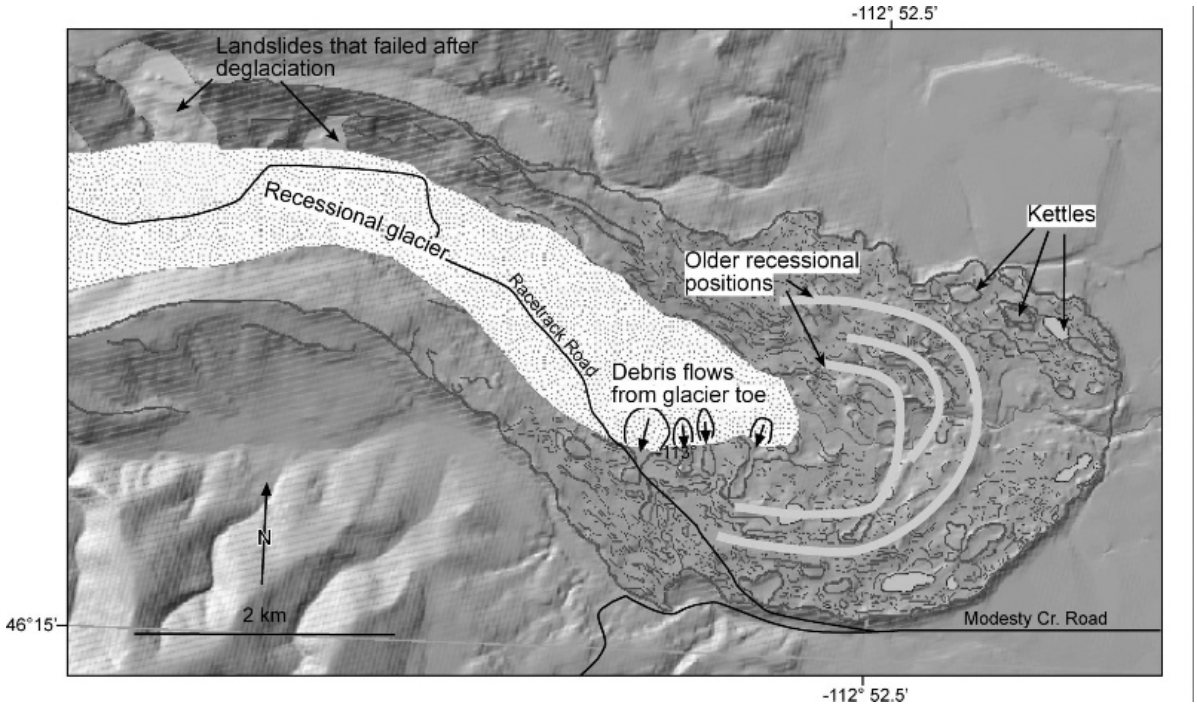

Published by The Tobacco Root Geological Society, Inc.
P.O. Box 2734
Missoula, Montana 59806
http://trgs.org

Edited by: Bruce E. Cox and Richard I. Gibson

Cover: Montana's state seal, in the Deer Lodge County Court House, Anaconda (photo by R. Gibson).
Above: Glacial geology of Racetrack Area (see Smith et al., this volume).

The Tobacco Root Geological Society, Inc.

P.O. Box 2734
Missoula, Montana 59806

Officers, 2010:

President: Mike Stickney, Montana Bureau of Mines and Geology, Butte
Vice-President: Robert C. Thomas, Dept. of Environmental Sciences, U. of Montana-Western, Dillon, MT
Treasurer: Ted Antonioli, Montana Mining Association
Secretary: Ann Marie Crites, Libby, MT
Webmaster: Dick Gibson, Consultant, Butte

Board of Directors, 2010:

Richard B. Berg, Montana Bureau of Mines and Geology, Butte, MT
Bruce E. Cox, Hecla Mining Co.
Marie Marshall Garsjo, Natural Resources Conservation Service, Ft. Worth, TX
Richard I. Gibson, Gibson Consulting, Butte, MT
Larry Johnson, Consultant, Missoula, MT
Larry Smith, Montana Bureau of Mines and Geology, Butte
Robert C. Thomas, Dept. of Environmental Sciences, U. of Montana-Western, Dillon, MT

Conference Organizers, Anaconda Field Conference:

Ted Antonioli, Montana Mining Association
Katie McDonald, Montana Bureau of Mines & Geology

ISSN: 0096-7769

http://trgs.org

NORTHWEST GEOLOGY

The Journal of The Tobacco Root Geological Society

Volume 39, August 2010

The Anaconda Area

and other papers

Table of Contents

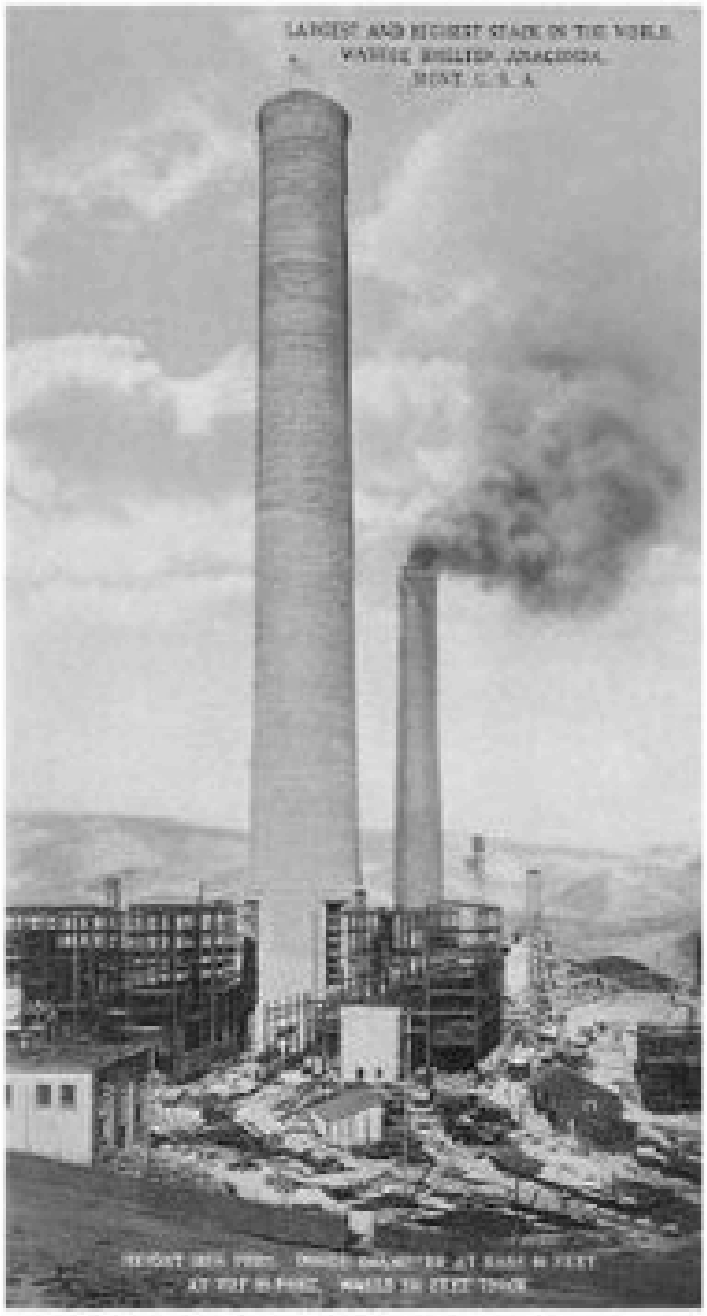

Anaconda Smelter Stack, Anaconda, Montana
—from an old post card

QUATERNARY MAPPING AND GLACIATION OF THE NORTHERN ANACONDA RANGE AND THE SOUTHERN FLINT CREEK RANGE, DEER LODGE, GRANITE, AND POWELL COUNTIES, MONTANA

Smith, L.N., Smith, M.G.A., Croft, T.O., Dutton, A.D., Sunwall, D.A., Gordon, L.M., Wright, J.R., and Dresser, H.W.*

Department of Geological Engineering, Montana Tech of the University of Montana
1300 W. Park St., Butte, MT 59701
*- retired

Introduction

The northern Rocky Mountains in western Montana experienced multiple glaciations over the course of the Pleistocene (2.6 – 0.12 Ma). However, the ages of glaciation are not well constrained in Montana (Locke and Smith, 2004). Most glacial advances have been ascribed either to the Pinedale or to the Bull Lake glaciations. During those periods, valley glaciers and local icecaps periodically dominated many of the mountain ranges in Montana. The Bull Lake glaciation occurred approximately 130 ka–300 ka (Fullerton et al., 2004). The Pinedale was the last of the major glaciations in the Rocky Mountains, occurring approximately 14 ka–40 ka (Fullerton et al., 2004). In most locations the Pinedale glaciers were apparently less extensive than those of the Bull Lake. Without reliable age control and only general mapping of glacial features in much of Montana, details of the history of glaciation are poorly understood outside the Yellowstone region (Pierce et al., 1976; Pierce, 1979, 2004)

The primary goal of this project was to improve the mapping of glacial and other Quaternary features in the Anaconda and Flint Creek ranges in southwestern Mon-

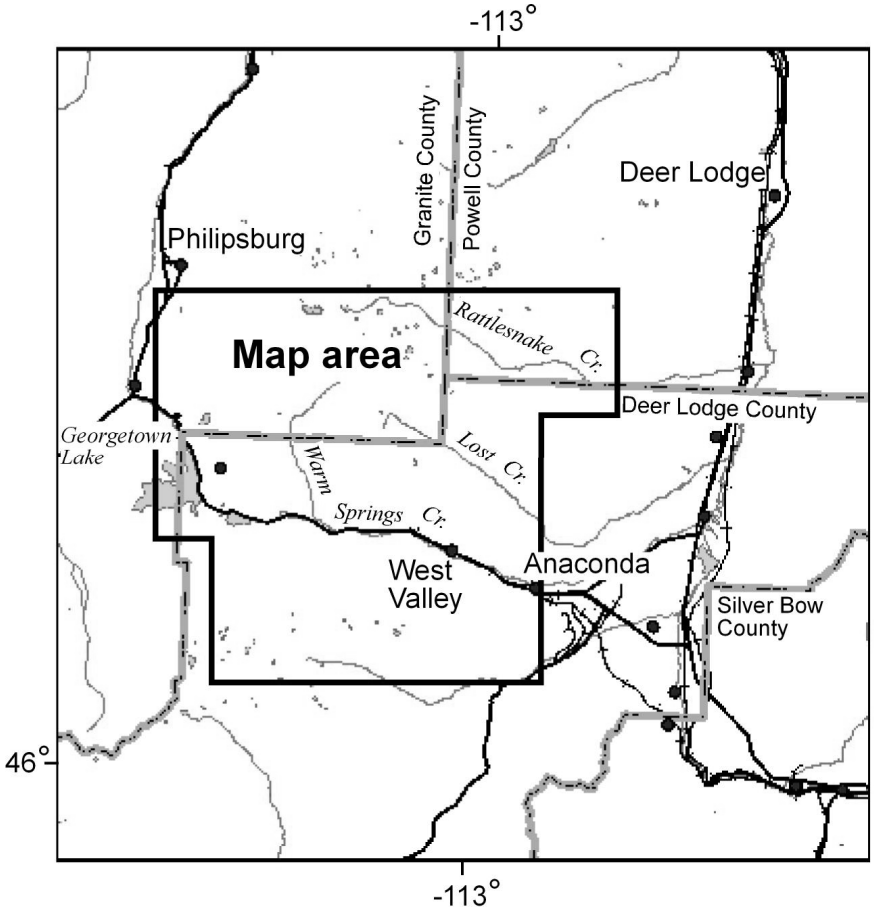

Figure 1. Location of the mapping area in the northern Anaconda and southern Flint Creek ranges.

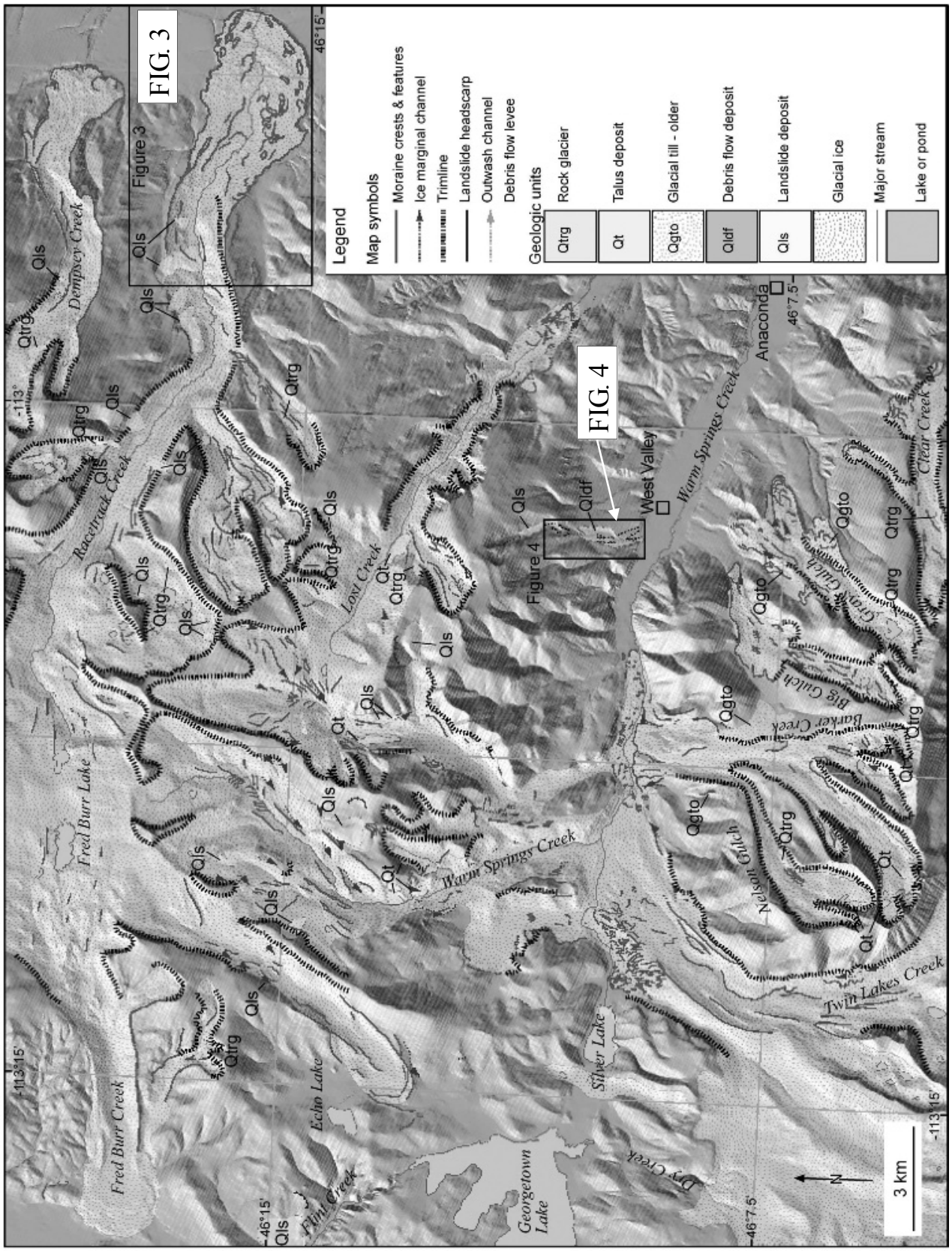

Figure 2. Simplified geomorphic and geologic map of Quaternary features, ice extent at the maximum recognized glaciation are shown. The boxes show the locations of Figures 3 and 4.

tana (Figures 1 and 2). The glacial features include moraines, till, outwash channels, trimlines, and ice-marginal channels. This is the first time that many of the area's glacial features have been mapped in detail. Observations on glacial features were made during early work in the area (Emmons and Calkins, 1913; Alden, 1953). Recent geologic mapping focused on bedrock units and were made mostly at the 1:100,000 and 1:250,000 scales (Lonn et al., 2003; Lewis, 1998; respectively). The general extent of ice in western Montana was shown by Locke and Smith (2004).

This report provides new information on landslides and the former extent of ice coverage in these mountain ranges. Some of the mapped moraines and till deposits show evidence for multiple glacial advances, while others help define the occurrence of the local icecaps in the Flint Creek Range and the probable creation of an ice-dammed lake, namely glacial Lake Georgetown, first proposed by Hugh Dresser (oral comm.).

The mapping of glacial features has been a useful technique for determining the extent and history of mountain glaciation. Another goal of this project was to determine the ancient equilibrium line elevations (ELAs) for area glaciers. Estimation of equilibrium line altitudes (ELAs) of ancient glaciers and comparison to glaciers found today allows for paleoclimate reconstruction. Studies of the decrease in ELA altitudes in western Montana showed average temperatures during the last glacial period (Pinedale) were about 10 °C lower than present (Locke, 1989; 1990). Others have used similar methods to reconstruct regional climate patterns for the northwestern United States (Meyer et al., 2004). ELAs for late Pleistocene alpine glaciers were estimated using our detailed photogeologic map, and were then compared to the results from previous studies.

Glacially related morphological features helped to unravel the geologic, climatic, and glacial history of the area. End moraines indicate the maximum extent of glaciers. Lateral moraines and ice marginal channels show maximum lateral extent of glaciers and a series of recessional moraines may contain significant information regarding the retreat history of a specific glacier. Crosscutting relationships between glacial landforms and till deposits indicate multiple stages in glacial history. Cross cutting relationships between glacial features, landslides, and rock glaciers help in the understanding of processes that occurred during deglaciation and post-glacial times.

Methods

The map of geologic features shown in Figure 2 was created by a group effort of mapping glacial features on stereoscopic aerial photos taken in August 1947 (DFH series including portions of lines 2, 3, 5, 6, 7, and 10). Because the Anaconda and Flint Creek ranges encompass a large aerial extent, participants were responsible for individual east-west flight lines to interpret and map using acetate plastic overlays. The features were mapped by hand, showing the location and extent of erosional and depositional landforms. Map units included: glacial features, landslide deposits and headscarps, alluvial deposits, rock glaciers, and extensive talus deposits. The main emphasis of mapping was to depict those features not shown, or mapped differently, on either Lewis (1998) or Lonn et al. (2003).

Individual features were mapped first in areas where they appeared on published maps and had distinctive forms, such as continuous moraine crests that correspond to clear glacial trimlines. Features were then traced into valley systems where exposures were less clear. Correlations between

mapped features were done based on similar photogeologic descriptions, and were ultimately made consistent throughout the map area. Old photos provided an interpretive advantage over modern aerial images because heavy logging in years prior to the 1940s removed much of the forest vegetation in the area. Many of the glacial features that were mapped in this study are now currently covered with plant growth and would never have been seen without these photos. No specific field checking of the mapping was done.

The maps created by hand were then digitized by each mapper using ArcMap™. Linear features were digitized as "arcs" and deposits were digitized as "polygons". The arcs and polygons were referenced to base layers available from the Natural Resource Information Service (NRIS), including orthophotographs made from 2009 color aerial photographs, hillshaded 10 m digital elevation models (DEMs), digital topographic base maps, and digital versions of published geologic maps from the Montana Bureau of Mines and Geology. The areas overlapped by multiple flight lines were evaluated and corrected for any discrepancies.

There are many different methods to approximate paleo-ELAs, including the elevation of cirque floors (CIR), the highest elevations of lateral moraines, and two different elevational and areal relationships of former glacier extents. These are based on either the terminus to headwall altitude ratio (THAR) or the area-altitude ratio (AAR) of the former glaciers (Richmond, 1965; Flint, 1971; Andrews, 1975; Meierding, 1982; Locke, 1990). The THAR method, an estimate of 40% of the vertical distance between the glacier toe and the top of the cirque headwall, was found to be the most useful for this study (see ELA estimates). The successes of the THAR or AAR methods depend on the ability to map the extent of Pleistocene glaciation, specifically the extent of isolated alpine glaciers. Methods for calculating ELAs cannot be easily applied to ice-sheet outlet glaciers or to multiple converging glaciers, both of which were observed in the study area.

Results - Description of Landforms

Moraines and Moraine Crests

Glacial moraines are one of the most common glacial features found in the mapped area. Moraines are depositional glacial landforms that were created by debris from an active glacier. There are several types of moraines found in a glaciated area, including lateral, medial, terminal, and recessional. However, the different types are not distinguished in Figures 2 and 3. Moraine crests include the raised portions of moraines, which appear as elevated, sometimes lumpy mounds, distinct from the relatively flat, smooth area around the moraine. Many moraines are also darker in color/reflectance compared to the surrounding area, making them easier to identify.

Lateral moraines are mostly sharp crested landforms that define the maximum height and extent of a glacier in a valley, or on the piedmont in the case of the outlet glacier along Racetrack Creek (Figure 3). Debris incorporated into the landforms likely fell onto the ice from the slopes of the glacial valley and was carried by the glacier or pushed up the side of the valley from the force of the ice during glacial movement. Landslide debris is commonly carried long distances from the origin on the surface of an active glacier. Debris that has been pushed up from the valley floor may have originally come from talus piles on the valley side, or even from the valley floor bedrock. These lateral moraines are always located on, or parallel to, the glacial valley walls and are locally continuous for more than 4 km along

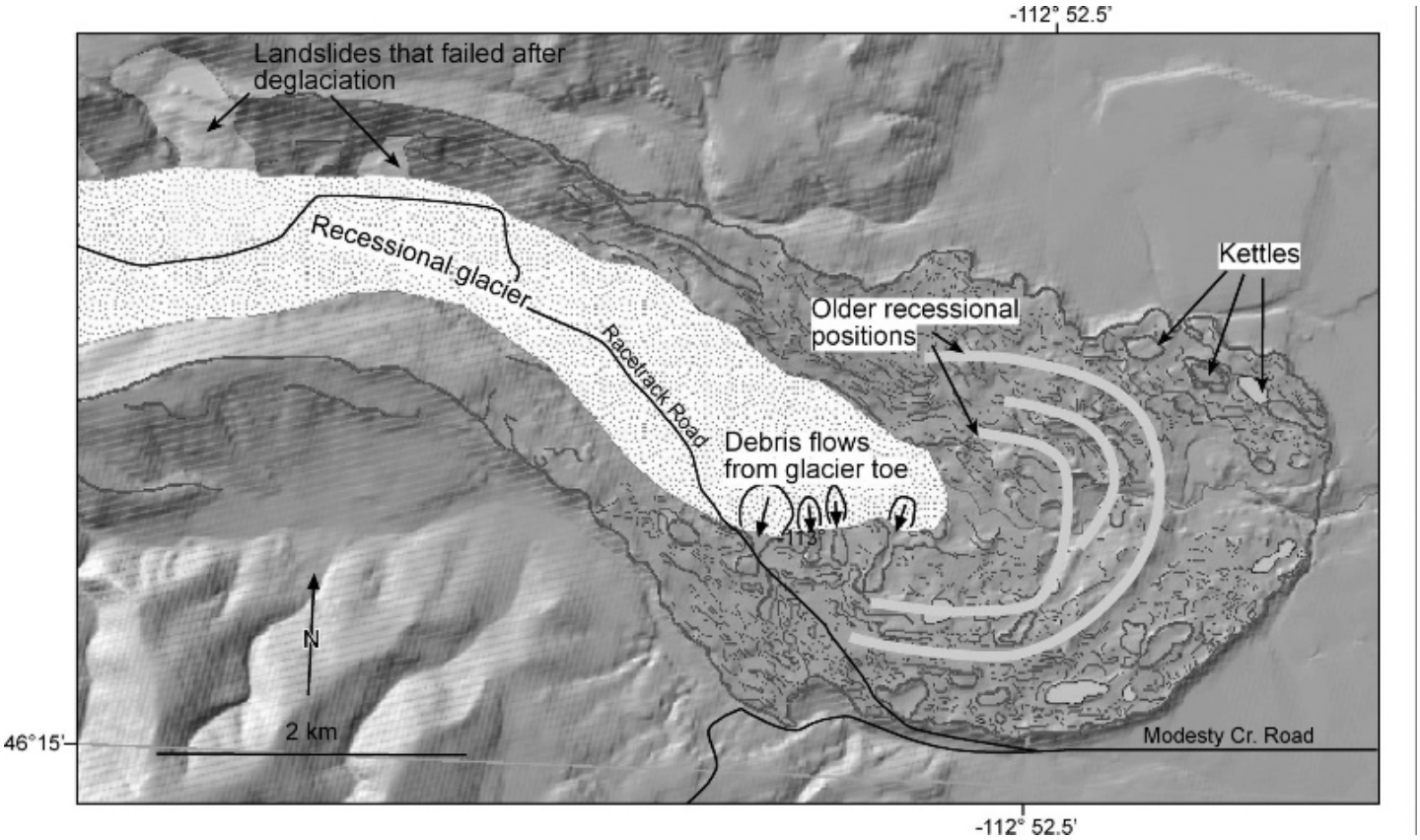

Figure 3. Large-scale map of the moraines left by a receding outlet glacier as it retreated up Racetrack Creek. Glacial retreat created two distinct features, kettles and debris-flow deposits. The kettles formed as large chunks of glacial ice were left behind, which then blocked sediment from being deposited there. These are now seen as bowl-shaped depressions in the moraine. The debris flow channels can be clearly seen on the south-facing side, where sediment-laden ice flowed off of the glacier creating a teardrop-shaped moraine. This process happened repeatedly, which piled these channels on top of each other, creating closely spaced parallel moraines. This glacial toe is characteristic of valley glaciers that exit the mountains onto piedmonts near the Anaconda and Flint Creek ranges. Symbology explained in Figure 2.

valleys. Lateral and recessional moraines near outlet-glacier termini include some landforms that suggest deposition by rock-falls or landslides from the glacier itself (Figure 3).

Terminal moraines have the same source and depositional process as lateral moraines, but the location of the moraine is different. Terminal moraines are typically arc-shaped at the mouth of a glacial valley and sometimes appear as large mounds or walls, where the glacier became inactive until it retreated/ melted. These landforms are very important for determining the glacial extent and possibly the ELA in an area.

Trimlines

Trimlines, which mark the highest extent of glaciations, were mapped to correspond with visible lines on the side of a valley. In a few areas, such as in the Lost Creek and Racetrack Creek valleys, trimlines can be traced directly into lateral moraines. The lines are visible due to either changes in color to the rock or to changes in vegetation on either side of the line. In some cases, the trimline is

indicated by an increase in the slope of the valley wall. Valleys may also show multiple trimlines where recent glacial events overprint older glacial surfaces. In the project area, some trimline segments have been obscured by post-glacial erosion and vegetative growth. In such cases, the trimlines were mapped based on the nearby, visible segments of un-eroded trimline.

Along the northern half of the Anaconda Range, the well-defined valleys have a southwest to northeast orientation and trimlines are continuous the along the steep valley walls . There are also a few examples of trimlines which extend beyond recently eroded valley boundaries (e.g. Grays Gulch and Big Gulch valleys) (Figure 2). These trimlines, and the associated glacial till (discussed later), indicate that there were larger, older glacial events once active through those valleys (possibly Bull Lake time). In a few locations (western Anaconda Range, Racetrack Creek, and Lost Creek valleys), most landslide headscarps are at or near the trimlines. This indicates that the change in slope at the trimline is an area of weakness and therefore, more prone to mass movements.

Some valleys in the Flint Creek Range, such as parts of the Warm Spring Creek valley, have less well-defined glacial morphologies; they are not everywhere U-shaped, but display local moraines. This made mapping difficult, because the trimlines are less apparent. However, trimlines such as those near Fred Burr Lake show that glacial icecaps can be locally continuous across multiple valleys. Multiple trimlines in the area of an icecap suggest that the ice may have been more extensive in an older glaciation and was thinner and less extensive in the most recent Pinedale glaciation. This observation agrees with earlier studies in the area, which suggests that multiple local icecaps existed in the highlands of southwestern Montana (Locke, 1990).

Ice-marginal channels

Ice-marginal channels are anomalously deep channels or discontinuous valleys located on the lateral margins of glaciers and are parallel or sub-parallel to the axis of the glacial valley. Many ice-marginal channels are dry and sit high above the floor of the glacial valleys, but some channels have been re-occupied by streams. Most observed ice-marginal channels are not continuous along the length of the valley, and only small portions of the channels have been preserved. The channels commonly have one bank defined by a lateral moraine. Many examples of ice-marginal channels are shown on Figure 2.

Headwall Scarps

Headwall scarps characterized by over-steepened vertical walls are typically found at the upper extent of glaciers.. These scarps usually give way down-slope to a shallow sloping bowl-shaped depression called a cirque. If no cirque is present, a U-shaped valley would extend down from the headwall scarp. Typical features of a headwall scarp, other than over-steepened walls, include a talus field and pre-existing topography. The talus field is usually near the base of the headwall slope, while the pre-existing topography is above the headwall. A distinct feature of headwall scarps is the abrupt change in ground slope from lower angle above and below the scarp to the very steep characteristic near-vertical walls. Headwall scarps are traceable into trimlines along some valleys.

Hanging Valleys

Hanging valleys commonly develop where two U-shaped glacial valleys come together. The characteristic feature associated with

hanging valleys is the abrupt ending of one valley that gives way to the side walls of another. If water is flowing along the upper valley, a waterfall will typically form at the intersection of the hanging valley and the lower valley. Angles near 90 degrees between the two valleys produce the most significant elevation changes, and as the angle decreases, the valleys tend to be closer to the same elevation. Hanging valleys are the product of one glacier being more erosive than the other and down-cutting farther into the bedrock. Some hanging valleys in the Flint Creek Range show development of a lateral moraine marginal to the larger valley, impounding sediment that was being carried down the smaller, hanging valley. This cross-cutting relationship suggests that the upper valley was deglaciated prior to the larger lower valley. Some examples are in Racetrack Creek and Lost Creek drainages.

Description of Map Units

Glacial Till

Glacial till is characterized by lumpy uneven ground. It can contain moraine crests and ice marginal channels, and can be located below a number of features including cirques and trimlines. Some of the till may be covered by outwash channels or eroded by drainage canals. In stereo-photos, the till appears grey to light grey in color and has a smooth to undulating surface texture; some boulders on the surface can be recognized. Till is extensive throughout the area covered by glacial ice but is not shown in Figure 2.

Older Glacial Till

Relatively older glacial till shown on Figure 2 is morphologically similar to the younger glacial till. Older glacial till is distinguished from newer glacial till by cross-cutting relationships. The older glacial till has been cut through by glacial valleys and is higher in elevation than the trim lines of those glacial valleys, but newer glacial till is lower in elevation than the observed trim lines. Like the younger glacial till, the older glacial till has a hummocky texture and is predominately characterized by a dense network of moraines. Trends in moraine orientations are observed within these older till deposits, but most moraines are randomly orientated. Good examples of older till are along Barker Creek, Big Gulch, and Grays Gulch (Figure 2).

Debris Flows

Different types of mass wasting may have caused debris flows in the Anaconda and Flint Creek Ranges. Debris flows have generally smooth interiors, are bounded by prominent levees, and locally show a braided pattern in distal channels. The levees look very similar to moraine crests, however, their relief is typically too low to host ice or there is little evidence of glacial action in the area. A few debris-flow features are indicated on Figure 2; most were too small to depict. Figure 4 shows a prominent debris flow deposit that emanated from an unnamed gulch between Geary and Priebe Gulches, north of West Valley. Priebe Gulch is defined by the westernmost levee of the flow. The deposit traveled downslope for at least a mile once leaving the constricted lower end of the canyon. Multiple debris flow levees can be traced near the canyon mouth, and up into the watershed, suggesting that older debris flows may have been much larger than the younger, mapped, deposit. The lower portion of the debris flow apparently bifurcated. The previous pathway defined by the levees has been truncated by downcutting of the unnamed gulch, suggesting a significant age of the mapped deposit (Holocene or late Pleistocene?). In general, the locations of debris flows can be good indicators of future hazards in the area. Mass wasting tends to reoccur in the same areas so, if past debris flows can be identified, future precautions can be made to avoid such hazards.

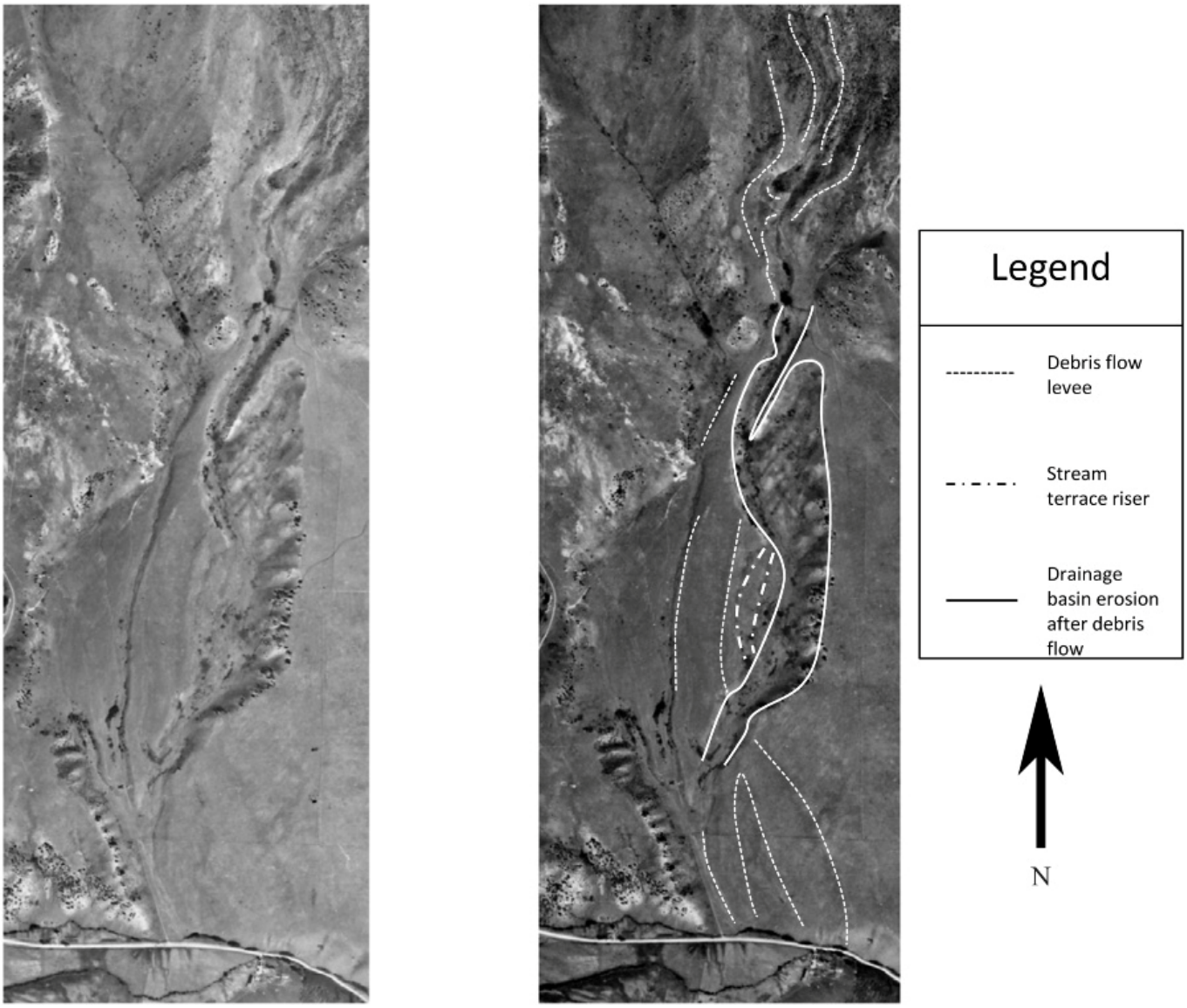

Figure 4. A stereoscopic photo pair of a debris flow deposit and the lower reaches of its source area near the West Valley area of Anaconda, Montana. Debris flow levees, terraces inset into the debris flow, and drainage channels are shown. Note the multiple paired levees near the canyon mouth that suggest multiple debris-flow events.

Landslides

Landslides in the Anaconda and Flint Creek Ranges include rotational debris slides, rock falls, and slab or deep-seated bedrock failures. Most observed landslides consist of a mass of colluvial debris with a definite headscarp of origin upgradient from a rotational failure and/or slump. These deposits typically consist of a hummocky texture surface apparently made up of colluvial or rock-fall material at the base of a slope. Most range in size up to about one square km. A sharp cliff-like arc-shaped headscarp can be seen upgradient from the slumped material. Large talus piles or rock falls were also mapped as separate units. These types of landslides often occur in areas where hard rock is present and weathering caused the rock material to weaken and fall. The headscarps for these types of landslides are typically very sharp and occur on a valley wall where the gradient of the wall is steep. These landslides are common in the river valleys and steep glacial valleys of the Anaconda Range. A few older landslides, which did not occur in very steep gradient areas, were identified based on an arc-shaped headscarp. The landslides were identified by their hummocky nature, and elevated shape upon a relatively even gradient area. There were several landslides identified based on the characteristics of high and low gradient slopes in the Anaconda Range.

Some noteworthy landslides have their headscarps near moraine crests in the lower Racetrack Creek valley (Figures 2 and 3). One instance of apparently open arcuate cracks in bedrock high above the valley bottom was mapped in a southern tributary to Lost Creek, directly north of West Valley (Figure 2). In this case, the headscarps are again at about the same altitude as the local trimline.

Outwash

Outwash is recognized as sediment, which was deposited downslope from the terminal moraine of a glacier. Meltwater transported poorly sorted sediments beyond the toe of the glacier. Outwash channels can be recognized as numerous, parallel, braided streams downslope from the glacier creating a "braided sandur surface."

Rock Glaciers

Rock glaciers were recognized as steep-sided, rocky, depositional features along valley margins. Some of these undulating landforms occur at the bottom of steep valley slopes, while others may extend farther into the valley floor ("protalus lobe" and "valley floor rock glacier," respectively; after Humlum, 1982). From aerial photographs, these features appear lobate, with banded areas of light and dark pressure ridges. There is uneven reflection on the landform, creating shadows among the dips and mounds.

Rock glaciers are common among valleys in the northern Anaconda Range, especially on north and east-facing, protalus slopes. Determination of rock-glacier activity is difficult using only the aerial photographs. Some rock glaciers have vegetation growing on them, while still showing distinct flow-like features. Rock Glaciers in the lower Flint Creek Range are smaller, less common and appear more deflated and vegetated.

ELA Estimates

Equilibrium line altitudes (ELAs) of alpine glaciers are a function of a suite of local and regional climatic and topographic factors that affect ice mass balance. These factors include air temperature, precipitation, patterns of wind erosion, deposition of snow, and insolation (Bradley, 1985). However, in continental

interiors, glacial mass balances are most strongly controlled by summer temperatures (Locke, 1990). Previous work has defined how present-day mountain glaciers of western Montana are related to the regional climate, and how an empirical relationship (between winter precipitation, mean summer temperature, and continentality) provides the mechanism to estimate former glacier ELAs (Meierding, 1982; Locke, 1989, 1990; Meyer et al., 2004). Locke (1990) concluded that Pleistocene continentality is the same as the present and that mean summer temperatures were ~10°C lower than the present. The proxy data which Locke (1990) used to interpret Pleistocene paleoclimates of the region are the ELAs of the glaciers which formerly occupied western and central Montana.

Multiple methods may be used to estimate paleo-ELAs. Due to poorly formed cirques, the CIR method was not employed in this area. In addition, due to the limited information available and the mapping techniques used in this project, it was not possible to accurately estimate the total ice-affected area for valleys, to be used in the AAR calculation. ELAs were estimated using the THAR method. It is important to remember that THAR (and AAR) calculations require the identification of maximum ice extent based on topographic features, which are only prominent from the last-glacial maximum, Pinedale glaciation. Therefore, the interpretation presented here represents the extent of ice at the peak of the last glaciation.

These calculations are also dependent on the elevations determined for ice-extent boundaries, as mapped from the photos. In some cases, it was difficult to correctly locate and determine the elevation of glacier toes, thus affecting these calculations. Due to valley shapes, the lack of simple cirque glaciers, and the icecap in the Flint Creek Range, only north-facing valleys from the Anaconda Range were used to estimate ELAs. The results are found in the Table 1.

It is clear that there is variability between ELAs in different valleys. However, the range of estimated ELAs is consistent with previous work performed in western Montana. In particular, Locke (1990) reports that a major trough in ELAs (generally below 2100 m) extended across the western part of Montana, south of the Northern Rocky Mountains. However, in the highlands of southwestern Montana (our area), the ELAs were higher (> 2100 m) and in some cases, local icecaps existed. The estimates from our study agree well with Locke's estimates. However, our estimates could be further refined by using the other methods, if better cirque data and glacial toe locations were available.

Discussion

Evidence for Multiple Glaciations

Throughout the map area, there are crosscutting relations and features that can best be explained by multiple periods of glaciations. Areas of older glacial till cut by younger till clearly show that periods of glacial advance, retreat, and re-advance took place. The freshness of landforms on the older till suggests that most, or all, of these deposits are Pinedale in age.

To the west in the Racetrack Creek drainage, there is a large area where the surface has been eroded down to hummocky bedrock by the icecap that covered this area and fed the glaciers to both the west and east. Below this surface are some typical U-shaped valleys with trimlines below the eroded surface. This relationship suggests the most recent glaciation did not completely occupy the icecap area.

Multiple hypotheses could explain these features. One is that a glacial re-advance occurred during the end of a single glacial period. After the icecap reached its maximum extent, it retreated, and then reestablished and re-advanced to a lesser extent. Inset trimlines and moraines were then produced at lower elevations. The substantial recessional moraines along Racetrack Creek (Figure 3) and elsewhere could be evidence for these smaller glaciers.

A second hypothesis is that the some of the erosional features in the icecap area were formed during a much older period of glaciation. While many of the features appear to be similar in age, based on slope and degree of weathering, it is impossible to conclude one or the other without further research. Collection of field data on glacier-flow directions and application of relative or numerical dating techniques on deposits and landforms may provide the data necessary to test the different hypotheses.

Landslides

Mapping of the Anaconda and Flint Creek Ranges resulted in recognition of many landslides not shown on previous geologic maps. The age of these landslides is not known; however, crosscutting relationships suggest many are related to glacial retreat.

Rotational landslides were on the insides of the lateral moraines, near the terminus of the glaciers. Apparently, as glaciers retreated up their valleys, ice could no longer buttress the down-slope edges of these moraines. The melting glacier likely saturated the already over-steepened moraine and caused a failure. The plane of failure is most likely right along the base of the moraine and the underlying sediment or bedrock.

Farther up the valleys large rotational landslides can be found. The glacier acted as the toe for many of these areas and plucked the sides of the valleys into steep cliffs. Once the glacier retreated these areas were free to fail along natural planes of weakness.

A few landslides mapped in bedrock units in the upper reaches of the valleys have headscarps near glacial trimlines. This relationship suggests partial bedrock failure during lateral unloading during deglaciation.

Glaciation and Drainage History

Glaciation in the Anaconda and Flint Creek Ranges had a profound effect on the distribution of surficial materials and the landscape. Erosion of the high-mountain areas exposed large areas of granite that produced thin soils and sparse vegetation. Deposition of till and construction of moraines along and across valleys rearranged the drainages.

A spectacular example of drainage rearrangement is evident in the Silver Lake, Georgetown Lake, and Flint Creek drainage area. The topography of the Georgetown Lake area strongly suggests that the basin, now dammed at the headwaters of Flint Creek (Figures 1 and 2) initially flowed through the Silver Lake area and down what is now known as Warm Springs Creek. Evidence for this is the shape of the headwaters now drowned by Georgetown Lake. Additionally, the outlet to the lake is in a narrow gorge located on a low saddle at the northern end of the lake. Mapping shows that the stream valley from Georgetown Lake to north of Barker Creek was blocked by ice. Apparently, the glacier near Dry Creek and the glacier from the Twin Lakes basin advanced north from the Anaconda Range and flowed across the area on both sides of Silver Lake. The Twin Lakes glacier connected with south-flowing ice from the Flint Creek Range at the upper ex-

tent of Warm Springs Creek (Figure 2). This ice, and associated moraines, effectively blocked the east-flowing drainage.

This blockage would have formed an ice-dammed lake, named glacial Lake Georgetown. The lake is inferred to have overflowed at the lowest point in the upper basin, at the present site of the Flint Creek Dam. Low forested slopes, incised by the canyon, suggest an altitude of about 1950-1980 m for the pre-existing saddle. Overtopping of this divide by lake waters would have led to increased flows and sedimentation down the Pleistocene Flint Creek, which may be recognizable in outwash deposits. These ideas should be tested by looking for field evidence in the Georgetown Lake and Flint Creek valley areas.

Conclusions

1) Cross-cutting relationships between glacial deposits suggest multiple glaciations or multiple advances of a single glaciation. Additional work on dating the deposits and landforms is needed to better understand the glacial history.

2) Numerous landslides have occurred in glacial deposits, and a few as bedrock failures. Most of the recognizable headscarps on the failures developed near trimlines or near the crests of lateral moraines. The subdued appearance of debris slides and slumps and their association with glacial features suggest that most moved during, or shortly after deglaciation due to failure of oversteepened slopes or the reduction of lateral support provided by valley glaciers.

3) One or more large debris flows in the West Valley area of Anaconda were produced from a moderately large drainage basin, possibly during the Pleistocene or early Holocene(?). Debris flow levees near the canyon mouth look superficially like lateral moraines, but mapping clearly shows debris flow morphology. These ancient flows suggest the side valleys in the area could produce devastating events, given the right climatic conditions.

4) Drainage basin morphology and glacial deposits in the area suggest drainage rearrangement in the Georgetown Lake area during the last glaciation. The Georgetown drainage previously flowed east. Glaciers from the Anaconda Range dammed the drainage, forming glacial Lake Georgetown. The lake eventually spilled to the north across a low saddle forming the canyon along the upper reach of Flint Creek.

Acknowledgements

This report is the result of the Spring 2010 Geomorphology and Photogeology class at the Department of Geological Engineering at Montana Tech. Funding that was provided to many of the students by various scholarship funds and donors is graciously acknowledged.

References

Alden, W.C., 1953, Physiography and glacial geology of western Montana and adjacent areas: U.S. Geological Survey Professional Paper 231, 200 p.

Andrews, J.T., 1975, Glacial Systems: Duxbury Press, North Scituate, Mass., 191 p.

Bradley, R.S., 1985, Quaternary Paleoclimatology: Methods of Paleoclimatic Reconstruction: Allen and Unwin, Inc., Boston, 472 p.

Emmons, F.C., and Calkins, W.H., 1913, Geology and ore deposits of the Philipsburg quadrangle, Montana: U.S. Geological Survey Professional Paper 78, 271 p.

Flint, R.F., 1971, Glacial and Quaternary Geology: Wiley, New York, 892 p.

Fullerton, D.S., Colton, R.B., and Bush, C.B., 2004, Limits of mountain and continental glaciations east of the Continental Divide in northern Montana and north-western North Dakota, U.S.A.: *in* Ehlers, J., and Gibbard, P.L., eds., Quaternary Glaciations – Extent and Chronology, Part II: Elsevier, Amsterdam, p. 131-150.

Humlum, O., 1982, Rock glacier types on Disko, central West Greenland: Geografisk Tidsskrift 82, p. 59-66.

Lewis, R.S., 1998, Geologic map of the Butte 1ºx2º quadrangle: Montana Bureau of Mines and Geology Open File Report MBMG 363, scale 1:250,000.

Locke, W.W., 1989, Present climate and glaciation of western Montana, U.S.A.: Arctic and Alpine Research 21, p. 234-244.

Locke, W.W., 1990, Late Pleistocene glaciers and the climate of western Montana, U.S.A.: Arctic and Alpine Research 22, p. 1-13.

Locke, W.W., and Smith, L.N., 2004, Pleistocene mountain glaciation in Montana, USA: *in* Ehlers, J., and Gibbard, P.L. eds., Quaternary Glaciations – Extent and Chronology, Part II: Elsevier, Amsterdam, p. 117-121.

Lonn, J.D., McDonald, C.M., Lewis, R.S., Kalakay, T.J., O'Neill, J.M., Berg, R.B., and Hargrave, P., 2003, Preliminary geologic map of the Philipsburg 30' x 60' quadrangle, western Montana: Montana Bureau of Mines and Geology Open File Report 483, 29 p.

Meierding, T. C., 1982, Late Pleistocene glacial equilibrium-line altitudes in the Colorado Front Range: A comparison of methods: Quaternary Research 18, p. 289-310.

Meyer, G.A., Fawcett, P.J., and Locke, W.W., 2004, Late-Pleistocene equilibrium-line altitudes, atmospheric circulation, and timing of mountain glacier advances in the interior northwestern United States: *in* Haller, K.M., and Wood, S.H., eds., Geological field trips in southern Idaho, eastern Oregon, and northern Nevada: U.S. Geological Survey Open-File Report 2004-1222, p. 63-68.

Pierce, K.L., Obradovich, J.D., and Friedman, I., 1976, Obsidian hydration dating and correlation of Bull Lake and Pinedale glaciations near West Yellowstone, Montana: Geological Society of America Bulletin 87, p. 703-710.

Pierce, K.L., 1979, History and dynamics of glaciation in the northern Yellowstone National Park area: U.S. Geological Survey Professional Paper 729 F, 91 p.

Pierce, K.L., 2004, Pleistocene glaciations of the Rocky Mountains: *in* Gillespie, A.R., and Porter, S.C., eds., The Quaternary Period in the United States: Elsevier, Amsterdam, p. 63-76.

Richmond, G.M., 1965, Glaciation of the Rocky Mountains: *in* Wright, H.E., Jr., and Frey, D.G., eds., The Quaternary of the United States: Princeton University Press, Princeton, NJ, p. 217-230.

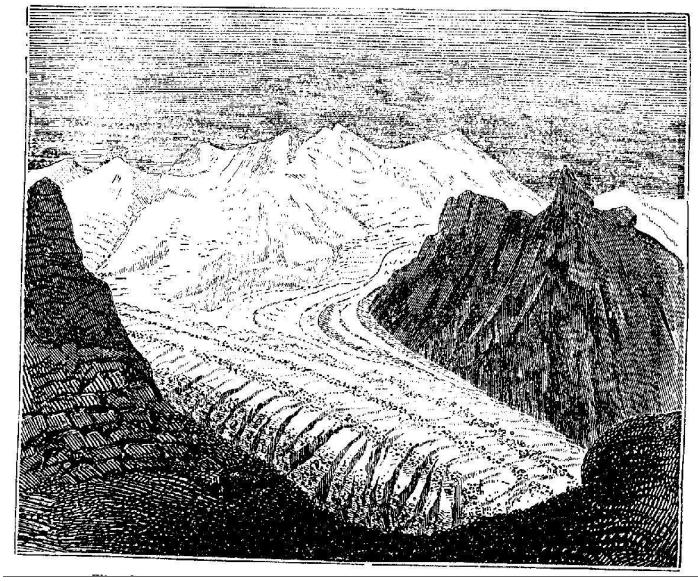

SECONDARY ENRICHMENT OF COPPER AT THE MADISON GOLD SKARN DEPOSIT, SILVER STAR DISTRICT, MONTANA

Christopher H. Gammons[1], Jill Sotendahl[1], and Dan Everett[2]
[1]*Montana Tech, Dept. of Geological Engineering, Butte, MT 59701*
[2]*Coronado Resources, PO Box 18, Silver Star, MT 59751*

Introduction

The Madison Gold skarn deposit is located near the southeastern margin of the Highland Mountains, near Silver Star, Montana. This deposit shares many similarities to other Au-Cu skarns in Montana and elsewhere in the world (Meinert et al., 2005), but is also unique in several aspects. Whereas previous workers (Foote, 1986) have examined the paragenesis and geochemistry of the primary skarn mineralization at Madison Gold, the current paper focuses on the chemical reactions responsible for secondary enrichment of copper. Secondary enrichment is a common phenomenon in copper deposits, including many skarns and porphyry deposits in the western U.S. (e.g., Sillitoe, 2005). Such enrichment is usually the result of weathering processes in the near-surface environment, and is therefore referred to as "supergene". At Madison Gold, we argue that most of the secondary Cu enrichment occurred during a late hydrothermal event that replaced the high temperature skarn mineral assemblage with hematitic jasperoid. Evidence favoring this "hypogene" Cu enrichment hypothesis is presented below, after a brief summary of the geology and mining history of the Silver Star district.

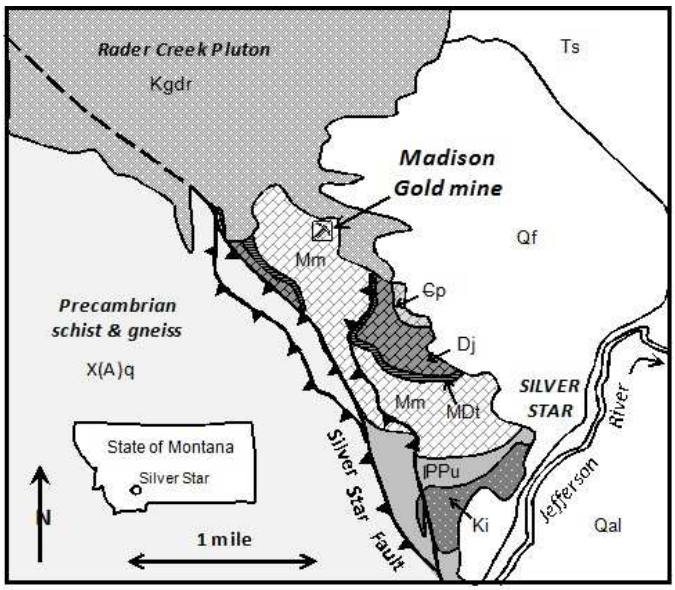

Fig. 1. Geology of the Silver Star area (modified from O'Neill et al., 2005). The geology of the Paleozoic block is simplified, as there are several faults and small intrusions not shown. Rock units: X(A)q = Precambrian quartzose schist and gneiss; Cp = Pilgrim Fm.; Dj = Jefferson Fm.; MDt = Three Forks Shale; Mm = Madison Limestone; PPu = Pennsylvanian and Permian, undivided; Ki = hypabyssal basalt and andesite; Kgdr = Rader Creek granodiorite; Ts = Tertiary sediments, undivided; Qf = alluvial fan; Qal = alluvium.

Local Geology

The Madison Gold deposit is a copper-gold skarn developed along the contact between the Cretaceous (80.4±1.2 Ma, Lund et al., 2002) Rader Creek granodiorite to the north and a NW-trending belt of folded and thrusted Paleozoic metasediments to the south (Fig. 1, modified from O'Neill et al., 1996). A major NW-trending reverse fault (termed the Green Campbell fault by early workers but renamed the Silver Star fault by O'Neill et al., 1996) separates the structural block of Paleozoic sediments from Precambrian basement to the southwest. The latter consists mainly of quartz-rich gneiss and amphibolite. According to the mapping of O'Neill et al. (1996), the outcrop pattern of the Paleozoic rocks at the

northern end of the Paleozoic structural block defines a synform, overturned to the west (Fig. 1). However, in detail the structure is more complicated than this, with some contacts being structural rather than stratigraphic. There has also been disagreement in the published literature regarding the identity of some of the sedimentary rocks (e.g., Amsden formation vs. Jefferson formation). Part of the confusion comes from the fact that the rocks are contact metamorphosed and therefore differ in color and texture from their unaltered appearance. However, all previous workers agree that the major skarn deposits in the district, including the Madison Gold deposit, are hosted by the Mississippian Madison Group limestone. The study area is sparsely vegetated with fair-to-good outcrop exposures, except in low-lying areas that are covered by alluvial fans.

Mining History

The Silver Star area is one of the oldest lode-gold mining districts in Montana. Two types of gold deposits are present: 1) fissure veins cutting Precambrian schist and gneiss; and 2) gold-rich skarns. Examples of the former include the Green Campbell and Iron Rod mines (Sahinen, 1939). Most of the gold production from the district has come from skarns developed along the contact between the Madison Group and the Rader Creek pluton. The Broadway (also known as Victoria) was the largest of several historic mines exploiting this skarn zone. An estimated 450,000 tons of ore was mined from the Broadway between 1870 and 1942, at an average grade of around 0.32 ounces per ton (144,000 oz Au) (Price, 2005). The Broadway mine has several thousand feet of horizontal workings extending to a maximum of 650 feet below surface. Three small open pits (American, Victoria, and Black) are located a short distance to the NW of the main Broadway mine.

Prior to 1900, ore from the Broadway mine was hauled to the towns of Silver Star and Iron Rod for milling. A 100-ton mill and cyanide plant was later built on the property, and gold bars were poured on site and shipped directly to the U.S. mint (Price, 2005). The mine shut down in 1942 owing to the general ban on gold mining during WWII. The Broadway-Victoria property has changed owners several times in recent decades, with sporadic exploration drilling. The property was renamed the "Madison Gold" mine in 1986. The current owners, Coronado Resources, are advancing an elliptical decline to explore the down-dip extension of copper and gold-rich skarn below the Black and Victoria pits. At the time of this writing, the decline has been driven over 1420 feet and locally to a depth of 265 feet below surface. Many of the observations and ideas that follow have come from underground mapping and examination of rock samples collected from this active underground operation.

Economic Mineralization

Three types of ore exist at the Madison Gold property: 1) unweathered skarn, locally rich in primary Fe-Cu sulfides and gold; 2) secondary chalcocite with subordinate native copper; and 3) Au-bearing, Fe-rich jasperoid. Most of the copper production to date has come from the chalcocite bodies, whereas most of the gold production has come from the primary sulfide and jasperoid zones.

Primary Skarn

Like most skarns, the Madison Gold deposit is mineralogically zoned and includes both *endoskarn* (i.e., metasomatized intrusive rock) and *exoskarn* (metasomatized country rock). Foote (1986) described the mineralogy and geochemistry of the Madison Gold skarn in detail. A simplified summary is included here.

The Rader Creek pluton is a medium-grained, non-porphyritic granitoid with a slabby outcrop pattern defined by low-angle joint sets. Near its contact with the Madison limestone, the pluton is altered to a light-green color with abundant epidote veins and replacements. A thin band of black Mn-oxide often occurs near the boundary between the epidote alteration and fresh granodiorite. Although disseminated sulfides are present, the endoskarn has generally low Cu and Au grades. The exoskarn which developed within the Madison limestone has a gangue mineralogy dominated by grossular-garnet + diopside closest to the intrusive contact grading to massive hedenbergite skarn and calcitic marble with greater distance from the intrusion. The garnet-diopside skarn has a mottled, green- to light-brown color and is disappointingly fine-grained with few collectable mineral specimens. In contrast, the hedenbergite skarn is very coarse-grained, with radiating clusters of dark-green to jet-black pyroxene crystals up to 5 cm long. The outer contact of the hedenbergite zone is very abrupt, with black pyroxene on one side and white calcitic marble on the other (Fig. 2). Primary sulfide minerals, including pyrite, pyrrhotite, chalcopyrite, and bornite, are present throughout the entire exoskarn, but are especially abundant in the garnet-diopside zone, locally forming pods or bands of nearly 100% sulfide. In sulfide-rich zones, the primary anhydrous skarn assemblage has been retrograde-metamorphosed to hydrous minerals, including Fe-rich amphibole, chlorite, and epidote (Foote, 1986). These sulfide-rich zones are oxidized to hematite/limonite near the surface, and at depth where they are cut by jasperoid (see below).

The primary gangue mineral zonation described above for Silver Star is typical of many skarns (e.g., see Meinert et al., 2005), and can be explained by differences in the hydrothermal mobility of Al, Mg, Si, and Fe (Fig. 3). Because Al and Mg are relatively immobile, garnet and diopside are found closest to the intrusive contact. Fe and Si are more soluble, resulting in the formation of hedenbergite at the outer margins of the exoskarn. Simplified reactions can be written as follows:

$$3CaCO_3 + 2Al^{3+} + 3SiO_2(aq) + 3H_2O \rightarrow Ca_3Al_2(SiO_4)_{3,grossular} + 6H^+ + 3CO_2 \quad (1)$$

$$CaCO_3 + Mg^{2+} + 2SiO_2(aq) + H_2O \rightarrow CaMgSi_2O_{6,diopside} + 2H^+ + CO_2 \quad (2)$$

$$CaCO_3 + Fe^{2+} + 2SiO_2(aq) + H_2O \rightarrow CaFeSi_2O_{6,hedenbergite} + 2H^+ + CO_2 \quad (3)$$

Beyond the furthest extent of metasomatism (i.e., hydrothermal mass transfer), dissipation of heat from the intrusion causes recrystallization of micritic limestone to coarse-grained marble. At Silver Star, the marble is creamy-white to bluish-gray, with large crystals that sparkle in the sun, in contrast to the unaltered Madison limestone that has a dull gray luster.

Jasperoid and Secondary Copper Enrichment

Three of the features of the Madison Gold deposit that set it apart from typical Cu-Au skarns are: 1) the presence of gold-bearing, Fe-rich jasperoid cut by calcite veins; 2) the presence of small but very high-grade bodies of chalcocite ore; and 3) the presence of unusual concentrations of native copper. The remainder of this article will attempt to show how these observations might be linked.

Jasperoid and jasperoid breccia crop out in the vicinity of the Victoria and American pits. This material locally carries good gold grades (> 0.1 opt), and obviously was mined for gold in the early days. The deep orange-

Fig. 2. Black, hedenbergite skarn (left) in near-vertical contact with light-colored marble (right). Tree for scale. Photo taken from the north rim of the Black Pit, looking south.

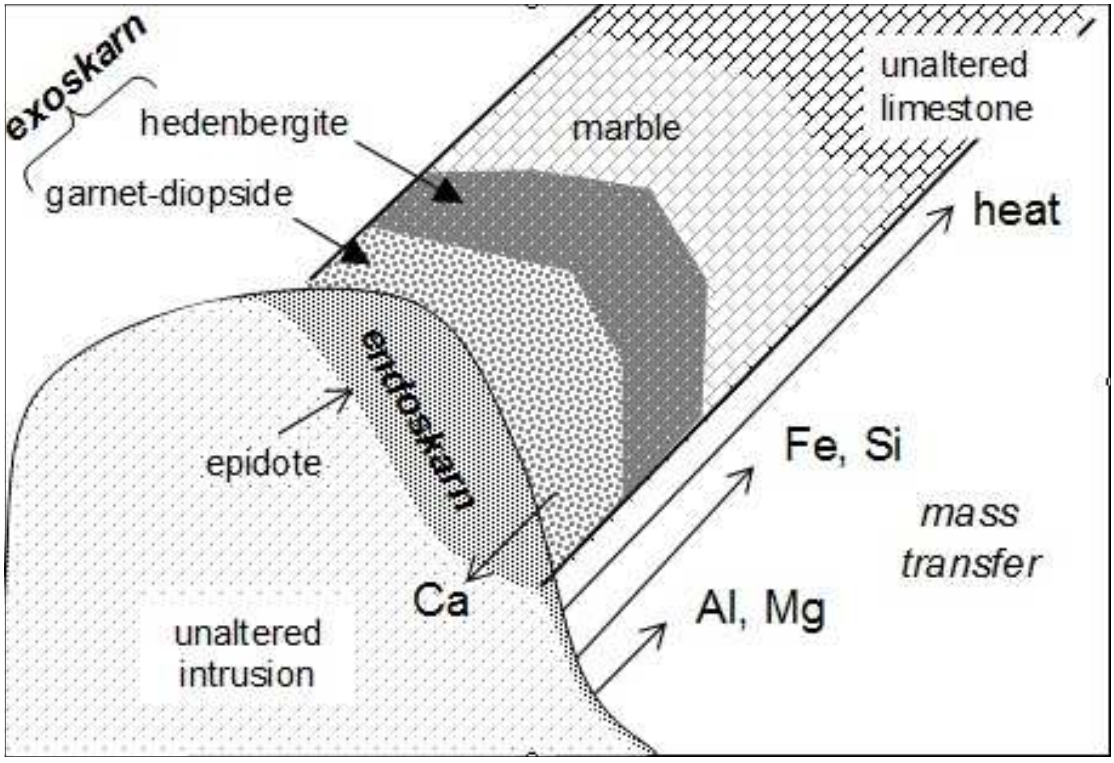

Fig. 3. Schematic diagram showing how differences in the hydrothermal mobility of different elements can explain the observed zonation of primary skarn minerals at Madison Gold.

Fig. 4. Photographs of hydrothermally-altered skarn and secondary copper minerals. A) Fe-rich jasperoid with stockwork of white calcite veins. The field of view is roughly 3 m across; B) Jasperoid with bright red pods of pure hematite, most likely replacing primary sulfide minerals: white veins are calcite; C) Massive chalcocite (dark gray) replacing pyrite. Small remnants of pyrite appear as light spots. D) Native copper stockwork in bleached skarn; E) Podiform native copper in garnet-diopside skarn: white is calcite (quarter for scale); F) Large native copper nugget (weight 47 lbs!) with malachite stains (quarter for scale).

brown to red color attests to its high Fe-oxide content, which is confirmed by chemical assay. Exposures of the same jasperoid body in the Madison Gold decline show that it is cut by a stockwork of anastomosing calcite veins (Fig. 4A). Quartz is comparatively rare, with the exception of the siliceous jasperoid itself. Jasperoid is commonly resistant to the strike of a rock hammer but locally contains soft patches of bright red hematite (Fig. 4B). Gold grades in the jasperoid body are locally good, but also unpredictable. From visual inspection, it is not possible to discern ore from waste. The jasperoid body is not restricted to the near-surface environment, and extends to deep levels of the mine. In certain areas, the jasperoid is located along the boundary between the aforementioned garnet-diopside and hedenbergite skarns, although elsewhere it is in direct contact with the Rader Creek pluton.

Adjacent to the jasperoid are localized pockets of chalcocite ore. The chalcocite bodies have irregular shape and are generally small (< 1000 tons), but extremely high-grade (25 to 50% Cu). When encountered during underground drilling, these chalcocite bodies are mined out and stockpiled at the surface for direct shipment to a smelter; no milling is necessary. Examination of hand samples and polished thin-sections shows that the chalcocite has replaced pre-existing sulfides, chiefly pyrite (Fig. 4C). Some rocks are essentially pure chalcocite, whereas others are mainly pyrite, with chalcocite invading along grain boundaries and cracks. Although chalcocite is a very common secondary mineral in weathered, hydrothermal copper deposits, the chalcocite bodies at Silver Star are unusually high-grade, due to whole-scale replacement of massive pyrite by secondary Cu-sulfide. For comparison, supergene-enriched copper ore at the Berkeley Pit of Butte, Montana, typically graded < 1% Cu, but was nonetheless significantly richer than the deeper ore that had not seen secondary enrichment (< 0.5% Cu) (McClave, 1973).

>From a mineralogical standpoint, the most fascinating aspect of the ore being mined at Madison Gold is the localized occurrence of native copper pods and veins. Native copper is definitely subordinate to chalcocite in terms of abundance; an estimated 350 lbs of copper nuggets have been hand-picked during the current mining operation, compared to an estimated *1 million* lbs of Cu mined from chalcocite. Nonetheless, native copper is fairly common, even in the deep underground workings. Copper occurs in two main forms: stockworks of anastomosing veins (Fig. 4D), and pods or irregular masses several cm in diameter (Figs. 4E, 4F). The copper stockworks are particularly striking, with cross-cutting veins of native copper up to 1 cm in thickness. In some samples, the copper veins cut skarn that is still hard and intact, whereas in other samples the skarn matrix has been severely altered to clay, making it difficult to obtain sawn slabs. Although at first glance the veins appear to be filled entirely by copper, reaction with dilute hydrochloric acid shows that many of the veins have thin selvages of calcite, which is a clue to their origin. Another clue is that the overall geometry of the copper veins resembles that of the calcite stockworks that cut the nearby Fe-rich jasperoid bodies (compare Figs. 4A and 4D). Although native copper exists in minor quantities throughout the mine, some of the richest native copper zones were found adjacent to the aforementioned chalcocite bodies. At the boundary between the two mineral zones, arborescent masses of native copper have been found encasing marble-to golf-ball-sized pods of chalcocite.

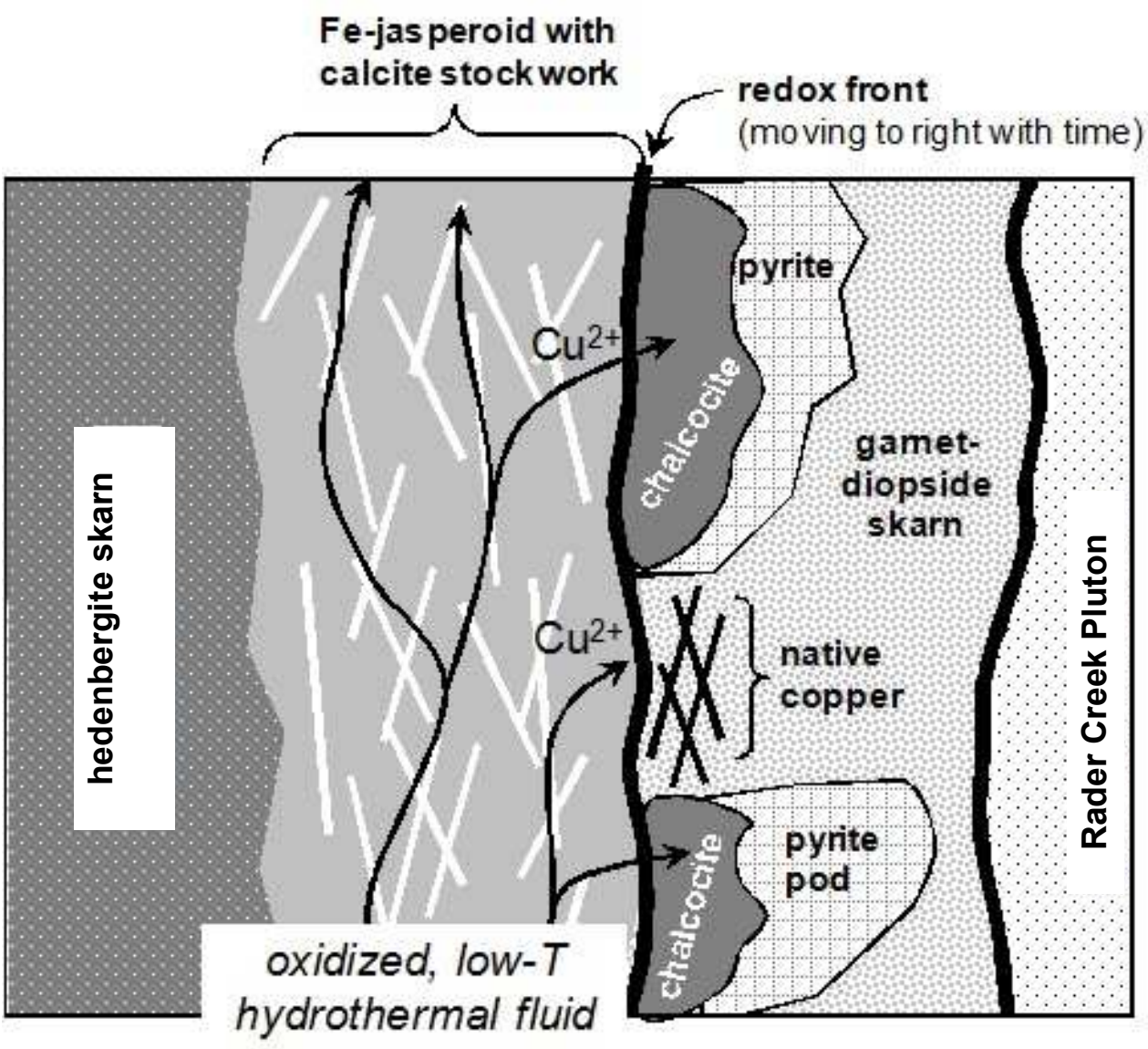

Fig. 5. Conceptual model of low-temperature hydrothermal alteration of the Madison Gold skarn. Oxidized geothermal waters infiltrate through the prograde skarn, converting hedenbergite to hematite + amorphous silica (Fe-jasperoid). Copper is leached out of the skarn protore and is re-deposited at an advancing redox front as either chalcocite (where pre-existing pyrite is present) or native copper (where no sulfides are present).

Genetic Model

The following is a preliminary geochemical model that attempts to link together the spatial association of Fe-rich jasperoid, chalcocite bodies, and native copper at the Madison Gold deposit. A cartoon of the overall process is shown in Fig. 5.

To begin with, the occurrence of Fe-rich jasperoid cut by calcite veins can be explained by interaction of a lower-temperature geothermal water with pre-existing hedenbergite skarn, as shown by the following simplified reaction:

$$2CaFeSi_2O_{6,\text{hedenbergite}} + 2CO_2 + \tfrac{1}{2}O_2 \rightarrow Fe_2O_{3,\text{ hematite}} + 4SiO_{2,\text{ quartz}} + 2CaCO_{3,\text{ calcite}} \quad (4)$$

The stoichiometry of reaction (4) predicts a molar ratio of 1:4:2 for hematite:quartz:calcite, which is in qualitative agreement with visual inspection of the jas-

peroid outcrops on the walls of the Madison Gold decline (Fig. 4A). The silica that was liberated from the breakdown of hedenbergite now exists as siliceous cement within the jasperoid itself, and did not form discrete quartz veins. Instead, most of the veins cutting the jasperoid are filled with calcite. This is a clue that the invading geothermal waters were rich in dissolved inorganic carbon (i.e., CO_2), but not rich in silica. In other words, they were probably low-temperature hydrothermal waters (T < 200°C), the type that would form a travertine mound at the surface as opposed to a silica sinter. Also, reaction (4) shows that it is necessary to oxidize iron from its ferrous (+2) valence state in hedenbergite to its ferric (+3) valence state in hematite. This is an important observation, and suggests that the invading geothermal fluids had a high concentration of dissolved oxygen, further evidence that this was a low temperature (and most likely shallow) geothermal system.

If we assume that the Fe-jasperoid bodies at Madison Gold were caused by a low-temperature hydrothermal fluid that was strongly oxidized, it follows that any pre-existing sulfide minerals that these fluids encountered would have been destroyed. Pyrite would have been altered to hematite, as shown by the following reaction:

$$2FeS_{2,pyrite} + 4H_2O + 15/2O_2 \rightarrow Fe_2O_{3,hematite} + 4SO_4^{2-} + 8H^+ \quad (5)$$

Primary Cu-bearing sulfides such as chalcopyrite would also have been converted to hematite, liberating Cu^{2+} ions in the process:

$$2CuFeS_{2,chalcopyrite} + 2H_2O + 17/2O_2 \rightarrow 2Cu^{2+} + Fe_2O_{3,hematite} + 4SO_4^{2-} + 4H^+ \quad (6)$$

The soft "pods" of hematite in the otherwise hard jasperoid bodies (Fig. 4B) most likely owe their origin to replacement of pre-existing sulfides, e.g., via reactions (5) or (6).

Due to the oxidized nature of the late hydrothermal waters, any primary Cu-bearing sulfide minerals would have dissolved in the main zone of jasperoid development. We envision that most of the Cu^{2+} ions liberated in this way migrated laterally into the garnet-diopside skarn and precipitated as chalcocite and/or native copper at an advancing reduction front (Fig. 5). This is the key step in the formation of the unusually rich secondary copper ores at Madison Gold. In instances where pyrite was already present, the Cu^{2+} reacted to form chalcocite, via the classic pyrite replacement reaction first described by Zies et al. (1916):

$$14Cu^{2+} + 5FeS_{2,pyrite} + 12H_2O \rightarrow 7Cu_2S_{chalcocite} + 5Fe^{2+} + 3SO_4^{2-} + 24H^+ \quad (6)$$

The fact that the oxidized fluids were geothermal (and not supergene) allowed the replacement of pyrite by chalcocite to advance to completion, rather than being a thin reaction rim. In areas of the skarn where pre-existing sulfide minerals were absent, chalcocite did not form, and instead Cu^{2+} precipitated at the reduction front as native copper:

$$Cu^{2+} + H_2 \rightarrow Cu_{\ native\ copper} + 2H^+ \quad (7)$$

This could explain the existence of cm-wide veins of nearly pure copper cutting bleached and clay-altered skarn. It is also possible to form native copper by oxidation of chalcocite:

$$Cu_2S + H_2O + 3/2O_2 \rightarrow 2Cu + SO_4^{2-} + 2H^+ \quad (8)$$

Reaction (8) could explain the localized intergrowths of native copper nuggets and chalcocite.

Unlike copper, gold is immobile in low temperature, oxidized environments (Gammons and Williams-Jones, 1997). Much of the gold from the historic Broadway mine was recov-

ered from a single drift of oxidized skarn ore, located within 200 feet of surface (Price, 2005). The grade of gold in this oxide ore was probably close to what it would have been in the primary skarn ore, on average ~ 0.3 opt. Preliminary examination of polished sections of primary, sulfide-rich skarn from the Madison Gold mine has revealed the rare presence of micron-sized inclusions of gold within other sulfides, including pyrite and chalcopyrite. Gold has also been identified as micron-sized inclusions within jasperoid. Our current hypothesis, which agrees with the conclusions of Foote (1986), is that most of the gold in the Madison Gold deposit was introduced, along with Fe-Cu-sulfides, during the late stages of the main skarn event. The lower-temperature hydrothermal system responsible for jasperoid development and calcite veining was incapable of remobilizing gold, due to its inferred oxidized character. Thus, oxidation and silicification of the skarn protore resulted in the complete remobilization of copper to form chalcocite and native copper along the margins of the jasperoid, whereas gold remained in place.

Concluding Statements

The above model for hypogene secondary enrichment of copper at the Madison Gold deposit should be considered preliminary. The authors are still at an early stage in their study, and have quite a bit of mineralogy and geothermometry work yet to accomplish. Nonetheless, the general model appears robust in the sense that it explains many of the mineralogical observations at the deposit, while at the same time being geochemically and geologically plausible. If correct, one of the more significant implications of the hypogene enrichment model is that zones of high-grade chalcocite ore may persist to even greater depth than currently seen in the Silver Star district. This is opposed to conventional wisdom which would predict that this type of secondary copper mineralization would only be present near surface, e.g., at or near the present-day water table. Another important idea to keep in mind is that the late geothermal fluids, if oxidized, could not have introduced any new gold into the deposit. Thus, the grades and distribution of gold within the jasperoid most likely reflect the grades and distribution of gold within the skarn protore.

References Cited

Foote, M.W., 1986, Contact metamorphism and skarn development of the precious and base metal deposits at Silver Star, Madison County, Montana: Ph.D. thesis, Univ. of Wyoming, Laramie, WY, 233 p.

Gammons, C.H., and Williams-Jones, A.E., 1997, Chemical mobility of gold in the porphyry-epithermal environment: Economic Geology, v. 92, p. 45-59.

Lund, K., Aleinkoff, J.N., Kunk, M.J., Unruh, D.M., Zeihen, G.D., Hodges, W.C., du Bray, E.A., and O'Neill, J.M., 2002, SHRIMP U-Pb and 40Ar/39Ar age constraints for relating plutonism and mineralization in the Boulder batholith region, Montana: Economic Geology, v. 97, p. 241–267.

McClave, M.A., 1973, Control and distribution of supergene enrichment in the Berkeley Pit, Butte District, Montana: *in* Miller, R.N., ed., Guidebook for the Butte field meeting of the Society of Economic Geologists, Butte, MT: August 18-21, 1973, p. K1-K4.

Meinert, L.D., Dipple, G.M., and Nicolescu, S., 2005, World skarn deposits: *in* Hedenquist, J.W., Thompson, J.F.H., Goldfarb, R.J., and Richards, J.P., eds., Economic Geology, One Hundredth Anniversary Volume: Society of Economic Geologists, p. 299-336.

O'Neill, J.M., Klepper, M.R., Smedes, H.W., Hanneman, D. L., Frazer, G.D., and Mehnert, H.H., 1996, Geologic map and cross sections of

the central and southern Highland Mountains, southwestern Montana: U. S. Geological Survey Miscellaneous Investigations Series, Map I-2525.

Price, B.J., 2005, Madison Gold Property, Silver Star area, Madison Co., Montana, USA: Technical Report prepared for Minera Capital Corp., 118 p.

Sahinen, U.M., 1939, Geology and ore deposits of the Rochester and adjacent mining districts, Madison County, Montana: Montana Bureau of Mines and Geology Memoir 19, 53 p.

Sillitoe, R.H., 2005, Supergene oxidized and enriched porphyry copper and related deposits: *in* Hedenquist, J.W., Thompson, J.F.H., Goldfarb, R.J., and Richards, J.P., eds., Economic Geology, One Hundredth Anniversary Volume: Society of Economic Geologists, p. 723-768.

Zies, E.G., Allen, E.T., and Merwin, H.E., 1916, Some reactions involved in secondary copper sulphide enrichment: Economic Geology, v. 11, p. 407-503.

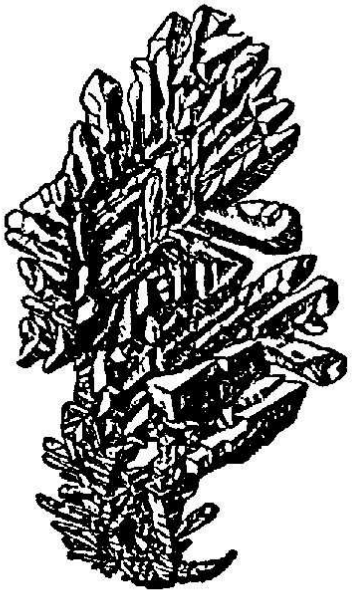

LATE HOLOCENE ROCK FALL ON A MOUNTAIN BISON IN THE ANACONDA RANGE, MONTANA

Chris Shaw
Mine Geologist, Turquoise Ridge Joint Venture, Golconda, NV 89414

Abstract

A bison skull and skeleton were found by the author in 1977 at an elevation of 2515 m in the Anaconda Range, 40 km southwest of Anaconda, Montana. The remains were pinned under several heavy rock slabs in Maloney Basin near the base of Warren Peak, 1.6 km east of Warren Pass, in the Anaconda-Pintler Wilderness. During a field visit in 1985, the skull showed signs of being eaten by porcupines. In 2008, the character of the site and skull were documented in preparation for this paper. A radiocarbon date has not been obtained, although some of the bones are available for radiocarbon dating. The condition of the bones suggest the bison died at a relatively young age, dating perhaps to the time of the last wild bison in the area in the 1800's (Haines, 1955). The bison is likely a mountain or wood bison (*Bison bison athabascae*) because the width of the horn core at 97.4 cm is much wider than the world record plains bison's horn spread of 89.8 cm. However, there is a possibility it is an extinct ancient bison (*Bison antiquus*) due to the measured horn core width nearly one meter wide. A deformed left horn core shows this animal was infected with either bovine brucellosis or tuberculosis, which may indicate this animal was old, injured, or was suffering from environmental stress. The site documents the time of the collapse of the rock shelter, and the time of mountain bison in the area. The bison could have been killed by the collapse of the rock shelter as the skull was pinned by a large rock slab. It is also possible the bison died of natural causes and was later covered by the rock fall. No evidence of human occupation was observed in the rock shelter.

Introduction

During a seven-day horse pack trip into the Anaconda Mountains in August 1977 (Figure 1), the author found a bison skull and skeleton in a rock fall in Maloney Basin (Figure 2). Snowstorms at the time made for a cold late summer wilderness trip (Figure 3).

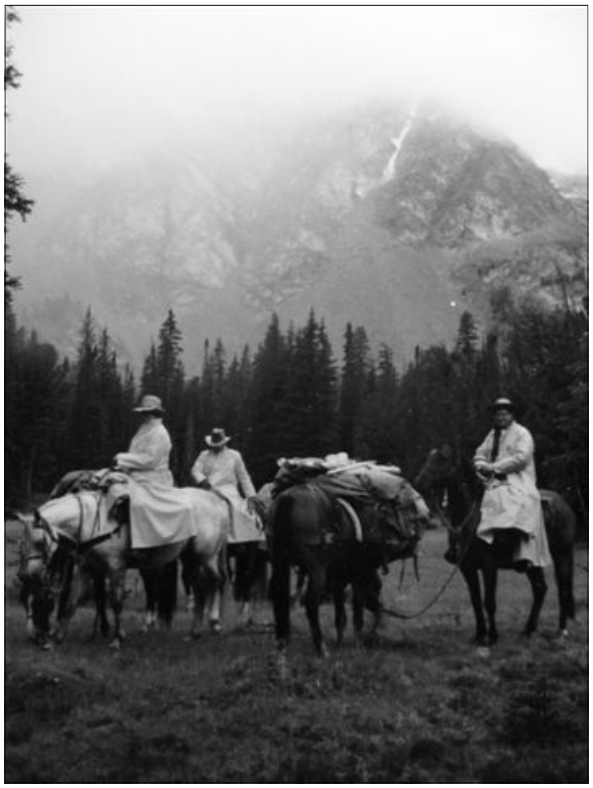

Figure 1. The Shaw family below Warren Pass in the Anaconda Range, Montana, in August 1977. From left to right are Linda, Tim and Carlton Shaw on horses. The author found a bison in a rock fall in Maloney Basin on the north side of the Continental Divide while exploring.

Figure 2. The Maloney Basin bison skull with a knife 9 cm long for scale.

Figure 3. During August 1977, early storms hit during the pack trip. Carlton and Sarah Shaw prepare supper at a camp below Warren Lake after crossing Cutaway Pass from Maloney Basin in a snowstorm.

Discovery Site

Maloney Basin is an alpine cirque located 8 km inside the Anaconda-Pintler Wilderness and 40 km southwest of Anaconda, Montana (Figure 4). The rock shelter in which the bison remains were discovered is located immediately northeast of Warren Peak (Figure 5). The rock shelter and rockslide are composed of Cretaceous quartz monzonite. A large amount of blocky quartz monzonite lies along the base of Warren Peak. A grass-covered mountain meadow (which at one time probably was a small lake) is directly downhill from the rock shelter, and a small mountain stream is about 30 m to the east of the site. A 10 cm-thick white clay layer (which may be Mazama ash) is exposed at springs in the meadow.

Bison in the Anaconda Range

A radiocarbon date to determine the radiocarbon age of the bison has not been obtained. The freshness of the bones suggests an 1800's age of death. The Maloney Basin bison may represent a remnant of some of the last free-roaming bison in the west. The discovery of gold in 1865 by Hector Horton caused a gold rush to the Phillipsburg area (Wolle, 1963). The influx of prospectors nearby and later settlers may have caused the last remaining bison to go toward the continental divide to find seclusion and safety. Raup (1933) described the rapid decline of bison in the western U.S. between 1840 and 1900, which is about the time the evidence suggests this bison died in Maloney Basin.

Figure 4. Location of the Maloney Basin Bison, Anaconda Range, Montana.

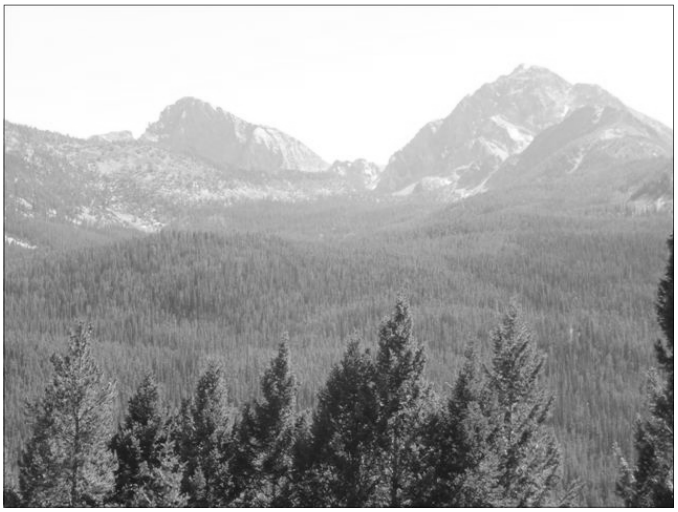

Figure 5. The continental divide looking south from Carpp Ridge. Warren Pass, elevation 2626 m, is to the left of the tree tops in the center of the photo. This is mountain bison habitat.

Mountain Bison or Plains Bison?

The bison lived in the habitat of mountain bison or wood bison (*Bison bison athabascae*). Alternatively, the bison may have been a very large plains bison (*Bison bison bison)* that lived in the mountains. A remnant population of wood bison was found in northeastern Alberta Canada in 1959, and some individuals from this remnant population have been reintroduced into Alaska (Gates, 1992, and Alaska Department of Fish and Game**,** 1994). The Maloney Basin bison horn core spread of 97.4 cm is about the same spread as the reported 1 m horn core for the extinct ancient bison (*Bison antiquus*, Jefferson, 2001). The relative freshness of the skull and the discovery habitat suggest this is a mountain bison and not an ancient bison. The Maloney Basin bison horn core is wider than the largest measured Boone and Crockett plains bison (Boone and Crockett Club, 2010). The mountain or wood bison may be a larger and more primitive subspecies of American bison (Skinner and Kalsen, 1947).

Bison Taxonomy

There is some controversy concerning the taxonomy of bison subspecies. Skinner and Kalsen (1947) proposed that mountain or wood bison may be a larger and more primitive subspecies of American bison. Van Zyll de Jong (1986, 1993) and van Zyll de Jong et al. (1995) contend that there are two subspecies of bison, the wood bison and the plains bison. Geist (1996) wrote that the wood bison was an ecotype of the plains bison and not a subspecies of the plains bison.

Most recently, Jackson (2008) observed that plains bison introduced into Yellowstone National Park migrate out of the Park during the winter. In contrast, the Mirror Plateau herd (300 bison) appear to have some mountain bison characteristics. These bison summer on the Mirror Plateau and winter in the Pelican Valley. Jackson suggests that the Mirror Plateau herd may be a remnant population of the original mountain bison native to Yellowstone National Park as described by Hague (1893). Jackson reported that they may have interbred with the introduced plains bison but they do retain the secretive and shy nature of the original mountain bison, even if they do not possess the larger, flatter horns, heavy front end, and overall larger stature of the wood bison of Canada.

Skull Measurements

Using the official scoring system for North American Big Game Trophies by Boone and Crockett (Boone and Crockett Club, 2010), the following are measurements for the Maloney Basin bison (Table 1). Since only the horn core remains, these are minimum measurements and do not give a full measurement for the skull.

The world record American plains bison is a skull found in Yellowstone National Park (YNP), Wyoming, by Sam T. Woodring in 1925; measurements recorded in Table 2.

Table 1. Boone and Crockett Club, Maloney Basin Bison, 1977.

Greatest Spread	97.4 cm, measuring horn core only
Tip to Tip Spread	97.4 cm, measuring horn core only
Length of Horn	Right Horn Core 27.2 cm, Left Horn Core 25 cm
D-1 Circumference of Base	Right Horn Core 26 cm, Left Horn Core 24.4 cm
D-2 First Quarter Circumference	Right Horn Core 22.8 cm, Left Horn Core 24 cm
D-3 Second Quarter Circumference	Right Horn Core 21.4 cm, Left Horn Core 20 cm
D-4 Third Quarter Circumference	Right Horn Core 18.8 cm, Left Horn Core 18.8 cm

Table 2. Boone and Crockett Club, World Record Bison, YNP, Wyoming, 1925.

Greatest Spread	89.85 cm
Tip to Tip spread	68.58 cm
Length of Horn	Right Horn 53.98 cm, Left Horn 59.80 cm
D-1 Circumference of Base	Right Horn 40.64 cm, Left Horn 38.10 cm
D-4 Third Quarter Circumference	Right Horn 20.96 cm, Left Horn 20.32 cm

Discussion of Skull Morphology

Comparison of Tables 1 and 2 suggest that the Maloney Basin bison is a mountain or wood bison. The horn core alone is nearly 8 cm longer than the world record plains bison and the horn core has a much wider and flatter profile.

The left horn core contains a 2.5-cm-deep cavity on the lower outer one-third of the horn core has produced a deformation on the outer seven cm of the horn core. This deformation was likely caused by infection or injury, which is a common affliction of old, injured, or stressed animals at the margins of their habitat. Common infections were bovine brucellosis and tuberculosis (Jolly and Messier, 2004). Many similar deformations in other bison skulls have been found in the Holocene, especially in animal populations showing increased environmental stress.

Rock slabs at the back of the collapsed shelter shifted some time between 1985 and 2008. This shift opened the site for greater deterioration of the bison remains by weathering and porcupine chewing (Figure 6) which have taken much of the skull forehead.

Conclusion

The Maloney Basin bison skull and skeleton found in a rock fall at the northern base of Warren Peak are most likely a mountain or wood bison (*Bison bison athabascae*). However, there is a less likely possibility that the

Figure 6. Russell Shaw shows where a porcupine chewed on the forehead of the Maloney Basin bison.

animal was an ancient bison (*Bison antiquus, now extinct*) due to the nearly one-meter-wide measured horn-core width. The mountain bison or wood bison is also extinct in the United States except for plains-mountain bison hybrids in Yellowstone National Park, and wood bison reintroduced to Alaska from Canada. The deformed left horn core shows this animal was infected with either bovine brucellosis or tuberculosis, which is common in old or injured animals, or animals suffering from environmental stress. No evidence of human occupation was found in the rock shelter that collapsed on the Maloney Basin bison. A more definitive age for the animal will require application of laboratory dating methods.

References

Alaska Department of Fish and Game, 1994, Reintroducing wood bison to the upper Yukon valley, Alaska: a feasibility assessment: Alaska Dept. of Fish and Game, Fairbanks, p. 94.

Boone and Crockett Club, 2010, data and on-line scoring of American plains bison and world record American plains bison: online at www.boone-crockett.org, 5/22/10.

Bork, A.M., Strobeck, C.M., Yeh, F.C., Hudson, R.J., and Salmon, R.K., 1991, Genetic relationship of wood bison and plains bison based on restriction fragment length polymorphisms: Canadian Journal of Zoology, v. 69, p. 43-48.

Gates, C.C., 1992, Cursory evaluation of the habitat potential of the Yukon River Flats, Alaska, for a reintroduction of wood bison: Unpublished Report, p.7.

Geist, V., 1991, Phantom subspecies: The wood bison (Bison bison "athabascae", Rhoads 1897) is not a valid taxon, but an ecotype: Arctic, v. 44, p. 283-300.

Hague, A., 1893, The Yellowstone Park as a game reservation: American Big Game Hunting, the book of the Boone & Crockett Club, Forest & Stream Publishing Co., New York, p. 240-270.

Haines, A., ed., 1955, Osborne Russell's Journal of a Trapper: Oregon Historical Society, Portland, 179 p.

Jackson, B., 2008, The mountain bison of Yellowstone, a breed apart: peer.org/docs/nps/08_23_4_yellowstone_mountain_bison.pdf, p. 1-2.

Jefferson, G.T., 2001, Rancho La Brea bison: Terra, v. 38, p. 33.

Jolly, D.O., and Messier, F., 2004, Factors affecting apparent prevalence of tuberculosis and brucellosis: Jour. of Animal Eco., v. 7, n. 4, p. 623-631.

Raup, H.M. 1933, Range conditions in the Wood Buffalo Park of western Canada with notes on the history of the wood bison: Spec. Pub. Am. Comm. for Int. Wildlife Prot., v. 1, n. 2, 52 pp.

Skinner, M.F., and Kalsen., O.C., 1947, The fossil bison of Alaska and preliminary revision of the genus: Bull. Am. Mus. Nat. His. v. 89, p. 127-256.

van Zyll de Jong, C.G., 1986, A systematic study of recent bison, with particular consideration of the wood bison: Nat. Mus. Nat. Sci. Publ.: Nat. Sci. n. 6. p. 69.

van Zyll de Jong, C.G., 1993, Origin and recent geographic variation of recent North American bison: Alberta, v. 3, n. 2, p. 21-35.

van Zyll de Jong, C.G., Gates, C., Reynolds, H., and Olson, W., 1995, Phenotypic variation in remnant populations of North American bison: J. Mammology, v. 76, p. 391-405.

Wolle, M.S., 1963, Montana Pay Dirt: Sage Books, Athens, Ohio.

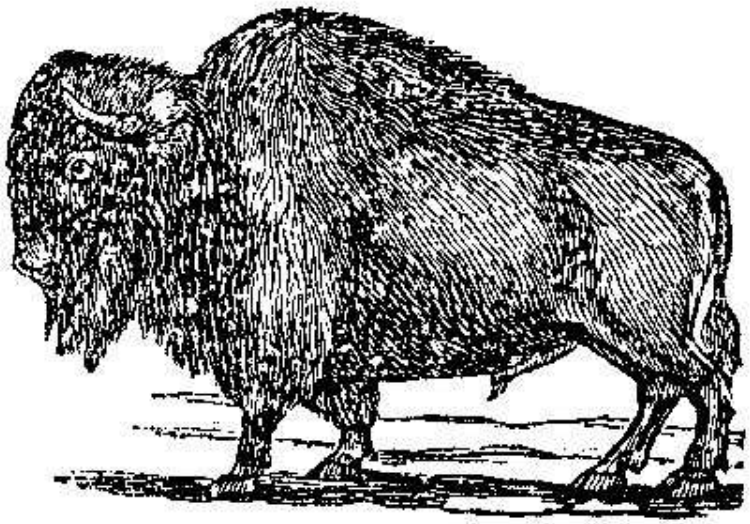

MICROSTRUCTURAL ANALYSIS OF BELT SUPERGROUP METAPELITES IN THE CLARKIA AREA OF NORTHERN IDAHO: IMPLICATIONS OF 1.0-1.1 GA GARNET

Timothy O. Nesheim[1], Jane A. Gilotti[1], William C. McClelland[1], Helen M. Lang[2], C.T. Foster Jr[1], and Jeff D. Vervoort[3]

[1] *Geoscience Department, University of Iowa, Iowa City, IA 52242*

[2] *Department of Geology and Geography, West Virginia University, P.O. Box 6300, Morgantown, WV 26506-6300*

[3] *School of Earth and Environmental Sciences, Washington State University, Pullman, WA 99164*

Abstract

Belt Supergroup metapelites in the Clarkia area of northern Idaho contain evidence of coeval deformation and metamorphism dating back to the Mesoproterozoic. Previous studies in the area attributed regional metamorphism and deformation to Cretaceous tectonism, associated with the emplacement of the Cretaceous Idaho Batholith. Recent studies in the Clarkia area of northern Idaho, however, have reported Lu-Hf garnet ages of 1.2-1.0 Ga within pelitic schist of the Belt Supergroup (e.g. Zirakparvar, 2010). Here we report three fabrics present within Belt schist of the Clarkia area that have relevance to the long tectonothermal history of these rocks: (1) S1 compositional layering, (2) S2, a metamorphic cleavage defined by the preferred orientation of planar matrix minerals which shows a syntectonic relationship to garnet growth, and (3) a poorly developed crenulation cleavage, S3, which deforms S2 and post-dates garnet growth. Coeval deformation and metamorphism in northern Idaho at approximately 1.1 Ga indicates that western Laurentia (North America) was tectonically active during the construction of the supercontinent Rodinia.

Introduction

Recent Lu-Hf garnet geochronologic studies of Belt Supergroup metapelites of northern Idaho have reported old ages of 1.2-1.0 Ga (Sha et al., 2004; Vervoort et al., 2005; Zirakparvar et al., 2010). The Mesoproterozoic garnet ages call for a reevaluation of the previous inferences of Cretaceous metamorphism and deformation. Previous work has determined that Belt Supergroup metasedimentary rocks in northern Idaho contain evidence for as many as three metamorphic events (Hietanen 1984; Lang, 1985a,b,c; Grover et al., 1992) and polyphase deformation with some outcrops preserving as many as three separate fold sets (Hietanen, 1963a; 1963b). These prior studies correlated their observed geologic events with Cretaceous tectonism on the basis of close proximity to the Idaho Batholith (Fig. 1).

Garnets within the Belt Supergroup metasedimentary rocks in northern Idaho display two different Lu-Hf age characteristics. Garnets in close proximity to the Idaho Batholith have cores and rims that give Lu-Hf ages of 1.2-1.0 Ga and 100 Ma, respectively, and garnets farther from the batholith give only Mesoproterozoic ages with no evidence for Cretaceous rims (Sha et al., 2004; Vervoort et al., 2005; Zirakparvar, 2007; Zirakparvar et al., 2010). The purpose of this study is to reexamine the timing

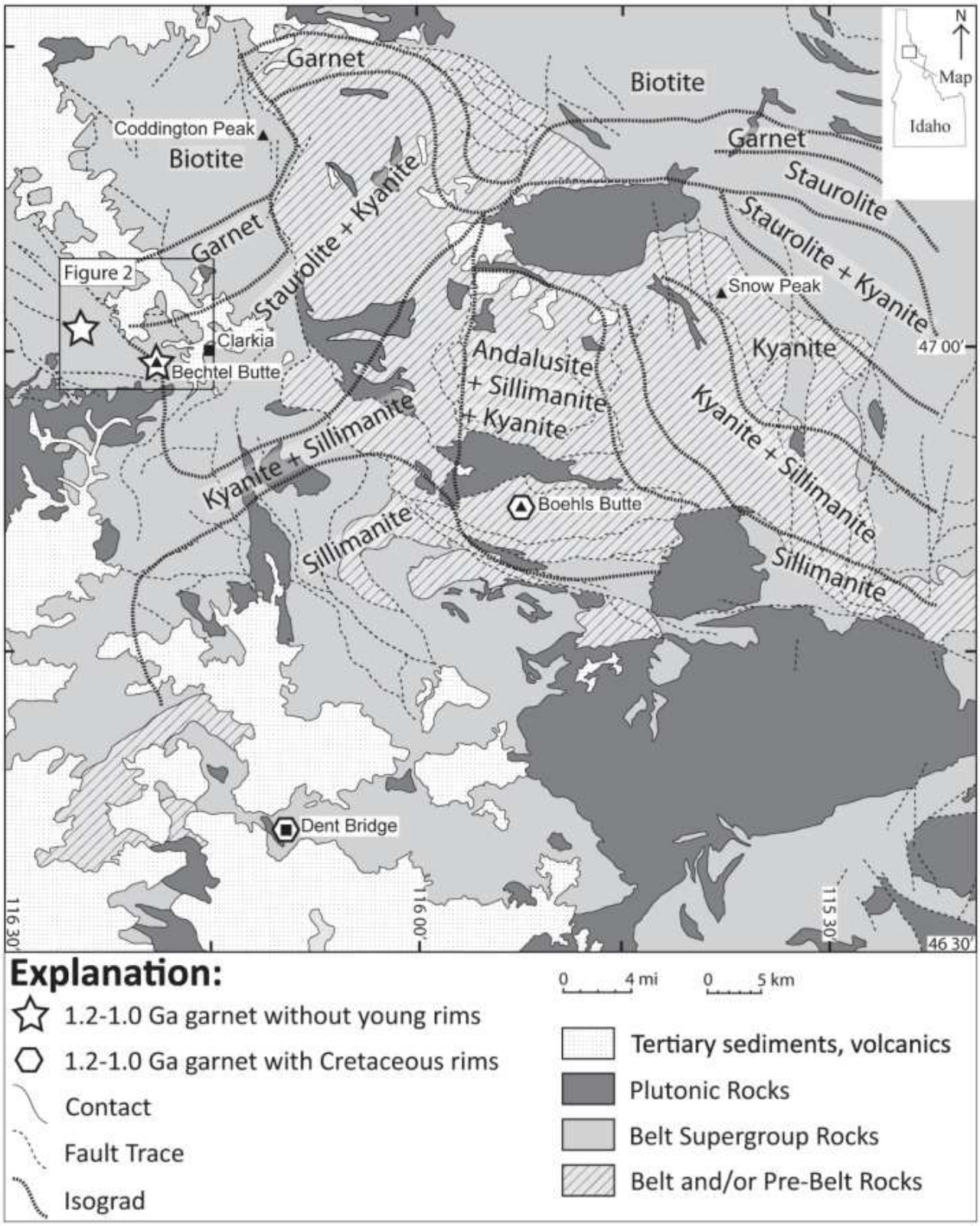

Figure 1: Simplified geologic map from northern Idaho with locations of known >1.0 Ga garnet (Vervoort et al., 2005; Zirakparvar et al., 2010). Geology is modified after Lewis et al. (2000; 2005; 2007) and the Wallace Quadrangle (Lewis, unpublished). The isograds are from Hietanen (1984).

of deformation in relation to garnet growth within the Clarkia area of northern Idaho where only the older, 1.2-1.0 Ga Lu-Hf garnet ages have been reported (Fig. 1).

Between 1.3 and 1.0 Ga, all of the Earth's major continents are thought to have merged to form the supercontinent Rodinia, which later broke apart between 0.7-0.5 Ga (e.g., Hoffman, 1991). As a result, 1.3-1.0 Ga orogenic belts are common to many paleo-continents. The Grenville orogenic belt in particular has played a key role as a piercing point for plate reconstructions of Rodinia (Dalziel, 1991; Hoffman, 1991; Moores, 1991). While reconstructions commonly place Laurentia (North America) toward the center of Rodinia, there is debate regarding what continental fragment was juxtaposed against the western margin of Laurentia (see review in Li et al., 2008). Regardless of which model is preferred, all reconstructions indicate relative tectonic quiescence along the western Laurentian margin by 1.3 Ga.

Geologic Setting

The Belt Supergroup is a 15-20 km thick sedimentary package that extends across eastern Washington, northern Idaho, western Montana, and southern British Columbia (Winston, 1978; Link et al., 1993). Sediments of the Belt Supergroup were deposited semi-continuously between 1.47 and 1.40 Ga (Evans et al., 2000). Metasedimentary rocks in the Clarkia area that contain Mesoproterozoic garnets are correlated with the Wallace Formation which lies in the middle portion of the Belt Supergroup. The Wallace formation consists of both carbonate and siliciclastic units thought to have been deposited in a lacustrine setting (Winston, 2007). The section has been metamorphosed and now occurs as interlayered quartzites, meta-carbonates, and, the most important to this study, garnet-bearing metapelites.

In Montana and Idaho, the Belt Supergroup was intruded by Cretaceous to Tertiary granitic plutons of the Idaho Batholith (Hyndman, 1983). Initial emplacement of the Idaho batholith began in the mid-Cretaceous within the Bitterroot lobe in northern Idaho (Fig. 1). The main phase of plutonism in the area of interest occurred during the early Eocene between ~66 and 54 Ma (Foster and Fanning, 1997; Gaschnig et al., 2009). Northern Idaho underwent regional extension at approximately 52-44 Ma, during the final stage of plutonism (Hodges and Applegate, 1993; House and Hodges, 1994; Foster and Fanning, 1997).

Multiple studies over several decades have contributed to understanding the metamorphic history of the metasedimentary rocks in northern Idaho. Initial work by Hietanen (1956; 1963a; 1963b; 1984) recognized a southward increase in metamorphic grade from greenschist facies rocks in the biotite zone to amphibolite facies rocks in the sillimanite zone (Fig. 1). Later studies in the eastern Snow Peak area (Fig. 1; Lang and Rice, 1985a, b, c), and the southern Boehls Butte area (Fig. 1; Grover et al., 1992), concluded that northern Idaho experienced two regional metamorphic events, M1 and M2, associated with crustal thickening followed by late-stage retrograde metamorphism, M3, associated with the emplacement of the Idaho Batholith (Grover et al., 1992).

Garnet Growth in Relation to Deformational Fabrics

The increasing number of Mesoproterozoic Lu-Hf garnet ages point a metamorphic event early in the history of the Belt Supergroup. This study examines the relationships between deformation and metamorphism to address the question of whether the Mesoproterozoic garnet growth in the Clarkia area (Fig. 1; Zirakparvar et al., 2010) is associated with a regional orogenic

event. Thin sections from oriented samples of garnet-bearing schist (Fig. 2) were used to characterize the timing relationships between deformational fabrics and garnet growth (Nesheim, 2009). In particular, porphyroblast-fabric relationships were examined using the methodology and terminology outlined in Passchier and Trouw (2006). The degree of matrix grain deflection around garnet porphyroblasts observed in thin sections cut perpendicular to planar fabrics is the critical factor in defining the fabric-porphyroblast timing relationship.

Most schist samples contain two planar fabrics: an older fabric defined by compositional layers and grain size variation (S1, Fig. 3) and a younger foliation defined by the preferred orientation of planar minerals, primarily biotite and muscovite (S2, Fig. 3). In the southern part of the area, S2 is cut by third fabric, an S3 crenulation cleavage. Typically S1 and S2 are oblique to one another, but are locally approximately coplanar (locality 13 and 31 in Fig. 2). Garnet can be seen overgrowing the S1 compositional layers (Fig. 3c, d), indicating that garnet growth post-dated the development of S1. While S1 records compositional layering within the metasedimentary rocks, its nature and degree of deformation associated with metamorphism is uncertain and beyond the scope of this study.

The relationship between garnet and S2 in the Clarkia area (Fig. 2) varies from syntectonic, where garnet grew during the development of S2, to post-tectonic growth, where garnet grew after the development of S2. In the northwestern part of the Clarkia area, garnets typically have inclusion-poor cores and inclusion-rich rims. Grains of elongate quartz, muscovite and biotite that define S2 show a slight (Fig. 4a, b) to moderate (Fig. 4c, d) deflection around garnet grain boundaries. S2 grains do not form well-defined strain caps or strain shadows as is commonly observed with pre-tectonic garnet growth. On the basis of these observations, garnet is interpreted to be syntectonic with respect to S2. The lack of inclusion trails across the garnet interiors may indicate that early garnet growth pre-dated S2, while later garnet growth was syntectonic. The above relationships were observed in samples from outcrops 01, 02, 13, 14, and 31 in the northwestern Clarkia area (Fig. 2).

In contrast, garnet in samples from around Bechtel Butte in the southwestern Clarkia area (Fig. 2) shows a post-tectonic relationship to S2 and a pre-tectonic relationship to S3. Garnet in this area is thus referred to as inter-tectonic garnet. The critical relationships are best observed at locality 27 (Fig. 2) where S2 is subparallel to compositional layering (Fig. 3c, d). Grains that define the S2 foliation show negligible deflection around garnet grain boundaries and form inclusion trails across the garnet interiors (Fig. 3c, d) indicating that garnet grew after the development of S2. In the matrix, S2 is deformed by a poorly developed crenulation cleavage, S3, that is absent in the inclusion trails within the garnet (Fig. 3c, d); therefore, garnet growth is interpreted to have pre-dated development of S3. Relationships that define inter-tectonic garnet growth are observed at localities 03, 26, and 27.

Implications

The porphyroblast-fabric relationships defined above indicate that at least one phase of coeval deformation (S2) and metamorphism occurred in the Clarkia area of northern Idaho. Garnet with Lu-Hf ages of 1.2-1.0 Ga (Sha et al., Vervoort et al., 2005; Zirakparvar, 2007; Zirakparvar et al., 2010) appear syntectonic to post-tectonic with respect to S2, a regional penetrative deformational fabric that is accordingly interpreted to be Mesoproterozoic in age. Garnet in the southeastern part of the study area is pre-

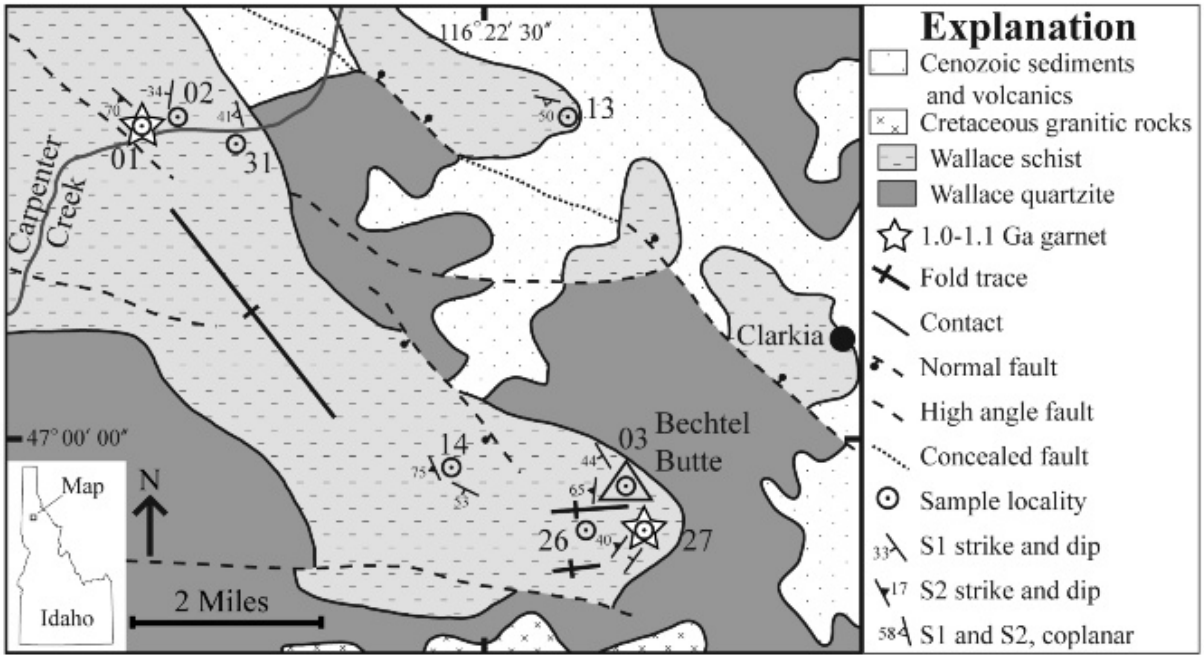

Figure 2: Geologic map of the Clarkia area showing sample locations and fabric orientations (this study) along with >1.0 Ga garnet localities from Zirakparvar (2007). Geology is modified after Lewis et al. (2000; 2005).

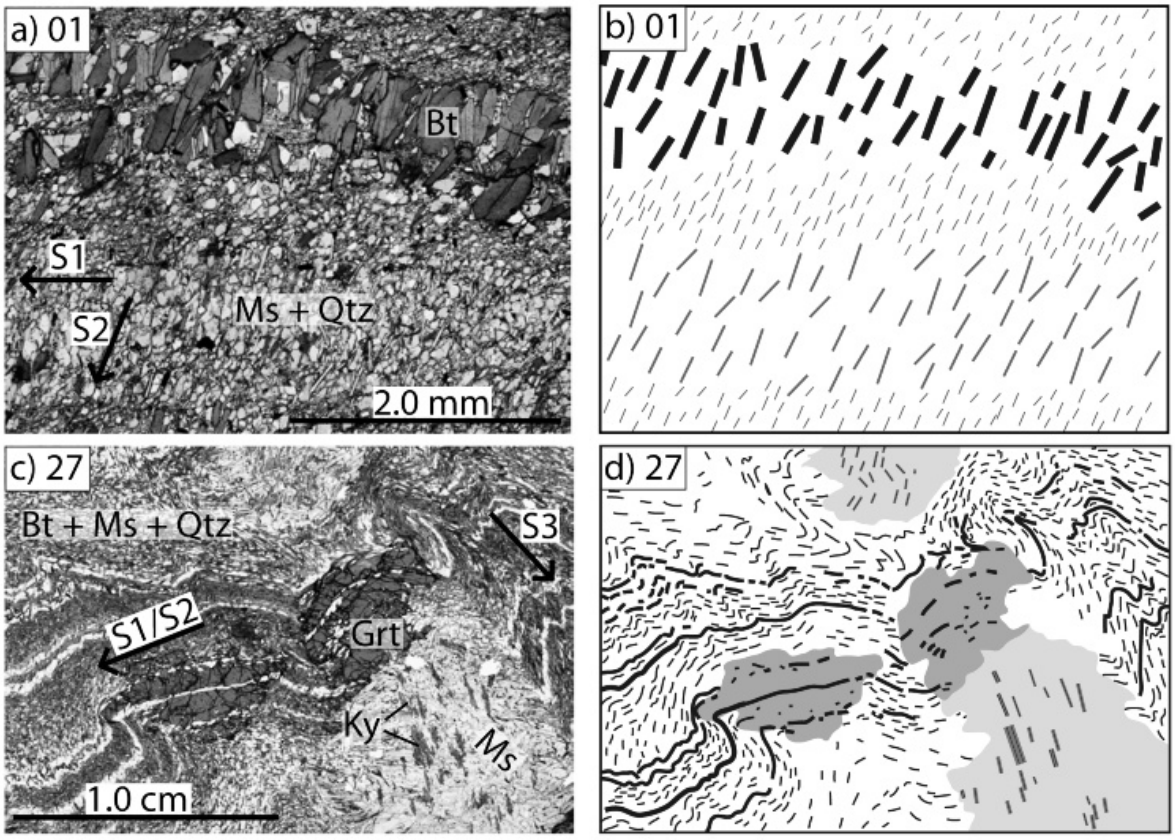

Figure 3: Plane polarized light (PPL) photomicrographs (a & c) and corresponding sketches (b & d) of Clarkia area fabrics. a-b) Horizontal compositional layering, S1, is oblique to a preferred mineral orientation, S2. c, d) S2 grains in the matrix are micro-scopically folded and show negligible deflection around garnet grain boundaries. S2 grains also form relatively undeformed inclusion trails across the garnet grain interior. Mineral Abbreviations: Bt-biotite, Grt-garnet, Ky-kyanite, Ms-muscovite, and Qtz-quartz. Numbers in the top left corner of each figure refer to localities on Fig. 2.

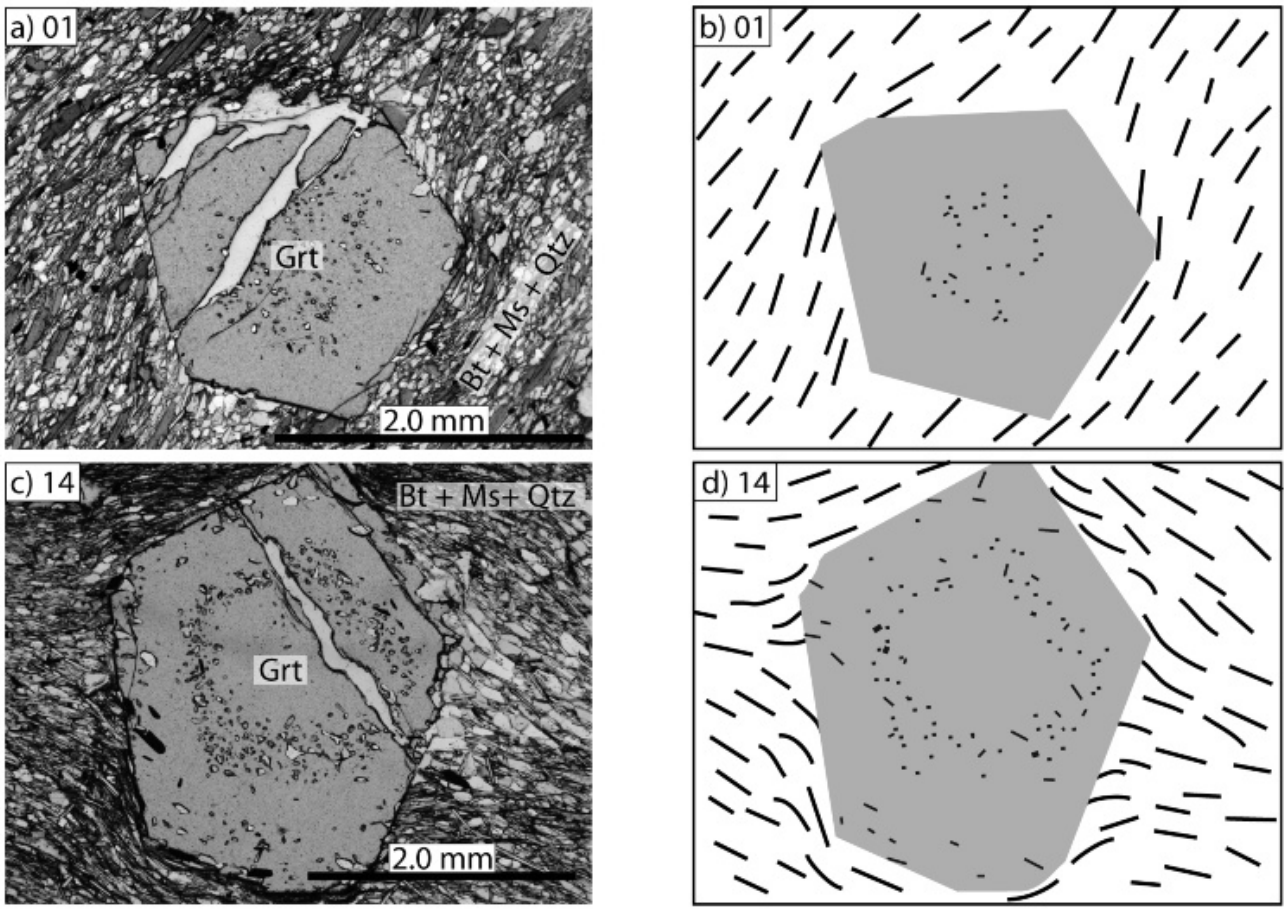

Figure 4: PPL photomicrographs (a & c) and corresponding sketches (b & d) show garnet porphyroblast-fabric relationships in the Clarkia area. a-d) S2 grains show slight (a, b) to moderate (c, d) deflection around, yet still trace into, garnet grain boundaries indicating that garnet growth was syntectonic with the development of S2 at these localities. Overall at locality 27, garnet is inter-tectonic, post-tectonic with respect to S2 and pre-tectonic to the microscopic folds. Mineral Abbreviations: Bt-biotite, Grt-garnet, Ms-muscovite, and Qtz-quartz. Numbers in the top left corner of each figure refer to localities on Fig. 2.

tectonic with respect to a poorly developed crenulation cleavage, S_3. This younger deformation is most likely either a late phase of Mesoproterozoic deformation or localized fabric associated with Cretaceous pluton emplacement. These observations indicate that northern Idaho was tectonically active during the Mesoproterozoic, but the extent and significance of such tectonism is still poorly defined.

Plate reconstructions of the Proterozoic supercontinent Rodinia generally rely on the correlation of approximately 1.1 Ga metamorphic belts found across continental blocks (e.g., Dalziel, 1991; Hoffman, 1991; Moores, 1991). Plate reconstructions of Rodinia have placed East Antarctica (Hoffman, 1991), Australia (Brookfield, 1993; Karlstrom et al., 2001), both East Antarctica and Australia (Dalziel, 1991), Siberia (Sears and Price, 1979, 2003), or the South China block (Li et al., 2008) next to western Laurentia. All of these scenarios portray the northwest Laurentian border as a tectonically passive margin with the Belt Supergroup lying within an intracratonic setting. Combining the textural evidence reported in this paper with the existing Lu-Hf geochronology (Sha et al., 2004; Vervoort et. al., 2005;

Zirakparvar, 2007; Zirakparvar et al., 2010), it is likely that northwest Laurentia was tectonically active during the formation of Rodinia, and may have been a collisional margin. Evidence for 1.2-1.0 Ga regional tectonism involving Belt Supergroup metasedimentary rocks of northern Idaho indicates that new reconstructions of Rodinia should incorporate western Laurentia as a piercing point that links Grenville-aged orogenic belts.

The coeval deformation with metamorphism at approximately 1.1 Ga observed in this study needs to be put in context with multiple metamorphic and deformation events documented by previous studies. In particular, two regional metamorphic events, M1 and M2, and a late stage retrograde metamorphism, M3, have been documented in the Snow Peak and Boehls Butte areas (Fig. 1; Lang and Rice, 1985a, b, c; Grover et al., 1992). Multiple phases of deformation defined by fold sets have been documented in these areas as well (Hietanen, 1963a, b). These observations in combination with the >100 My age span observed in the existing Lu-Hf garnet ages (Zirakparvar et al., in review) suggest that Proterozoic deformation and metamorphism may have been prolonged and have encompassed two or more metamorphic and deformational episodes. Additional Lu-Hf geochronology in conjunction with microstructural analysis is needed to document additional Proterozoic fabrics and metamorphic assemblages associated with regional Grenville-age tectonism along the Western Laurentian border.

Acknowledgements

Reed Lewis (Idaho State Geological Survey) and John Watkinson (Washington State University) provided valuable discussion with Nesheim while in the field. Funding for this project was provided by a Graduate Student Research Grant from the Geological Society of America, a field scholarship from the Tobacco Root Geological Society, and funds from the University of Iowa: Department of Geoscience, all awarded to Nesheim. Additional funding was provided by National Science Foundation grants EAR-0755392, Ear-0710939, and EAR-0711326 awarded to McClelland, Lang, and Vervoort, respectively.

References

Armstrong, R.L., Taubeneck, W.H., and Hales, P.O., 1977, Rb-Sr and K-Ar geochronometry of Mesozoic granitic rocks and their Sr isotopic composition, Oregon, Washington, and Idaho: Geological Society of America Bulletin, v. 88, p. 397-411.

Brookfield, M.E., 1993, Neoproterozoic Laurentia-Australia fit: Geology, v. 21, p. 683-686.

Dalziel, I.W.D., 1991, Pacific margins of Laurentia and East Antarctica as a conjugate rift pair: evidence and implications for an Eocambrian supercontinent: Geology, v. 19, p. 598-601.

Evans, K.V., Aleinikoff, J.N., Obradovich, J.D., and Fanning, C.M., 2000, SHRIMP U-Pb geochronology of volcanic rocks, Belt Supergroup, western Montana; evidence for rapid deposition of sedimentary strata: Canadian Journal of Earth Sciences, v. 37, p. 1287-1300.

Foster, D.A., and Fanning, C.M., 1997, Geochronology of the northern Idaho Batholith and the Bitterroot metamorphic core complex; magmatism preceding and contemporaneous with extension: Geological Society of America Bulletin, v. 109, p. 379-394.

Grover, T.W., Rice, J.M., and Carey, J.W., 1992, Petrology of aluminous schist in the Boehls Butte region of northern Idaho; phase equilibria and P-T evolution: American Journal of Science, v. 292, p. 474-507.

Gaschnig, R.M., Vervoort, J.D., Lewis, R., and McClelland, W., 2010, Migrating Magmatism in

the northern US Cordillera: in situ U-Pb geochronology of the Idaho batholith: Contributions to Mineralogy and Petrology, v. 159, no. 6, p. 863-883.

Hietanen, A.M., 1956, Kyanite, andalusite, and sillimanite in the schist in Boehls Butte Quadrangle, Idaho: American Mineralogist, v. 41, p. 1-27.

Hietanen, A., 1963a, Metamorphism of the Belt Series in the Elk River-Clarkia Area Idaho: United States Geological Survey Professional Paper 344-C, 49 p.

Hietanen, A., 1963b, Belt Series in the Region around Snow Peak and Mallard Peak, Idaho: United States Geological Survey Professional Paper 344-E, 34 p.

Hietanen, A., 1984, Geology along the northwest border zone of the Idaho Batholith, northern Idaho: United States Geological Survey Bulletin, p. 1-17.

Hodges, K.V., and Applegate, J.D., 1993, Age of Tertiary extension in the Bitterroot metamorphic core complex, Montana and Idaho: Geology, v. 21, p. 161-164.

Hoffman, P.F., 1991, Did the breakout of Laurentia turn Gondwanaland inside out?: Science, v. 252, p. 1409-1412.

House, M.A., and Hodges, K.V., 1994, Limits on the tectonic significance of rapid cooling events in extensional settings: Insights from the Bitterroot metamorphic core complex, Idaho-Montana: Geology, v. 22, p. 1007-1010.

Hyndman, D.W., 1983, The Idaho batholith and associated plutons, Idaho and western Montana: *in* Roddick, J.A., ed., Circum-Pacific plutonic terranes: Geological Society of America Memoir, v. 159, p. 213-240.

Karlstrom, K.E., Ahall, K.I., Harlan, S.S., Williams, M.L., McLelland, J., and Geissman, J.W., 2001, Long-lived (1.8-1.0 Ga) convergent orogen in southern Laurentia, its extensions to Australia and Baltica, and implications for refining Rodinia: Precambrian Research, v. 111, p. 5-30.

Lang, H.M., and Rice, J.M., 1985a, Regression modelling of metamorphic reactions in metapelites, Snow Peak, northern Idaho: Journal of Petrology, v. 26, p. 857-887.

Lang, H.M., and Rice, J.M., 1985b, Geothermometry, geobarometry and T-X(Fe-Mg) relations in metapelites, Snow Peak, northern Idaho: Journal of Petrology, v. 26, p. 889-924.

Lang, H.M., and Rice, J.M., 1985c, Metamorphism of pelitic rocks in the Snow Peak area, northern Idaho; sequence of events and regional implications: Geological Society of America Bulletin, v. 96, p. 731-736.

Lewis, R.S., Burmester, R.F., Kauffman, J.D., and Frost, T.P., 2000, Geologic Map of the St. Maries 30 x 60 Minute Quadrangle, Idaho: Idaho Geologic Survey.

Lewis, R.S., Bush, J.H., Burmester, R.F., Kauffman, J.D., Garwood, D.L., Myers, P.E., and Othberg, K.L., 2005, Geologic Map of the Potlatch 30 x 60 Minute Quadrangle, Idaho: Idaho Geologic Survey.

Lewis, R.S., Burmester, R.F., McFaddan, M.D., Kauffman, J.D., Doughty, P.T., Oakley, W.L., Frost, T.P., 2007, Geologic Map of the Headquarters 30 x 60 Minute Quadrangle, Idaho: Idaho Geologic Survey.

Link, P.K., Christie-Blick, N., Devlin, W.J., Elston, D.P., Horodyski, R.J., Levy, M., Miller, J., Pearson, R.C., Prave, A., Stewart, J.H., Winston, D., Wright, L.A., and Wrucke, C.T., 1993, Middle and late Proterozoic stratified rocks of the western U.S. Cordillera, Colorado Plateau, and Basin and Range Province: Precambrian: conterminous US: Geology of North America, v. C-2, Geological Society of America, p. 463-596.

Li, Z.X., Bogdanova, S.V., Collins, A.S., Davidson, A., De Waele, B., Ernst, R.E., Fitzsimons, I.C.W., Fuck, R.A., Gladkochub, D.P., Jacobs, J., Karlstrom, K.E., Lu, S., Natapov, L.M., Pease,

V., Pisarevsky, S.A., Thrane, K., Vernikovsky, V., 2008, Assembly, configuration, and break-up of Rodinia: A synthesis: Precambrian Research, v. 160, p. 179-210.

Moores, E.M., 1991, Southwest U.S.-East Antarctic (SWEAT) connection: a hypothesis: Geology, v. 19, p. 425-428.

Nesheim, T.O., 2009, Are 1.1 Ga deformational fabrics present in metasedimentary rocks of the Belt Supergroup in northern Idaho?: unpublished M.S. Thesis University of Iowa, 125 p.

Passchier, C.W., and Trouw, R.A.J., 2005, Micro-tectonics: Springer-Verlag Berlin Heidelberg, Germany, 366 p.

Sears, J.W., Price, R.A., 1978, The Siberian connection: a case for the Precambrian separation of the North American and Siberian cratons: Geology, v. 6, p. 267-270.

Sears, J.W., Price, R.A., 2003, Tightening the Siberian connection to western Laurentia: Geological Society of America Bulletin, v. 115, p. 943-953.

Sha, G.S., Vervoort, J.D., Watkinson, A.J., Doughty, P.T., Prytulak, J., Lee, R., and Larson, P.B., 2004, Geochronologic constraints on the tectonic evolution of the Boehls Butte-Clearwater Core Complex: Evidence from 1.01 Ga garnets: Geological Society of America Abstracts with Programs, v. 36, no. 72.

Vervoort, J.D., McClelland, W.C., Oldow, J.S., and Watkinson, A.J., 2005, Grenville age metamorphism on the western margin of Laurentia, northern Idaho: evidence from Lu-Hf garnet geochronology: Geological Society of America Abstracts with Programs, v. 37, p. 89.

Winston, D., 1978, Fluvial systems of the Precambrian Belt Supergroup, Montana and Idaho, U.S.A.: *in* Miall, A.D., ed., Fluvial sedimentology: Canadian Society of Petroleum Geologists Memoir 5, p. 343-359.

Winston, D., 2007, Revised stratigraphy and depositional history of the Helena and Wallace Formations, mid-Proterozoic Piegan Group, Belt Supergroup, Montana and Idaho, U.S.A.: *in* Link, P.K., and Lewis, R.S., eds., Proterozoic geology of western North America and Siberia: Society for Sedimentary Geology Special Publication 86, p. 65-100.

Zirakparvar, N.A., 2007, Lu-Hf Garnet geochronology of polymetamorphic assemblages on the western margin of Laurentia: Evidence for protracted history of deformation and metamorphism beginning in the Mesoproterozoic: unpublished M.S. Thesis, Washington State University, 117 p.

Zirakparvar, N., Vervoort, J., Lewis, R., and McClelland, W., 2010, Insights into the thermal evolution of the Belt-Purcell Basin: Evidence from Lu-Hf garnet geochronology: Canadian Journal of Earth Sciences, v. 47, no. 2, p. 161–179.

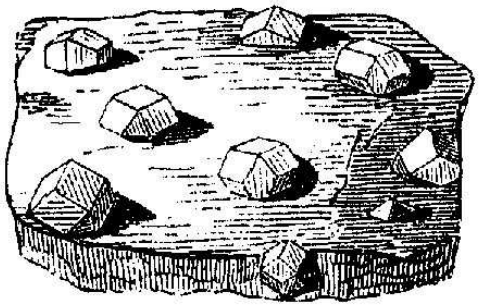

QUARTZITE OF ARGENTA, BEAVERHEAD COUNTY, MONTANA, REVISITED: DEFINITIVE EVIDENCE OF PRECAMBRIAN AGE INDICATES EDGE OF BELT BASIN

James W. Sears[1], Paul K. Link[2], Elizabeth A. Balgord[2], J. Brian Mahoney[3]
[1]University of Montana, Missoula MT; [2]Idaho State University, Pocatello ID;
[3]University of Wisconsin, Eau Claire WI

Introduction

In 2007 Sears and Link led a TRGS field trip to Argenta, Montana, to discuss the stratigraphic significance of a supermature, red quartz-arenite. The area is in the southern Pioneer Mountains (Fig. 1). We referred to this unit as the Quartzite of Argenta (Sears and Link 2007). It forms the walls of a small canyon along Rattlesnake Creek about 4 km west of the community of Argenta (see Stop 1 on p. 222 in the 2007 TRGS field guide and Fig. 2 in this paper). The unit is confined to the core of the Humbolt anticline, a hanging-wall anticline on the Ermont thrust (Fig. 3). The anticline plunges out to the south and passes to the north into the Pioneer batholith. The base of the quartzite does not crop out in the anticline, but the Cambrian WolseyShale stratigraphically overlies the quartzite on both flanks and on the south-plunging nose of the anticline, near Ermont.

Some of the field trip attendees held the opinion that the Quartzite of Argenta was a facies of the Cambrian Flathead Sandstone, and there was a discussion about possible Skolithus burrows at one outcrop on the nose of the anticline near Ermont (see Stop 5 in the 2007 TRGS field guide).

The consensus of the 30 field trip attendees was that stratigraphic assignment of the quartzite was inconclusive.

New evidence

Detrital Zircon Geochronology

Paul Link collected a specimen of the quartzite at Stop 1 (Sample 7PL09) for detrital zircon analysis and determined that the majority of the zircon grains formed a major Paleoproterozoic peak at 1882 Ma, with subordinate Archean grain-populations from 2770 to 2480 Ma. No zircons were younger than 1774 Ma (Fig. 4).

Figure 3 compares this detrital zircon 'barcode' with other Proterozoic and Cambrian quartzites in southwest Montana that could potentially be correlative with the Quartzite of Argenta (map locations on Fig. 1). The Argenta detrital-zircon populations (new data in this paper, see Table 2) match those of the early Mesoproterozoic Neihart Quartzite of the Little Belt Mountains of central Montana (data replotted from Ross and Villeneuve, 2003). This strongly suggests that the Argenta correlates with the Neihart (Mueller et al., 2003).

Missoula Group sandstones from Flint Creek Hill in the Pintlar Range (samples of Mt. Sheilds unit 2, Snowslip, and Bonner formations) have a major peak at 1744 Ma (data from samples 10, 11, and 12ES08; Stewart, 2009). Stewart et al. (in press) propose that the source area for the 1745 Ma peak was not the Yavapai and Mazatzal provinces far to the south as suggested by Link et al. (2007) and Sears (2007) but rather a more proximal area within the

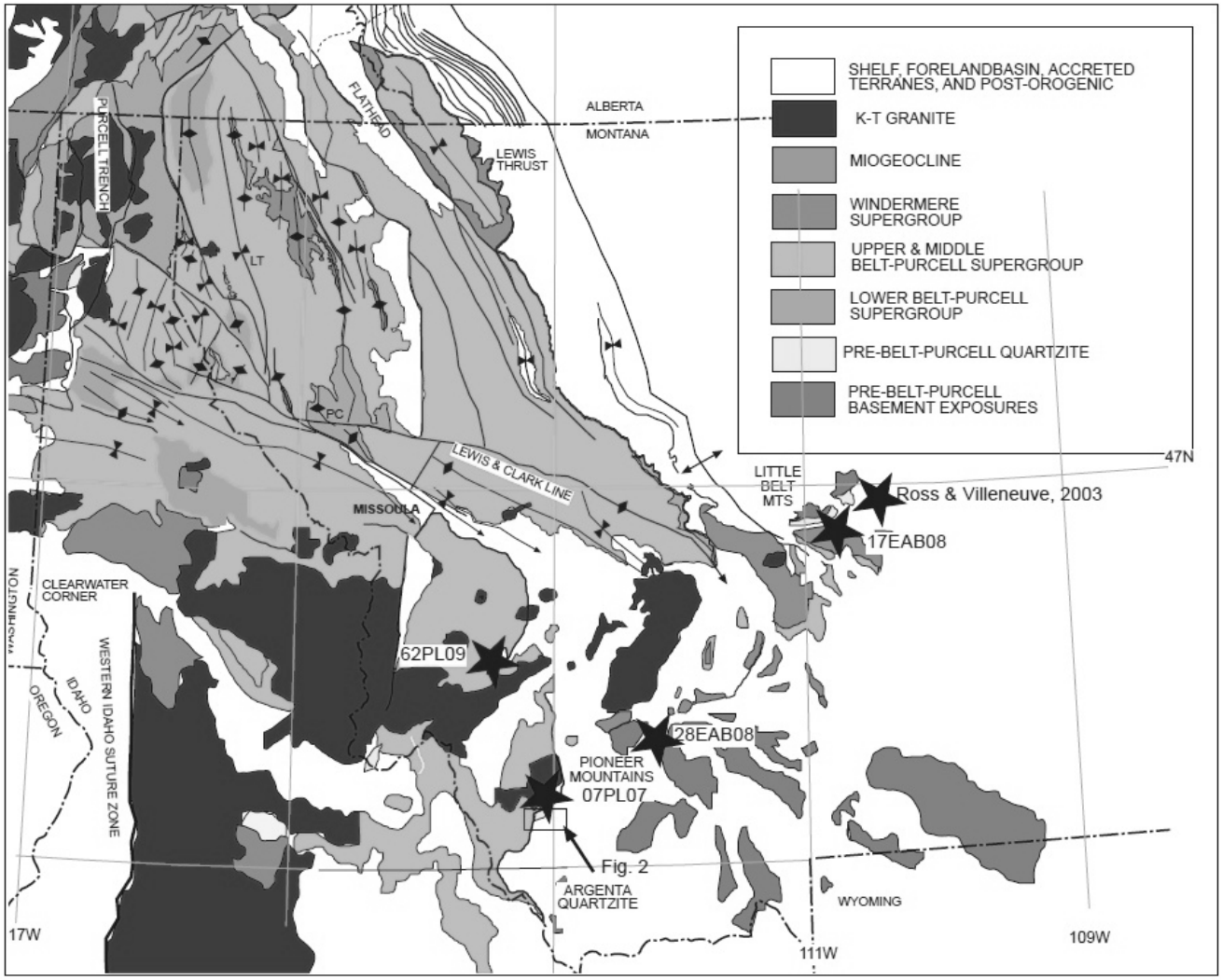

Figure 1. Map showing locations of detrital zircon samples presented in Figure 3. Area of Figure 2 in southern Pioneer Mountains shown by arrow.

northwest Mojave Province and/or a now-rifted fragment of proto-Rodinia.

Two samples of Cambrian Flathead Sandstone (28EAB09 overlying Archean basement in the Tobacco Root Mountains and 17EAB09 overlying Ravalli Group Spokane Formation in the Little Belt Mountains) and a sample of a black pebbly quartzite from the Cambrian Silver Hill unit (62PL09) in the Pintler Range all have a strong detrital-zircon peak at 1770 to 1790 Ma and few grains >1800 Ma (cf. Balgord et al., 2008; Balgord et al., in press). These new data are presented in Fig. 4. Data tables are available upon request from Paul Link. This ca 1780 Ma peak is at least 25 m.y. older than the 1745 Ma Missoula Group peak and perhaps 100 m.y. younger than the 1880 Ma Argenta Peak. The implications of these new data for regional Mesoproterozoic to Cambrian paleogeography are the subject of ongoing research by Mahoney, Link, and Balgord.

The lack of grains in the 1650 to 1780 Ma range in the Argenta unit suggests it had a completely distinct source area from the Missoula Group. This >1800 Ma source was proposed to be the Trans-Hudson province by Ross and Villeneuve (2003).

Geologic Mapping

In 2008, 2009, and 2010, Jim Sears designed mapping exercises for the University of Montana Geosciences Field Geology Course to define the map relations of the quartzite. The red quartzite (pCa1 on Figs. 2 and 3) was found to have an exposed thickness of ~150 m and to represent the lowest of three units that underlie the Cambrian Wolsey Shale. The red quartzite is overlain by a ~250-m thick section of rusty-weathering, light gray phyllite (pCa2) and by a second ~350-m thick, white quartzite unit (pCa3). Thus, the entire exposed section reaches ~750 m in thickness. The cross-section (Fig. 3) indicates that the entire pre-Wolsey section above the Ermont thrust, including the buried part, may exceed 1500 m. No *Skolithus* were observed.

The Wolsey Shale rests on the lower red quartzite along the east limb and nose of the anticline, but steps up through the section to the west to overlie the upper white quartzite on the west limb of the anticline (Fig. 3). Thus, the exposed Wolsey rests above a surface with 600 m of structural relief. The cross-section indicates that the Wolsey cuts out the entire quartzite section in the subsurface above the Ermont thrust and that the Wolsey may therefore cut out 1500 m of section. The mapping determined that the contact represents an angular unconformity beneath the Wolsey.

Locally, thin patches of Flathead sandstone and conglomerate are preserved between the Quartzite of Argenta and the Wolsey-Shale. On the east flank of the anticline, the Flathead conglomerate contains rounded pebbles of the underlying red quartzite, as well as coarse clasts of feldspar and vein quartz that suggest a nearby crystalline basement source.

The friable and brown Flathead sandstone contrasts with the recrystallized quartzite and phyllite of the underlying rock. Trilobite trails and worm burrows occur on Flathead sandstone lenses within green glauconitic shales. Over most of the anticline, however, the Flathead is missing, indicating that the older units formed a high ground that stood above the depositional edge of the Flathead, but was buried by the Woolsey. Similar relationships exist elsewhere in western Montana where the Cambrian buried quartzite hills of Precambrian rocks.

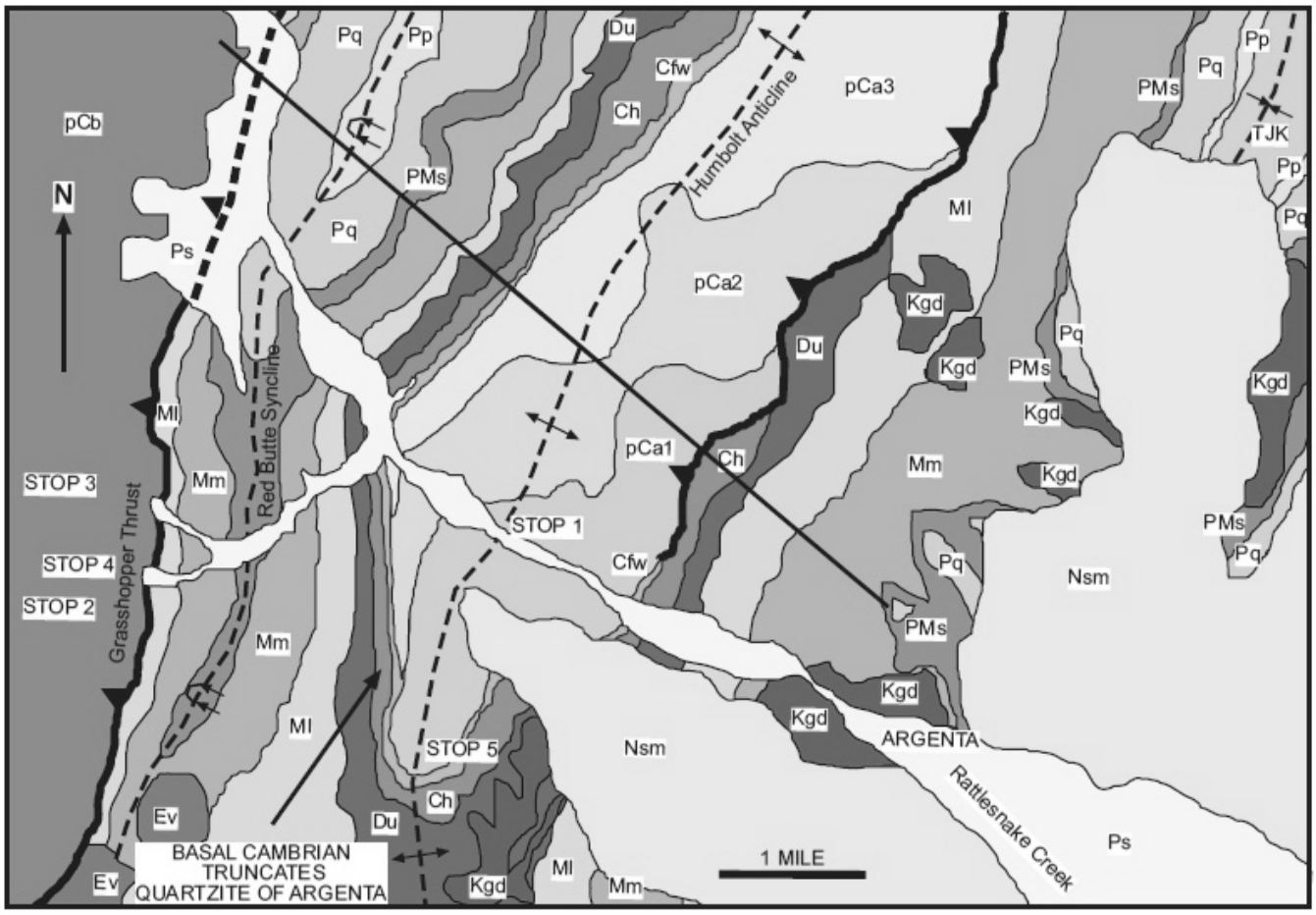

Figure 2. Geologic map of the Humbolt anticline and environs. After Thomas, 1981, Gonnerman, 1992, and mapping by Sears. Units: pCa1, pCa2, pCa3 - Quartzite of Argenta; pCb - Bonner; Cfw Flathead and Woolsey; Ch - Hasmark; Du - Jefferson and Three Forks; Ml - Lodgepole; Mm - Mission Canyon; PMs - Snowcrest; Pq - Quadrant; Pp - Phosphoria; TJK - Triassic, Jurassic, and Cretaceous strata undifferentiated; Kgd - granodiorite intrusives; Ev - Eocene volcanics; Nsm - Sixmile Creek; Ps - Pleistocene sediments. Black line - cross-section of Fig. 3.

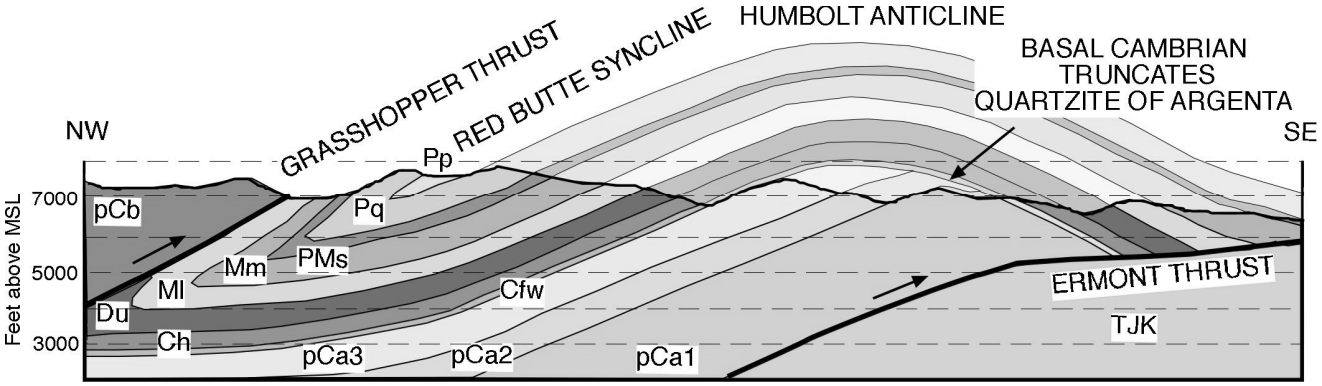

Figure 3. Geologic cross-section of Humbolt anticline, showing how the basal Cambrian (Cfw) truncates the Precambrian strata (pCa 1, 2, 3) from NW to SE. See Fig. 2 for location and symbols.

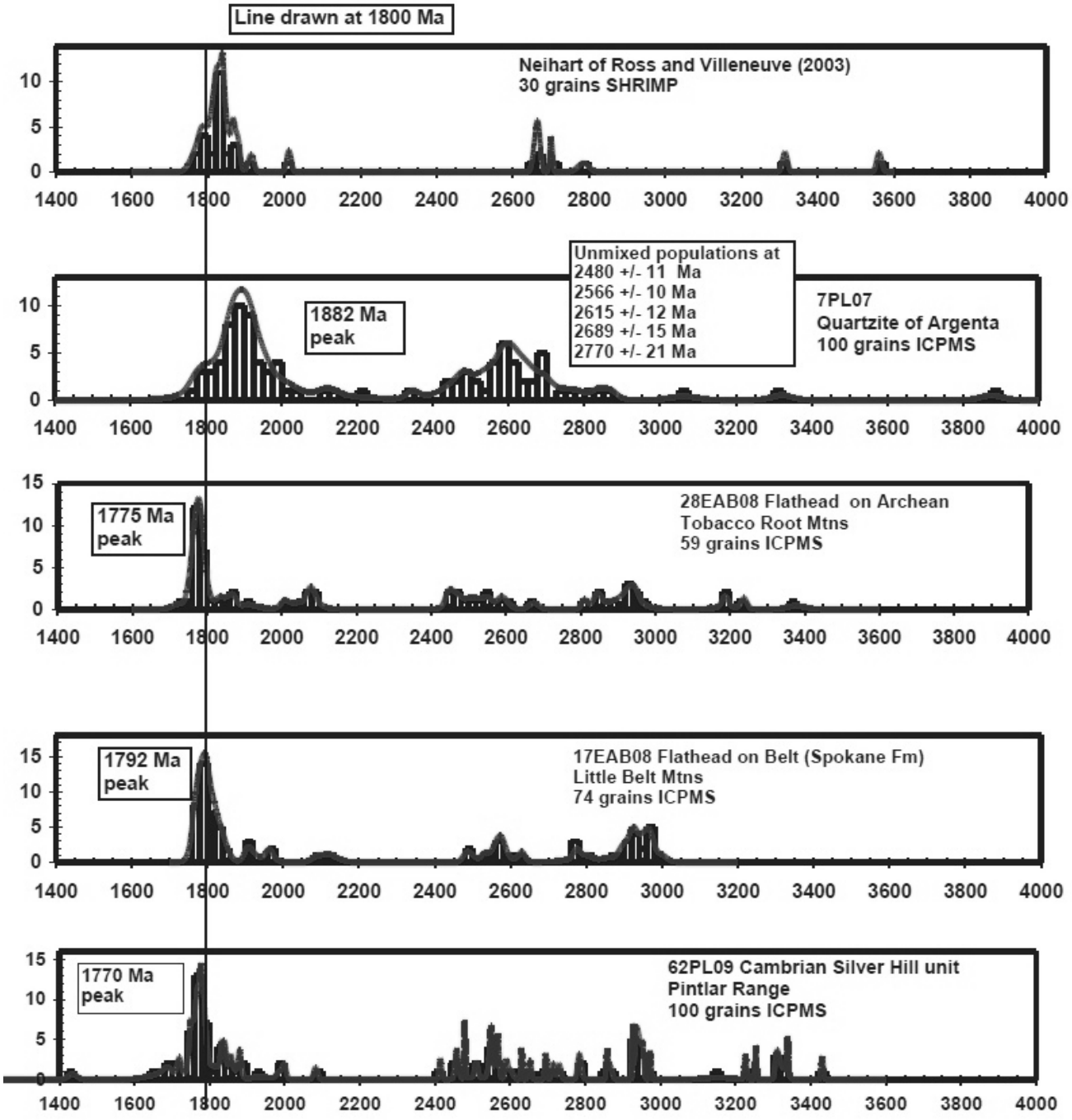

Figure 4. Detrital zircon histograms for Proterozoic and Cambrian quartzites from southern Montana. Locations of samples are shown in Fig. 1 and tabulated in Table 1. Data are from LA ICP MS at the University of Arizona or from SHRIMP at Australian National University, Canberra. From bottom to top the samples are A. Quartzite of Argenta (7PL07), B. Neihart Quartzite replotted from Ross and Villeneuve (2003); C. three samples of Missoula Group from Flint Creek Hill, Pintler Range (10, 11, 12ES08, data presented in Stewart et al., in press); D. Cambrian Flathead Sandstone, Tobacco Root Mountains (28EAB09); E. Cambrian Flathead Sandstone, Little Belt Mountains 17EAB09), and F. Cambrian Silver Hill unit, Pintler Range (60PL09).

	Locations for New Detrital Zircon Samples					
Flathead	28EAB08	12T 423930E	5065914N	NAD 27	45° 44' 33.3" N	111° 58' 40.4" W
Flathead	17EAB08	12T 494085E	5119564N	NAD 27	46° 13' 46.6" N	111° 4' 36.1" W
Argenta	07PL07	12T 350043E	5017806N	NAD 83	45° 17' 51.8" N	112° 54' 45.3" W
Silver Hill	62PL09	12T 314230E	5100675N	NAD 83	46° 02' 03.9" N	113° 24' 02.3" W

Table 1. GPS locations of samples presented in Figure 3.

We assign the Quartzite of Argenta to Precambrian age. We correlate the red quartzite unit (pCa1) with the Neihart Quartzite of the Little Belt Mountains on the basis of its purity, grain size, and detrital zircon signature. Link et al. (2007) have shown that most Belt quartzites are feldspathic and contain some detrital zircon grains younger than 1.6 Ga). The overlying phyllite (pCa2) and white quartzite (pCa3) are of uncertain assignment, and may be part of the Belt Supergroup.

Implications

If we flattened the Wolsey Shale, the underlying units would dip gently to the west. They may represent a west-tilted stratigraphic section at the east margin of the Belt basin onlapped by the Cambrian marine section. This pattern matches sections along the Rocky Mountain front in northern Montana and Alberta, where the Flathead steps down across the Belt Supergroup from west to east to directly overlie pre-Belt basement gneisses of Archean age in the subsurface of the foothills (Price and Mountjoy, 1970; Sears, 2007b).

A thin layer of Flathead Sandstone directly overlies Archean basement in the Armstead anticline, 25 km south of Ermont. The Flathead there contains angular clasts of fine grained red quartzite, as it does in the Humbolt anticline. The Armstead anticline occupies the next underlying thrust plate to the east of the Ermont thrust. Thus, the Precambrian quartzite pinches out from northwest to southeast.

Flathead Sandstone directly overlies pre-Belt basement in bore holes and all outcrops east of Argenta in the Ruby, Blacktail Deer, and Highland Mountains (Ruppel et al., 1981; O'Neill, 1997). Zen (1988) mapped Paleoproterozoic gneisses in the northern Pioneer Mountains. The Humbolt anticline may thus expose a rare section of the inverted east margin of the Belt basin.

We noted in the 2007 TRGS guidebook that the red quartzite stands in distinct contrast to the next exposures of Precambrian rock to the west, where the Bonner Formation of the Belt Supergroup overrides the Paleozoic section on the Grasshopper thrust (see Fig. 2 and 3). In this area, the Bonner comprises a thick, feldspathic, coarse-grained and locally conglomeratic sandstone (Winston, 1986). Its stratigraphic relationship to the Precambrian units of the Humbolt anticline remain undetermined.

This research was supported by NSF EAR 08-19884 to Link and NSF EAR 0911742 to Sears. Data tables are available upon request from Paul Link.

References cited

Balgord, E., Forgette, M., Mahoney, J.B., Ihinger, P., and Kimbrough, D., 2008, Redefinition of the Precambrian-Cambrian boundary in southwestern Montana: SEPM Annual Meeting, Abstract 152-5.

Balgord, E., Mahony, J.B., and Gingras, M.K., 2009, Detrital zircon evidence requires revision of Belt stratigraphy in southwestern Montana: GSA abstracts with programs, v. 41, no. 7, p. 590.

Gonnerman, H.M., 1992, An andesite-dacite stratovolcano within the Late Cretaceous Beaver-

head Group near Bannack, Montana: University of Montana B.S. thesis, 43 p.

Link, P.K., Fanning, C.M., Lund, K.I., and Aleinikoff, J.N., 2007, Detrital-zircon populations and provenance of Mesoproterozoic strata of east-central Idaho, USA: Correlation with the Belt Supergroup of southwest Montana: SEPM Special Publication 86, p. 101-128.

Meuller, P.R., Foster, D., Wooden, J., Mogk, D., and Lewis, R., 2003, Archean and Proterozoic sources for basal quartzites from the eastern and western margins of the Belt basin: Northwest Geology, v. 32, p. 215-216.

O'Neill, J.M., 1997, Stratigraphic character and structural setting of the Belt Supergroup in the Highland Mountains, southwestern Montana: *in* Berg, R.B., ed., Belt Symposium III: Montana Bureau of Mines and Geology, Special Publication 112, p. 12-16.

Price, R.A., and Mountjoy, E.W., 1970, Geologic structure of the Canadian Rocky Mountains between Bow and Athabasca Rivers: A progress report: *in* Wheeler, J.O., ed., Structure of the southern Canadian Cordillera: Geological Association of Canada, Special Publication 6, p. 7-25.

Ross, G.M., and Villeneuve, M., 2003, Provenance of the Mesoproterozoic (1.45 Ga) Belt basin (western North America): Another piece in the pre-Rodinia paleogeographic puzzle: Geological Society of America, Bulletin, v. 115, p. 1191-1217.

Ruppel, E.T., Wallace, C.A., Schmidt, R.G., and Lopez, D.A., 1981, Preliminary interpretation of the thrust belt in southwest and west-central Montana and east-central Idaho: *in* Tucker, T.E., ed., Field Conference and Symposium Guidebook to southwest Montana: Montana Geological Society, p. 139-159.

Sears, J.W., and Link, P.K., 2007, A field guide to the Quartzite of Argenta: Neihart Quartzite equivalent?, Northwest Geology, v. 36, p. 221-229.

Sears, J.W., 2007a, Rift destabilization of a Proterozoic epicontinental pediment: A model for the Belt-Purcell basin, North America: SEPM Special Publication 86, p. 55-64.

Sears, J.W., 2007b, Belt-Purcell basin: Keystone of the Rocky Mountain fold-and-thrust belt, United States and Canada: *in* Sears, J.W., Harms, T.A., and Evenchick, C.A., eds., Whence the Mountains? Inquiries into the Evolution of Orogenic Systems: A Volume in Honor of Raymond A. Price: GSA Special Paper 433, p. 147-166.

Stewart, E.D., Link, P., Fanning, C.M., Frost, C.D., and McCurry, M., 2009, Provenance of the upper Belt Supergroup and Lehmi Group: Constraints from Hf and Nd isotopes: GSA Abstracts with Programs, v. 41, no. 7, p. 687.

Stewart, 2010, Paleogeographic implications of non-North American sediment in the Mesoproterozoic upper Belt Supergroup and Lemhi Group, Idaho and Montana, USA: Geology.

Thomas, G.M., 1981, Structural geology of the Badger Pass area, southwest Montana: University of Montana M.S. thesis, 58 p.

Winston, D., 1986. Stratigraphic correlation and nomenclature of the Middle Proterozoic Belt Supergroup, Montana, Idaho, and Washington: *in* Roberts, S.M., ed., Belt Supergroup: Montana Bureau Mines and Geology Special Paper 94, 69-84.

Zen, E-an,1988, Bedrock geology of the Vipond Park 15-minute, Stine Mountain 7 1/2- minute, and Maurice Mountain 7 1/2 -minute quadrangles, Pioneer Mountains, Beaverhead County, Montana: U.S. Geological Survey, Bulletin 1625, 49 p.

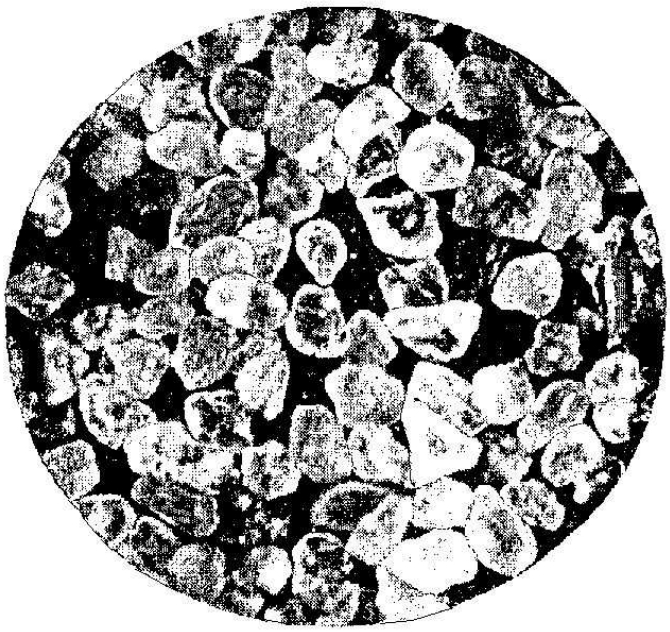

FRENCH GULCH PLACERS AND ANACONDA HOT SPRINGS, DEER LODGE COUNTY, MONTANA

Robin McCulloch and Katie McDonald
Montana Bureau of Mines and Geology, 1300 W. Park Street, Butte, MT 59701
Ted Antonioli
5907 Longview, Missoula, MT 59803

Introduction

The primary focus of this field trip will be visiting the historic French Gulch gold placer and lode deposits. We will hike approximately 3.6 miles (round trip) along a road to the mine and return through the placer workings. There will be a brief stop en route to French Gulch to look at the Anaconda Hot Springs travertine deposit which once was as extensive as the famous travertine deposits at Mammoth Hot Springs in Yellowstone National Park. Lunch will be at the Mule Ranch vista which provides panoramic views of the Anaconda Range and Pioneer Mountains and an ideal spot for an overview of regional geology. The location of the field trip stops is shown in Figure 1.

Road Log Miles

0.0 Miles Leave Anaconda High school, driving northward on Main Street.

0.3 Right on Park Street (Montana Highway 1).

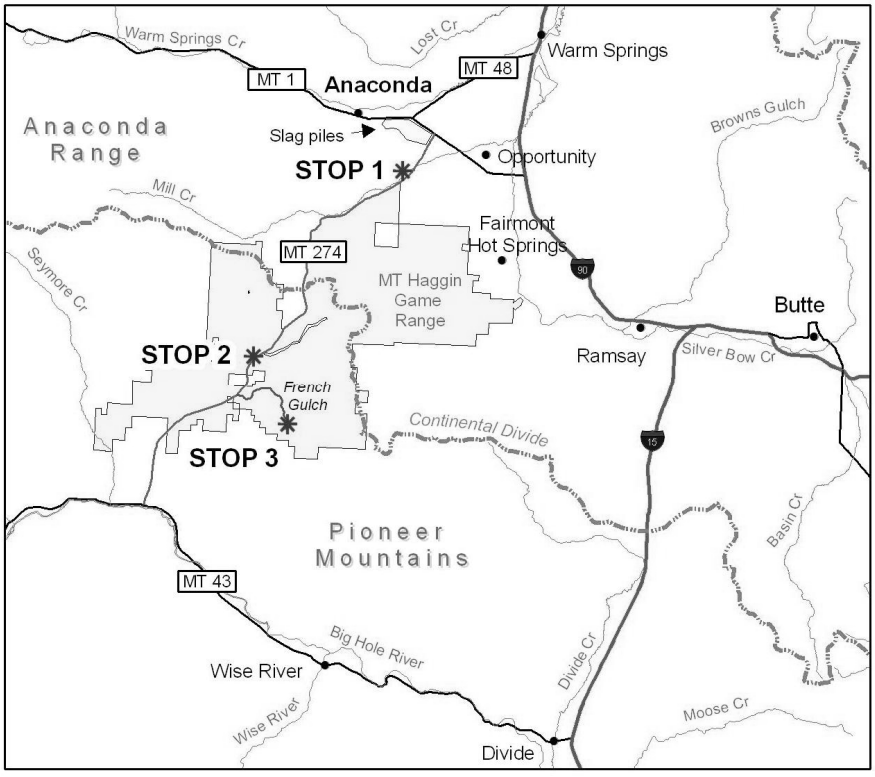

Figure 1. Road log route map showing field trip stops.

1.8 Original Anaconda Smelter (Old Works) was located on foothills to the left. This site has been partly converted into the Old Works Golf Course by BP/Arco, the successors to the Anaconda Company. The 1970's era buildings to the left are what remains of the Arbiter smelter, a hydrometallurical facility to process copper concentrates. High energy consumption meant that the process was never commercially successful. To the right are the black slag piles that were a waste product of the Anaconda smelter, an integrated pyrometallurgical facility located beneath the smelter stack. Copper slabs pro-

duced in the smelter were not quite pure enough for use in wire or pipe, so the slabs were shipped to Great Falls for electrowinning. The facility also produced various metal byproducts, and sulfuric acid from scrubbers. At various times, the acid was combined onsite with phosphate ore to produce fertilizer, or shipped to Butte to be used to leach low grade copper ore.

4.1 Turn right onto Hwy 274 toward Wisdom. The light colored waste material to the right is tailings from a large concentrator which processed raw ore from Butte until the construction of the current concentrating facility in Butte, which is still processing approximately 60,000 ore tons per day from the Continental pit.

4.7 Road to right is the main access for contractors who are reclaiming the smelter site.

5.6 Turn to right onto a dirt road. Please note this is private property owned by Arco. TRGS has been given advanced permission to visit this site.

STOP 1

7.9 STOP 1. Parking area for Anaconda Hot Springs deposit.

The following description is excerpted from Weed, W. H. (1904) **Economic value of hot springs and hot-spring deposits**. U.S. Geological Survey Bulletin 260, pages 598-604:

"THE LIMONITE AND TRAVERTINE DEPOSITS OF THE ANACONDA HOT SPRINGS, MONTANA.

For a number of years the limonite deposits found on the foothills between Mill Creek and the city of Anaconda were quarried and the ore shipped to the East Helena smelter. In 1902 the property was investigated by Mr. H. V. Winchell, chief geologist of the Anaconda Copper Company. He kindly took the writer over to see the property, and called attention to its unique character. It is now owned by and forms an important source of flux for the Washoe copper smelter, which lies but a half mile or so to the north.

The Anaconda Hot Springs are three miles from Anaconda, on the hillside south of the great Washoe smelting plant and west of the Deer Lodge Valley. The area of former and existing hot-spring action covers the slope north of Mill Creek and west of the main valley, the old travertine terraces of this place being formerly as extensive as the famous ones of the Mammoth Hot Springs of the Yellowstone Park. Prolonged degradation has removed the larger part of the Anaconda deposit and destroyed all the terracing. The underlying rocks are tilted Mesozoic limestones, which are probably of Jurassic age, but which have not been identified by fossils. Their eroded surface is covered by rhyolitic tuffs, on which the travertine cap was laid down.

The existing waters are tepid, inert, and feebly charged, and are incapable of adding to the great deposit of travertine that once covered the slopes. Several old cones still exist, and from an isolated one to the northwest of the main area a small quantity of warm water overflows. There is another cone to the extreme southwest, but the main outflow is from the open quarries and underground workings, where a deposit of limonite is extracted for a flux.

This limonite deposit is extensive, covering many acres. It comes to the surface in some places, but elsewhere lies beneath the travertine sheet, of which it is clearly a replacement formed by the existing springs.

The travertine has the surficial aspect of an ordinary limestone. Even in the cuts along the switch line to the new smelter, where 20 feet of curved and platy superimposed sheets of calcareous tufa are exposed, the travertine is easily mistaken for limestone unless compared with the similar old deposits of the Yellowstone Park. Aside from the water-filled cone just

noted, there are no recent deposits to give a clue to its origin. The old basins and terraces are gone, soil and vegetation cover a large part of the area, and the travertine is no longer loose, and friable, but hard and dense, though in part still porous.

The chief economic interest lies in the iron ore. The existing waters are distinctly ferruginous and are warm (100°±). They deposit limonite in their channels and in the drainage trenches, and are evidently replacing the travertine by limonite (not siderite) at a depth of 10 to 20 feet below the surface. The limonite not only forms a sheet, but sac-shaped masses, prongs, and tongues project into the travertine along joint cracks, etc. This ore is very low in silica, carries 2% or more of lime (gradations to travertine being, of course, common), and, according to assays, often carries from 50 cents to $1.50 in gold per ton. It is the chief source of flux for the great Washoe copper smelter."

Return to Hwy 274. Reset odometer and turn right. Proceed 11.8 miles up Mill Creek and over the Continental Divide.

11.8 (if you reset your odometer) STOP 2. Turn right to the Mule Ranch vista where we will eat lunch and have a brief discussion of the regional geology.

STOP 2

Mule Ranch Vista

The Mule Ranch vista provides beautiful panoramic views of the Anaconda Range to the west and the northern Pioneer Mountains to the east. The high peaks of the Anaconda Range are mostly underlain by Tertiary and Cretaceous intrusive rocks and metamorphosed Neoproterozoic Belt Supergroup rocks. The lower hills consist of unmetamorphosed sedimentary rock, volcanic rock, and unconsolidated valley fill deposits. The trace of the low-angle Anaconda Detachment fault approximately parallels the mountain front and separates lineated and mylonitic footwall rocks to the west from mostly strongly brecciated and broken hanging wall rocks to the east (O'Neill and others, 2004; Kalakay and Lonn, 2002; Kalakay and others, 2003; O'Neill and Lageson, 2003).

East of the vista are the Pioneer Mountains. The higher talus-covered peaks along the continental divide are underlain by Paleozoic and Neoproterozoic rocks that have been thrust eastward over Cretaceous rock along the regional Johnson thrust fault. The Johnson thrust marks the eastern edge of the Grasshopper thrust plate that underlies Pioneer Mountains in southwest Montana. (Ruppel and others, 1981).The lower hills to the north and south are underlain by rhyolite and dacite of the Tertiary Lowland Creek volcanics, granodiorite related to the Pioneer batholith, and some Paleozoic and Mesozoic sedimentary rock. Extensive aprons of colluvium blanket the west-facing slopes and isolated outcrops of sedimentary bedrock are typically very brecciated.

A number of northeast trending faults cut the Johnson thrust and appear to have been important in localizing mineral deposits, such as the Beal Mountain deposit to the west. Ruppel and others (1990) and Lewis (1998) compiled regional geologic maps for this area. Larger scale mapping in the north end of the Pioneer Mountains was completed by Moore (1956), Noel (1956), Lewis (1990), and McDonald (in review).

Get back on Highway 274 and proceed south 1.1 miles to French Gulch road which bears off to the left.

13.0 Turn left onto dirt road and travel approximately 1.2 miles for parking and vehicle turn around. The road narrows and is gated 0.3 miles ahead so parking is very limited beyond this point.

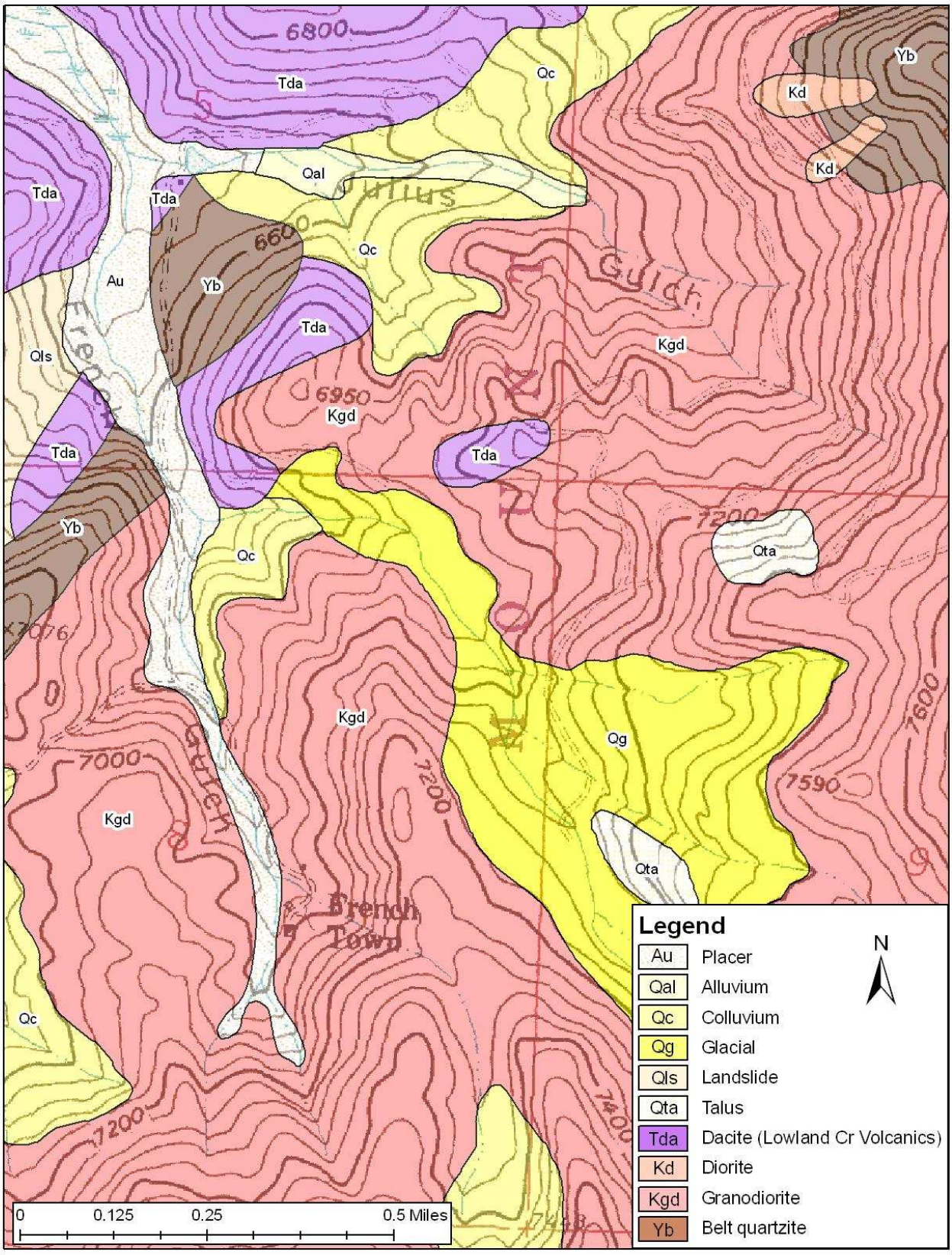

Figure 2. Geologic map of French Gulch (modified from Lewis, 1990).

STOP 3 13.2 STOP 3. Walking tour of French Gulch site begins here. We will proceed up the Gulch, to look at the placer deposits and continue to the hard rock mining area near the head of the gulch. We will cross one small stream where the culvert has washed out. Round trip distance is approximately 3.6 miles. At the end of the trip return to Anaconda by the same route.

French Gulch Geology Overview

The geology of French Gulch is shown in Figure 2. The lower part of the gulch is underlain by dacite flows and autobreccias of the Eocene Lowland Creek volcanics. Some of the dacite is scoriacious. South of Julius Gulch, bedrock is dominated by Cretaceous granodiorite associated with the Pioneer batholith. Isolated outcrops of Belt quartzite (Bonner formation) occur as roof pendants above the granodiorite. Glacial and surficial deposits occur along the slopes and in drainage bottoms. Historic placer and other mine workings (Figure 3) are found throughout the drainage.

Mining and Mineralization

The French Gulch mines and placers produced between $5,000,000 and $9,000,000 in gold between 1864 (discovery date) and 1925. The period from 1865 to 1880 was dominated by approximately 1,000 small-scale placer miners ground sluicing gravels in the drainage. By 1898 the claims were consolidated by William A. Allen. Old buildings, mine dumps, and other artifacts of past mining activity are still evident along the drainage.

In the lower part of the drainage, to the south of the road, Allen put in a Risdon Iron Worker bucket line dredge (Postlewaite type) outfitted with a 3.5-cubic-yard bucket and 16 Evans shaking tables, capable of 1,800 cubic yards per day production. This selection indicates that the gold was predominantly smaller than 10 mesh. Bedrock averaged 15-18 feet below ground surface. Bench gravels are visible along the road as it descends into the drainage. Some of these gravels were worked using an Evans hydraulic elevator, which was an educer or suction dredge similar to those used by hobbyists today.

Locked Gate, Start of walking tour:

Bedrock exposed along the road is dacite of the Lowland Creek volcanics, alluvium in the drainages formed the placer deposits. Several different types of placer deposits can be identified along the road. In the drainage bottom, the placer was in the stream alluvium and formed a transport deposit type. About a quarter mile upstream, a small alluvial fan type deposit formed at the mouth of the side drainage to the right (south) when the gold-bearing gravels were flushed out of the canyon. The extensive boulder piles along the drainage were stacked with a steam derrick and the fines were transported out with bedrock flumes. Note the increase in size and volume of the boulders upstream. In

Figure 3. Photograph showing historic placer piles along French Gulch. Placer mining began in 1864 and continued until around 1940.

general, the larger rocks were accompanied by larger nuggets, some up to 2 ounces each.

Stream crossing and junction with Julius Gulch:

Bedrock on the east side of the road along this part of the road is quartzite and diorite (Figure 2) that occurs mostly as float. An old fireplace and chimney and a small mine dump are visible along the road. In the drainage bottom, the many piles of stacked rock occupy the main pit that was the site of the most extensive placer mining (Figure 4). Near the upstream end of the pit, some unmined gravels remain and are bisected by a sluice-way built of stacked boulders. The current stream flows in the sluice-way. Quartzite bedrock is exposed just below the sluice in the pit floor.

Above the pit, the canyon is underlain mostly by granodiorite which intruded the Mesoproterozoic Bonner quartzite. Only isolated remnants of the quartzite remain. The gold-bearing veins occur in the granodiorite, near the contact with the overlying quartzite. The volume and richness of the placer is due to the stream eroding close to the quartzite contact. If the erosion had cut deeper into the granodiorite, the placer deposit would be further downstream and more deeply buried. Continuing upstream, the placer becomes a gulch placer. The boulders are large and an-

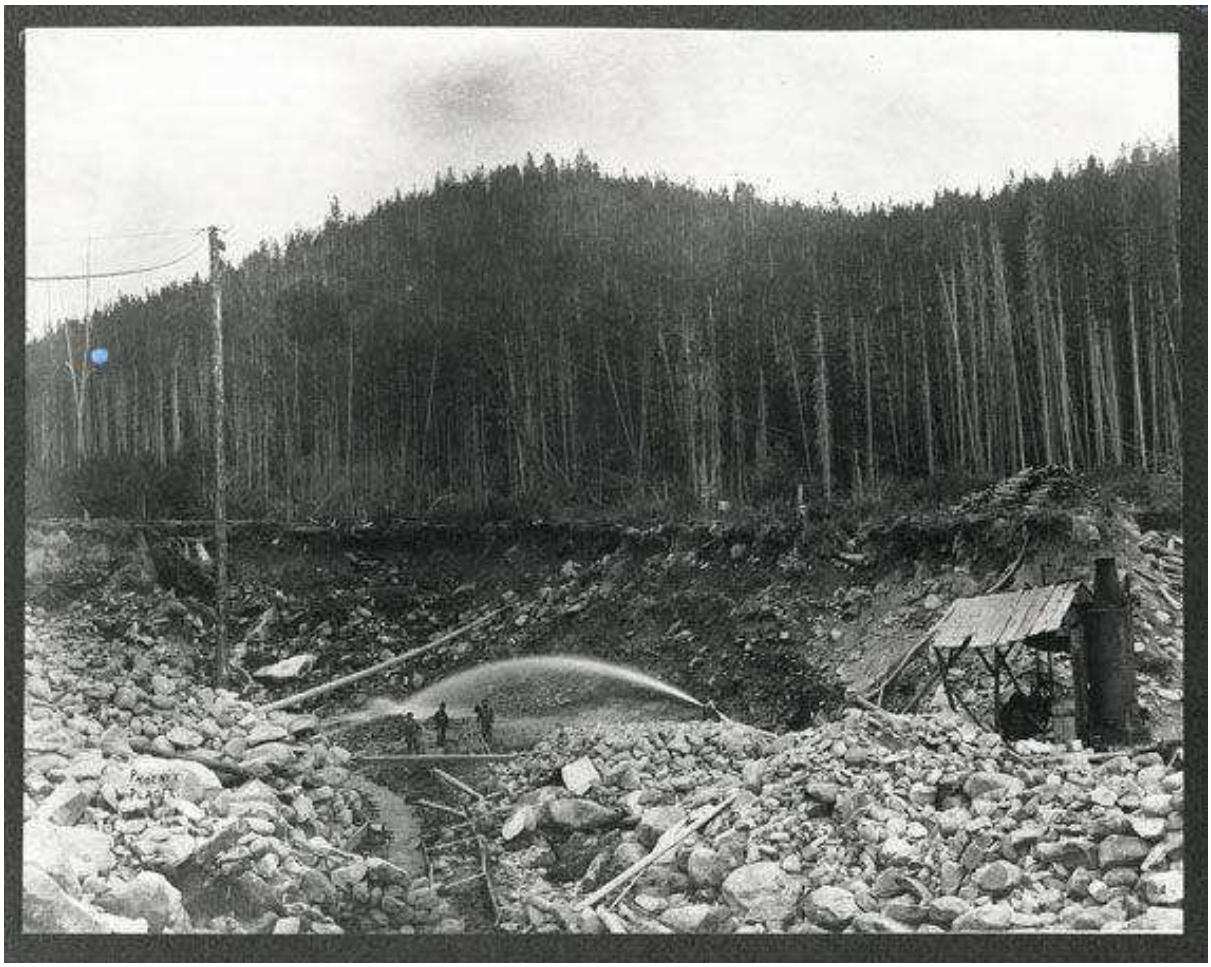

Figure 4. Photograph of historic hydraulic mining in French Gulch (photo courtesy of Archives and Special Collection, Mansfield Library, The University of Montana-Missoula).

gular. The workings all indicate ground sluicing methods. Several old ditches remain that provided water for sluicing.

Lode Mine and Camp:

Continue south up the road to the lode mine. The lode deposit was discovered during placer operations and drifts appear to follow structures. As reserves were exhausted, a shaft was sunk to continue following the structure. Samples from the dump indicate that the last ore encountered was sulfidic and mining ceased in 1925. It wasn't until 1928 that flotation methods were developed that would have allowed recovery of the gold from sulfidic ore.

Further upstream from the lode mine, placer mining of colluvial deposits continued up to the point where the ditches were cut in the hillside. Old reports indicate that values diminished south of the mine.

Old patent maps indicate the lode structures conform to a regional northeast and northwest stress pattern. One intersection of the two trends occurs in the main pit where an inclined shaft was sunk southward at an angle of 60°-70°. A similar intersection is indicated near the lode mine at the south end of the drainage. Early reports document a gold-bearing structure striking a southerly direction with a width of 300 to 600 feet. One author lists the host rock as aplite, another as quartzite. Shafts into these structures were approximately 100 feet deep with approximately 4,500 feet of total underground workings. Reported grades were 1 to 1.3 oz Au/ton. Underground maps and assays were lost in a fire in 1925.

References

Kalakay, T.J., and Lonn, J.D., 2002, Geometric and kinematic relationships between high-temperature and low-temperature faulting in the Anaconda detachment zone, southwest Montana: Geological Society of America Abstracts with Programs, v. 34, no. 6.

Kalakay, T.J., Foster, D.A., and Thomas, R.C., 2003, Geometry and timing of deformation in the Anaconda extensional terrane, west-central Montana: Northwest Geology, v. 32, p. 124- 133.

Lewis, S.E., 1990, Geologic map of the Dickie Peak quadrangle, Deer Lodge and Silver Bow counties, Montana: Montana Bureau of Mines and Geology Geologic Map 51, 6 p., 1 sheet, 1:24,000.

Lewis, R.S., compiler, 1998, Geologic map of the Butte 1 x 2 degree quadrangle: Montana Bureau of Mines and Geology Open File Report 363, 16 p., 1 sheet, 1:250,000.

Moore, G.T., 1956, The geology of the Mount Fleecer area, Montana: Bloomington, Indiana University, Ph.D. dissertation, 88 p.

McDonald, Catherine, *in review* 2010, Revised geologic map of the Dickie Peak quadrangle, Deer Lodge and Silver Bow counties, Montana: Montana Bureau of Mines and Geology, 1 sheet, 1:24,000.

Noel, J.A., 1956, The geology of the east end of the Anaconda Range and adjacent areas, Montana: Bloomington, Indiana University, Ph.D. dissertation, 74 p.

O'Neill, J.M., and Lageson, D.R., 2003, West to east geologic road log: Paleogene Anaconda metamorphic core complex: Georgetown Lake Dam – Anaconda – Big Hole Valley: Northwest Geology, v. 32, p. 29-46.

O'Neill, J.M., Lonn, J.D., Lageson, D.R., and Kunk, M.J., 2004, Early Tertiary Anaconda metamorphic core complex, southwestern Montana: Canadian Journal of Earth Science, v. 41, p. 63-72.

Ruppel, E.T., O'Neill, J.M., and Lopez, D.A., 1993, Geologic map of the Dillon 1 x 2 degree quadrangle, Montana and Idaho: U.S. Geological Survey Miscellaneous Geologic Investigation Map I-1803-H, 1 sheet, 1:250,000.

Ruppel, E. T., Wallace, C.A., Schmidt, R.G., and Lopez, D.A., 1981, Preliminary interpretation of the Thrust Belt in southwest and west-central Montana and east central Idaho: Montana Geological Society Field Conference and Symposium, Southwest Montana, p. 139-159.

CRETACEOUS STRUCTURES AND MINERALIZATION IN THE FOOTWALL OF THE EOCENE ANACONDA DETACHMENT FAULT, MONTANA: A FIELD TRIP ALONG WARM SPRINGS CREEK

Jeff Lonn
Montana Bureau of Mines and Geology, Montana Tech, 1300 W. Park Street, Butte, MT 59701
jlonn@mtech.edu

Larry Johnson
Missoula, Montana, 59801

This half-day field trip will take us west of Anaconda (Figure 1) into the structurally complex footwall of the Anaconda detachment fault to view mineralized structures of uncertain age, Cretaceous structures that affect the lower Paleozoic section, and the great unconformity. It includes one hike of about 2 miles that climbs 200 feet up a steep talus slope and traverses a wide but exposed ledge covered with loose rock.

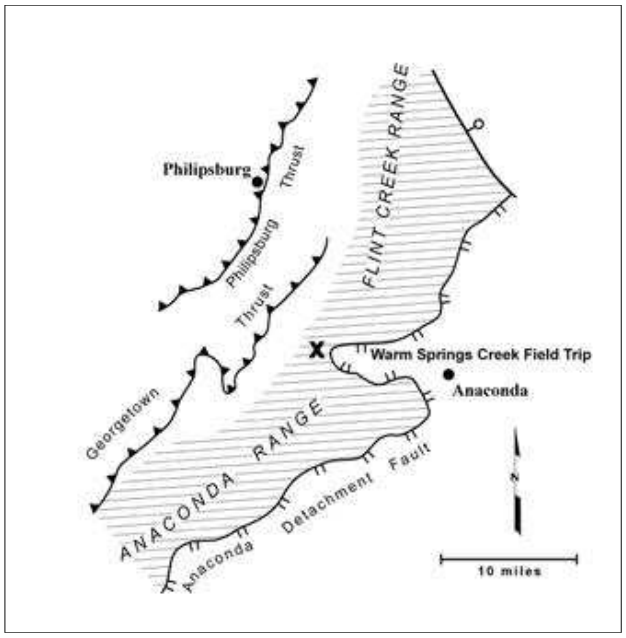

Fig. 1. Location of the field trip area with respect to major tectonic features of the Anaconda area. Hachured area contains amphibolite-grade metamorphic rocks.

Geologic setting

The eastern flanks of the Flint Creek Range and Anaconda Mountains are defined by the Eocene, top-east Anaconda detachment (low-angle normal) fault, the mylonitic core-bounding fault of the Anaconda metamorphic core complex (O'Neill and others, 2002, 2004). In its footwall are complexly folded, greenschist- to amphibolite-facies, Mesoproterozoic to Mesozoic metasedimentary rocks intruded by numerous plutons ranging in age from about 80 to 50 Ma. Metamorphic grade decreases westward from the Anaconda detachment, and near the northwestern side of the ranges, a major east-directed thrust system, the >78 Ma Georgetown-Philipsburg thrust system, is exposed. Emmons and Calkins (1913) were the first to note all of these features, including the Anaconda detachment fault that they compared to the "great Bitterroot fault", another core-bounding detachment fault located 60 miles to the west.

Metamorphism in the footwall occurred during a period of Cretaceous intrusion and crustal thickening produced by faults like the Georgetown thrust prior to 75 Ma. The deepest structural levels exposed by the Anaconda detachment fault, in the southeastern Anaconda Range, contain kyanite (Kalakay and others, 2003; Grice, 2006), indicative of a higher pressure metamorphic

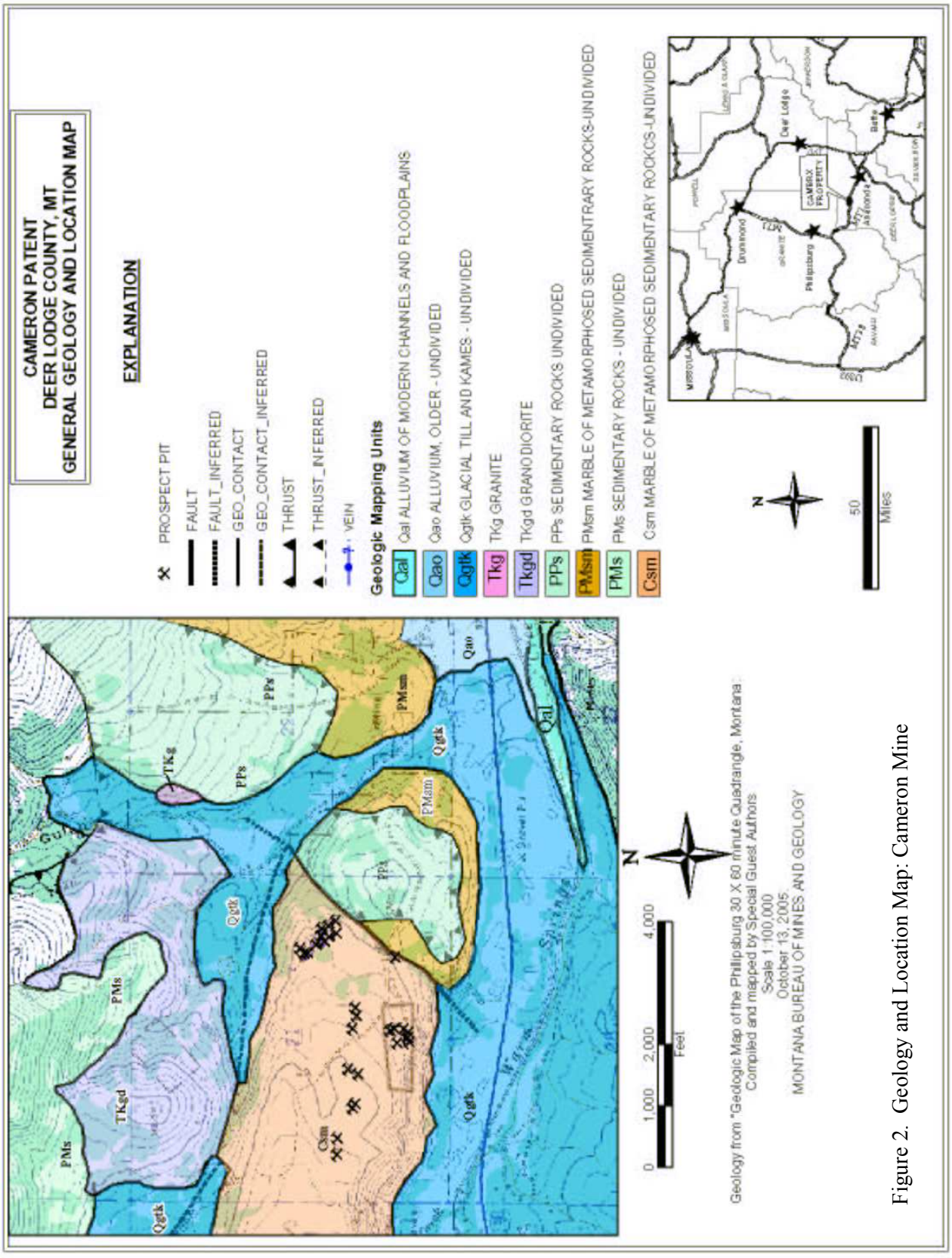

Figure 2. Geology and Location Map: Cameron Mine

event that was overprinted by high temperature-low pressure metamorphism from about 80-75 Ma (Stuart, 1966; Grice and others, 2004, 2005; Grice, 2006; Haney, 2008).

During the high temperature metamorphism, the still flat-lying 40,000-foot-thick Mesoproterozoic through Mesozoic section was tectonically thinned by an array of bedding parallel structures that include concordant mylonitic shear zones that cut out stratigraphic section, zones of vertical shortening that flatten the units through plastic flow, and brittle bedding-parallel faults that place younger units over older units. These structures are cut by plutons as old as 75 Ma; older intrusions were deformed along with the country rocks and developed strain fabrics parallel to them (Hawley, 1974; Desmarais, 1983; Grice and others, 2005; Grice, 2006). Because these bedding-parallel structures always omit stratigraphic section and occur throughout the entire 40,000-foot-thick sedimentary sequence, they have been attributed to a period of late Cretaceous synorogenic extension in the Sevier hinterland (Lonn and McDonald, 2004a,b; Lonn and Lewis, 2009) rather than to deformation along thrust faults.

Soon after the extensional period, tight, overturned, NNE-trending, *west*-verging folds formed; many in the structurally deep eastern parts of the Flint Creek and Anaconda Ranges are recumbent. These have been further deformed by open, upright NNE-trending folds. Voluminous plutonism also occurred between 80 and 50 Ma.

The top-east-southeast Anaconda detachment fault was active from 53 Ma to about 38 Ma, and exhumes the eastern part of the footwall from depths of 12-18 km (Grice and others, 2005; Grice, 2006; Foster and others, 2007). However, the Cretaceous extension described above may have been responsible for some of the exhumation.

The Field Trip

0.0 Anaconda High School. Exit the school parking lots and turn north on Main Street

0.3 Turn left/west on Commercial (MT Highway 1)

5.9 Entrance to quarries on right. Note that the rocks in this area are extremely brecciated as a result of their location in the immediate hanging wall of the Anaconda detachment fault. The quarries are developed in Madison limestone caught between two strands of the detachment.

6.6 Olson Gulch Road – the flat-topped mesa coming into view on the right is part of the lower plate of the Anaconda detachment fault core complex, although the detachment may cap the mesa (O'Neill and Lageson, 2003).

7.1 Cameron mine access road. Turn right through gate onto private land. TRGS has received permission to visit the mine via this 4WD road which winds its way up through the trees to the grassy mesa north of the main workings (Fig. 2).

STOP 1 9.0 STOP 1 - Cameron mine. "Y" intersection. Main road follows the right fork and gradually climbs the grassy bench. Left fork (along contour, west) is the mine access road. Park at the Y and walk west to the Cameron workings.

Mine History and Geology

The patent for the Cameron claim was issued to William A. Clark, Salton Cameron and Robert S. Kelly in 1881. The claim is located on silicified Cambrian (Hasmark?) carbonates with local breccia and silica veining. Silica alteration and breccias persist in float up to 2,000 feet to the north and in prospect pits to the northwest. Veining exposed in prospect pits appears to strike to the northwest. Mineralization may be related to a granodiorite intrusive outcropping to the north. The contact between the carbonate rocks and the intrusive is obscured by glacial deposits, as is most of the area around the old workings.

Several geologists for Anaconda Company have evaluated the property beginning with a cursory evaluation by L.H. Hart in 1935. Hart recognized "spotty, relatively low grade ore" occurring as bedding replacements controlled by two sets of "weak fissures". Hart thought the prospect offered potential to yield small tonnages of ore averaging 8 ounces per ton (opt) silver. Various lessees have shipped small quantities of ore, the largest shipment being 1941 tons grading 4.65 opt silver, 0.13% copper and 0.011 opt gold.

Robert G. Ingersoll and James G. Inderberg, again from the Anaconda Company, examined the property in 1958 targeting the siliceous alteration as a possible source of flux for the Anaconda smelter. Harold A. Braham evidently owned the patent at that time and had previously shipped around 1,000 tons to the smelter averaging a little better than 3 opt silver and seventy-eight percent silica. Braham's shipments cost more to process at the smelter than the value of flux and silver, and production was suspended. Ingersoll and Inderberg collected samples from the various workings and outcrops on the property which returned silica contents ranging from 48% to 89% and silver assays ranging from 1.39 opt to 2.38 opt silver along with some low grade gold credits. These sample results prompted Ingersoll and Inderberg to conduct a drilling program adjacent to the workings. From twenty-nine holes representing an area of approximately 40 feet by 60 feet, nine holes intercepted material suitable for flux (at that date: >70% silica and <8% calcium oxide). They calculated that there were approximately 1,900 tons of flux-grade ore which also contained 1.52 opt silver and minor gold credits.

Glen C. Waterman examined the property in 1973 and revisited some of Ingersoll and Inderberg's drill hole data. His recalculations indicated a weighted average grade of 1.93 opt silver over a fairly consistent thickness of nineteen feet. He also noted that "bluish silicified rock" sampled from float up to 1,000 feet north of the main workings ran up to 2.55 opt silver. These observations have encouraged more recent exploration which focuses on potential for concealed mineralization in favorable stratigraphy at depth and to the north of the Cameron patent.

Mineralization controls on the property are not well understood. Siliceous breccias appear to be structurally controlled but the structures are not well defined. The relationship between the wide area of silicification (up to at least 1,000 feet from the historic workings) and breccias is not apparent. One model (untested to date) employs high-angle structures to channel ore forming fluids southward from the granitic intrusions to form bedding plane replacement mineralization in one or more horizons.

Return to vehicles and follow the same route back to MT Highway 1. Reset mileage to 0.0

0.0 Junction - Cameron access road and MT Highway 1. Turn right (west). From here, the highway climbs onto terminal moraines from

glaciers which advanced from the high country of the Anaconda Range to the south. The lower strand of the Anaconda detachment fault is buried beneath the till.

1.5 Turn right on Foster Creek Road, marked by "Anaconda Job Corps" sign.

1.8 Pull off on right at old quarry.

STOP 2 STOP 2. At first glance this quarry appears to expose well-bedded marble (Cambrian Hasmark formation?), but a closer look reveals tight isoclinal folds within the layers. The axial planes appear to be parallel to the layers. Are these sheath folds? We attribute these folds to layer-parallel shear, but do not know whether they are the result of the Cretaceous tectonism discussed above or movement along the Eocene Anaconda detachment fault. The fault zone is at most a few hundred feet above us, but layer-parallel shear is also characteristic of the late Cretaceous strain event. As we have already discussed at the Cameron Mine, not all breccia in this region is of Tertiary age, nor is all mylonite. Breccia can be seen near the top of the cliff.

9.3 Return to Highway 1 and turn right.

10.2 Turn right into the DNRC Field Station.

STOP 3 STOP 3. Behind the DNRC station is a cliff that exposes the Precambrian-Cambrian unconformity and the Cambrian section. We will scramble up through these rocks at STOP 4. Note the subtle low-angle unconformity between dark colored Proterozoic sedimentary rocks near the bottom of the outcrop and the white Cambrian Flathead sandstone. The angular unconformity in this region averages only 2-5^{o}, and can usually only be seen from a distance (Fig. 3). The 25^{o} unconformity shown in a photo by Emmons and Calkins (1913) was relocated in 2009, and is interpreted by Lonn as a fault contact within the Belt Supergroup (Fig. 4).

Visible above the Flathead is the Silver Hill formation that here is only about 150 feet thick, in contrast to 325 feet on the northwest side of the Flint Creek Range (McDonald and Lonn, 2009). The local thinness of the Silver Hill Formation is attributed to severe internal deformation that we will examine closely at Stop 4. The white cliffs that cap the hill are Cambrian Hasmark dolomite.

3.1 Return to Highway 1 and turn right.

4.2 Turn right on the Warm Springs Creek Road.

4.5 Park near the Vermillion Trail Road on the right.

STOP 4 STOP 4. This hike will take about two hours. Follow the road across the creek to the first house, pass a basketball hoop, and then leave the road on a trail to the left. Stay on a faint trail through hummocky terrain to a knob where the cliff that we viewed from the DNRC station is visible. We will ascend the flank of this cliff, so continue working towards it. The easiest traveling is adjacent to the creek and floodplain.

Ascend loose talus, keeping the cliff

Fig. 3. a) View from Stop 3 of horizontal sedimentary section behind the DNRC station along Highway 1 west of Anaconda. Ym—Missoula Gp (Mount Shields Fm?); Cf—Flathead Fm; Csh—Silver Hill Fm; Ch—Hasmark Fm. A slight angular unconformity can be seen between Ym and Cf; b) The low angle unconformity between Mt. Shields Fm, member 2, and Flathead Fm on Olson Mountain a few miles NE of Stop 3.

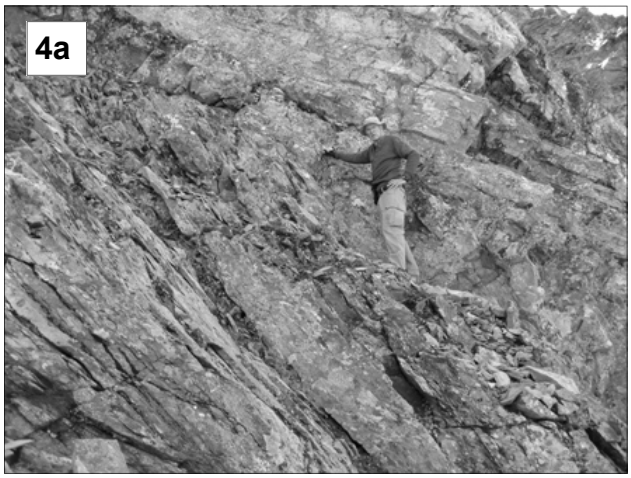

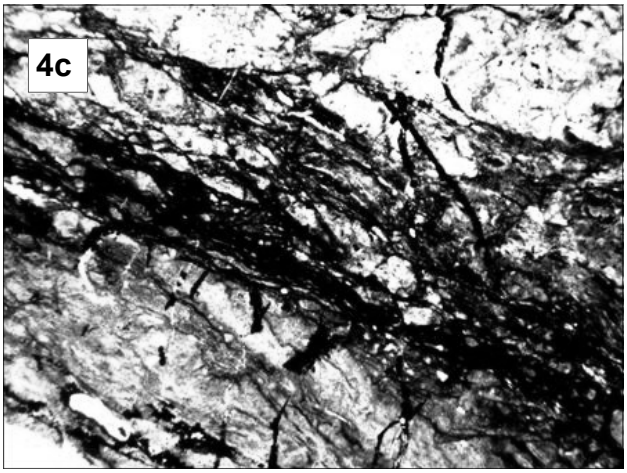

Fig 4. Photos from the area of Emmons and Calkins' (1913) unconformity near Spruce Lake, central Anaconda Range. Lonn interprets the unconformity as a fault contact separating Snowslip Fm below from overlying Mt. Shields 2: a) 2009 re-enactment of the original photo; b) close-up showing well-developed cleavage along the "unconformity"; c) photomicrograph showing cataclastic texture of the "unconformity"; d) the true Mt. Shields-Flathead contact located 300 feet above the photo location showing slight angular discordance.

on climber's right. The first outcrops you encounter are gray-green, rusty weathering, fine- to medium-grained quartzite. The dark color appears to be due to metamorphic biotite. Muscovite is also common. Is it detrital or metamorphic in origin? Some beds appear quite feldspathic; others do not. Flat laminations dominate over cross beds. In this region, everywhere the top of the Mesoproterozoic Belt Supergroup can be positively identified, it is Mt. Shields formation (Lonn and others, 2003), and so we have tentatively assigned these rocks to Mount Shields formation, member 2.

Continue upward, where the contact with the Cambrian Flathead formation can be easily identified. However, relationships between it and the Belt are obscured by fractures associated with a high angle fault. No angular unconformity is visible. The Flathead is white, feldspar-poor, fine- to medium-grained massive quartzite. It is usually less than 50 feet thick in the region.

Near the top of the Flathead, a cleft between outcrops ascends to the right. Follow this to a wide, but sloping ledge developed in the lower Cambrian Silver Hill formation. Note that the cliffs at eye level are composed of interbedded limestone and siltstone in wavy beds about an inch thick. This "ribbon rock" is characteristic of the middle member of the Silver Hill. *Carefully* traverse this ledge, which is covered in loose scree, to the right for 100 feet around a corner and onto flatter, more comfortable terrain.

Note the chaotic, disharmonic folds in the outcrops. Many fold sets can be seen to be bounded below and above by bedding-parallel shear zones (Fig. 5a,b). These folds, like the ones at Stop 2, are interpreted to have formed as a result of bedding-parallel shear. We attribute the deformation here to extension because the folds and shear zones appear to thin the stratigraphic section, just as similar fabrics do throughout the entire 40,000-foot-thick metasedimentary section below the Anaconda Detachment fault zone. Again we raise the question: has the deformation resulted from Eocene or Cretaceous extension? Since deformation here is indistinguishable from that found in the detachment footwall, it is likely that these features are Cretaceous as well.

Some of the fold sets that are nearly recumbent verge west (Fig. 5a), mimicking the megascopic folds of this area (Fig. 5c), and suggesting top west movement. Although shear sense indicators are rare in the Cretaceous strain fabrics, those that can be identified do show top-west shear sense (Fig. 5d). It is possible that the bedding-parallel shear zones and the slightly younger, megascopic west-verging folds are related and developed in the same tectonic regime.

Return to the cars via the same route, taking care not to roll rocks down on your colleagues during the descent.

7.1 Return to Highway 1 and turn right.

7.9 Silver Lake Dam on left.

8.1 Pull off the road on the right near mile marker 22.

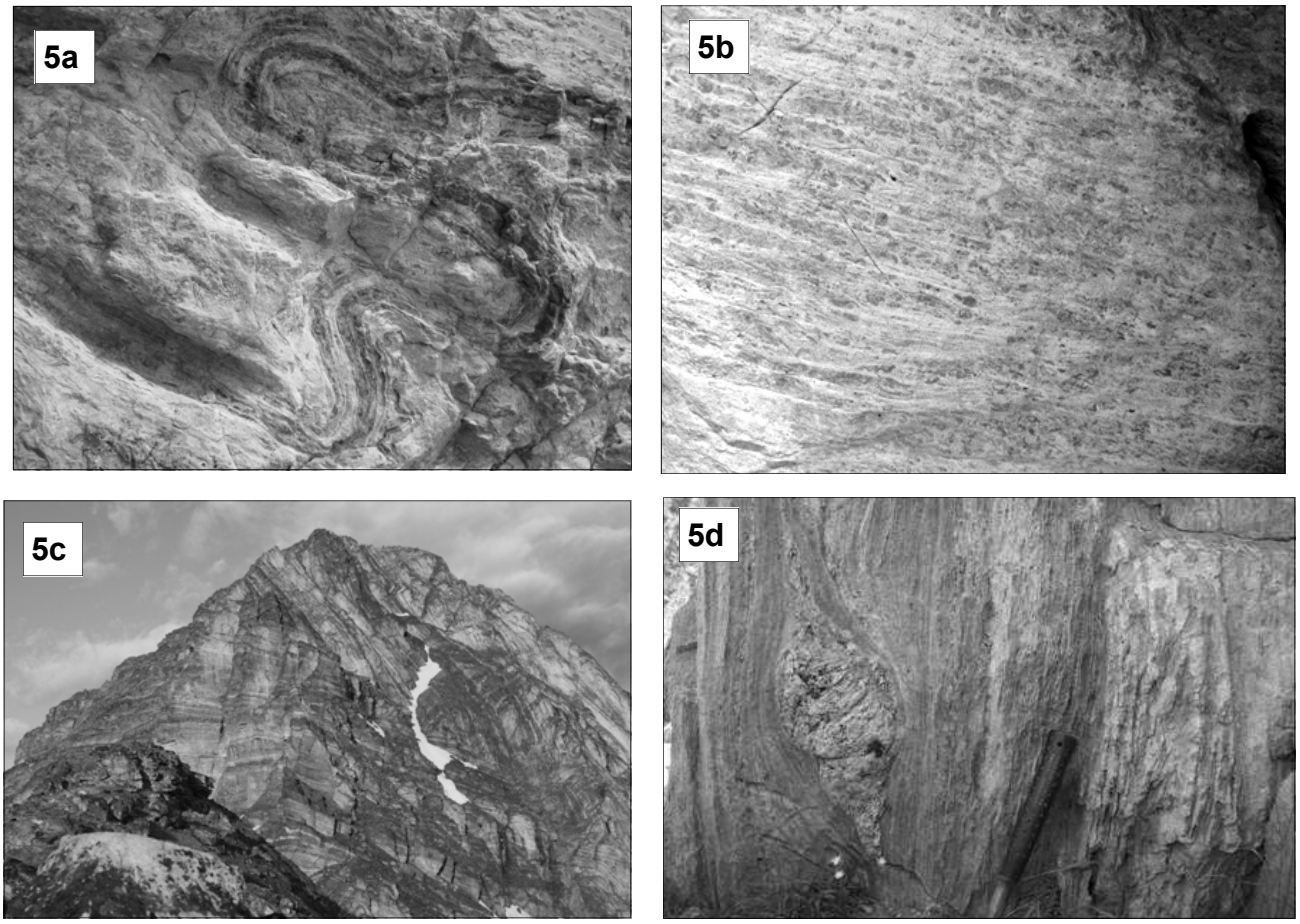

Fig. 5. Views of internally deformed Silver Hill Fm at Stop 4: a) disharmonic, west-verging folds between two bedding-parallel shear zones; b) the lower shear zone in a), showing dismembered silty layers in foliated matrix of calcite; c) huge west-facing recumbent anticline near Warren Peak, central Anaconda Range (Don Heffington photo); d) large σ-type quartzite porphyroclast in the Silver Hill Fm near Lost Creek, showing right-lateral shear sense that is top-west when rotated back to horizontal.

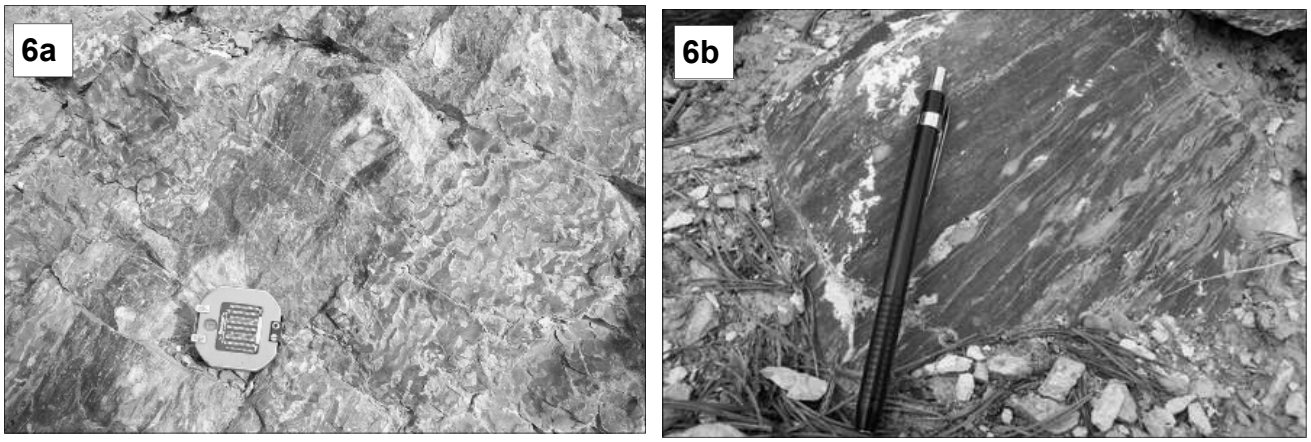

Fig. 6. a) Brunton marks dark mylonitic shear band between and parallel to relatively undeformed beds in the Red Lion Fm at Stop 5; b) mylonitic fabrics developed in the Jefferson Fm at Stop 6.

Fig. 7. a) Alternating dark-colored mylonitic and light-colored brecciated zones parallel to bedding within the Jefferson Fm south of Georgetown Lake; b) Breccia zone deformed by shear along the Anaconda detachment fault, Timber Gulch, southern Flint Creek Range.

STOP 5 STOP 5. Walk west along the highway to a long road cut. This "ribbon rock" looks similar to the middle member of the Silver Hill formation, but is actually upper Cambrian Red Lion formation. Close inspection will reveal bedding-parallel shear bands about 1 foot thick scattered throughout the section (Fig. 6). Although the strain fabrics here have been attributed to shear on the limbs of tight, overturned folds (O'Neill and Lageson, 2003), these folds are open and upright, and the strain fabrics can be found in their hinge areas as well. Therefore, these shear bands must have formed prior to the folding. We are now well below the Anaconda detachment fault and still two miles from the trace of the Georgetown thrust, and so we also assign these shear bands to the Cretaceous extensional event. The few shear sense indicators found along these road cuts show top-west shear sense (Tom Kalakay and Colleen Elliott, verbal communication, 2002).

Drive west on Highway 1 for 0.4 miles.

8.5 Pull over at an old two-track road ascending the slope between road cuts.

STOP 6 STOP 6. Walk west for 100 yards to the next road cut, composed of steeply NW-dipping Devonian Jefferson formation. The Jefferson also contains bedding-parallel mylonitic shear bands (Fig. 6b) like those of Stop 5. Also note the wide, nearly bedding-parallel breccia zone in this outcrop. While it is tempting to interpret the breccia as related to a Tertiary high-angle fault, bedding-parallel brittle faults are common throughout the region (Fig 5), and bedding-parallel breccia zones often alternate with the Cretaceous bedding-parallel mylonitic zones (Fig.7a). Numerous outcrops of sheared breccia (Fig. 7b) along the Anaconda detachment on the east side of the Flint Creek Range demonstrate that some breccia is pre-Tertiary. Therefore, both the brittle and ductile structures in this outcrop could be interpreted as Cretaceous age structures that have been folded into their near vertical attitudes.

END OF FIELD TRIP. On your return, don't forget about the Anaconda speed trap.

References

Anaconda Mining Company, 1935 to 1973, Intra-company reports on the Cameron mine were acquired by the mine owners but are not available in public documents.

Desmarais, N.R., 1983, Geology and geochronology of the Chief Joseph plutonic-metamorphic complex, Idaho-Montana: Seattle, University of Washington, Ph.D. dissertation, 150 p., map scale 1:48,000.

Earthworks, Inc., 1989, CAMBRX prospect submittal report: exploration summary report to Homestake Mining Company.

Emmons, W.C., and Calkins, F.C., 1913, Geology and ore deposits of the Philipsburg quadrangle, Montana: U.S. Geological Survey Professional Paper 78, 271 p.

Foster, D.A., Doughty, P.T., Kalakay, T.J., Fanning, C.M., Coyner, S., Grice, W.C., and Vogl, J., 2007, Kinematics and timing of exhumation of metamorphic core complexes along the Lewis and Clark fault zone, northern Rocky Mountains, USA: Geological Society of America Special Paper 434, p. 207-232.

Grice, W.C., Jr., 2006, Exhumation and cooling history of the middle Eocene Anaconda metamorphic core complex, western Montana: Gainesville, University of Florida, M.S. thesis, 260 p., map scale 1:100,000.

Grice, W.C., Jr., Foster, D.A., Kalakay, T.J., Bleick, H.A., and Hodge, K., 2004, Style and timing of crustal attenuation in the Anaconda metamorphic core complex, western Montana: Geological Society of America Abstracts with Programs, v. 36, no. 5, p. 546.

Grice, W.C., Jr., Foster, D.A., and Kalakay, T.J., 2005, Quantifying exhumation and cooling of the Eocene Anaconda metamorphic core complex, western Montana: Geological Society of America Abstracts with Programs, v. 37, no. 7, p. 230.

Haney, E.M., 2008, Pressure-temperature evolution of metapelites within the Anaconda metamorphic core complex, southwestern Montana: Missoula, University of Montana, M.S. thesis, 110 p.

Hawley, K.T., 1974, A study of the mafic rocks along the eastern flank of the Flint Creek range, western Montana: Missoula, University of Montana, M.S. thesis, 39 p., map scale 1:100,000.

Kalakay, T.J., Foster, D.A., and Thomas, R.C., 2003, Geometry and timing of deformation in the Anaconda extensional terrane, west-central Montana: Northwest Geology, v. 32, p. 124-133.

Lonn, J.D., and McDonald, C., 2004a, Geologic map of the Kelly Lake 7.5' quadrangle, western Montana: Montana Bureau of Mines and Geology Open File Report MBMG 500, 15 p., scale 1:24,000.

Lonn, J.D., and McDonald, C., 2004b, Cretaceous (?) syncontractional extension in the Sevier orogen, southwestern Montana: Geological Society of America Abstracts with Programs, v. 36, n. 4, p. 36.

Lonn, J., and Lewis, R., 2009, Late Cretaceous extension and its relation to the thin stratigraphic section in the Philipsburg area: A field trip to Carpp Ridge: Northwest Geology, v. 38, p. 141-152.

Lonn, J.D., McDonald, C., Lewis, R.S., Kalakay, T.J., O'Neill, J.M., Berg, R.B., and Hargrave, P., 2003, Preliminary geologic map of the Philipsburg 30' x 60' quadrangle, western Montana: Montana Bureau of Mines and Geology Open File Report MBMG 483, 29 p., scale 1:100,000.

O'Neill, J.M., and Lageson, D.R., 2003, West to east geologic road log: Paleogene Anaconda metamorphic core complex: Georgetown Lake Dam-Anaconda-Big Hole Valley: Northwest Geology, v. 32, p. 29-46.

O'Neill, J.M., Lonn, J.D., and Kalakay, T., 2002, Early Tertiary Anaconda Metamorphic Core Complex, southwestern Montana: Geological Society of America Abstracts with Programs, v. 34, no. 4, p. A10.

O'Neill, J.M., Lonn, J.D., Lageson, D.R., and Kunk, M.J., 2004, Early Tertiary Anaconda metamorphic core complex, southwestern Montana: Canadian Journal of Earth Sciences, v. 41, p. 63-72.

McDonald, C., and Lonn, J., 2009,The Cambrian Flathead and Silver Hill Formations in the northern Flint Creek Range near Maxville, Montana: Northwest Geology, v. 38, p. 111-120.

Stuart, C.J., 1966, Metamorphism in the central Flint Creek Range, Montana: Missoula, University of Montana, M.S. thesis, 103 p., map scale 1:6,000.

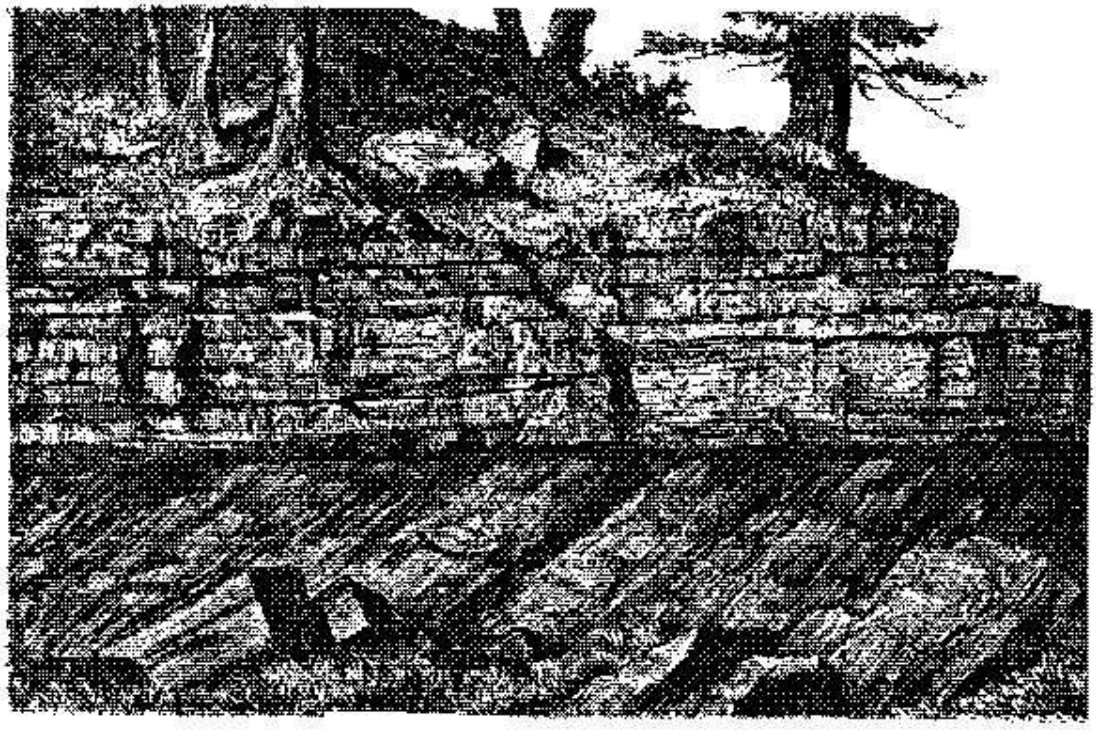

GEOLOGY AND MINERAL DEPOSITS IN THE NORTHERN HIGHLAND MOUNTAINS, MONTANA: A FIELD TRIP CROSSING THE GREAT DIVIDE (TWICE)

Christopher H. Gammons[1], Jill M. Sotendahl[1], and Bruce E. Cox[2]
[1]*Montana Tech, Dept. of Geological Engineering, Butte, MT 59701*
[2]*Geologist, Missoula, MT 59801*

Introduction

Numerous small but significant mineral deposits are located within a half-hour drive from the Richest Hill on Earth, Butte Montana. This field trip through the northern Highland Mountains (Figure 1) will visit two such deposits, a curious structural zone within the Boulder batholith and some inactive gold placer mines. Please note that three of the Stops are on private lands; owners have graciously given TRGS permission to visit and future visitors must secure the same permission.

Road Log

Leave Anaconda and drive east on Montana Highway 1 to its junction with I-90.

Set odometer to 0.0 Junction of MT Hwy 1 / I-90 (Exit 208). Turn southeast on I-90 and stay on I-90 for approximately 33 miles to the Pipestone exit.

10.5 Junction I-15 south. We will have the option of returning to Anaconda via I-15 when the field trip ends.

18.6 Junction I-15 north. For the next two miles (southbound), I-90 parallels the Continental fault, a west-side-down normal fault (~3,500 ft displacement) which forms the western boundary of the Continental Cu-Mo orebody currently operated by Montana Resources (Czehura and Zeihen, 2000).

24.1 Homestake Pass - Continental Divide. Vertical, N-trending shears, quartz-sulfide veins and aplite +/- pegmatite dikes are evident in road cuts for the next 6 miles. Locally strong argillic alteration along these structures and adjacent fractures has promoted deep weathering of the granitic rocks to yield the bouldery topography for which the batholith is named.

31.1 I-90 crosses the mouth of Dry Creek and the northeast projection of the Toll Mountain structural zone which we will examine at Stop 3. Shallow mine workings along Dry Creek (north of I-90) expose shears and veins and lenses of carbonate (Cambrian?) strata.

33.1 Pipestone Exit 241. Exit I-90, turn right (south) and immediately right again on the frontage road (Bluebird Lane) heading west.

33.8 Mailbox 75 - Brower Ranch. Turn left and go carefully across narrow bridge. Park single file in the turn-around on the valley floor.

STOP 1 **Stop 1. Gold placer workings at Brower Ranch.** John Brower will lead us on a short walking traverse through this reach of the Pipestone placer. Note the pattern of diversion ditchs and variety of rock types in the tailings piles. Figure 2 provides perspective on the size of these placer deposits (Map 9 from Lyden, 1987, revised).

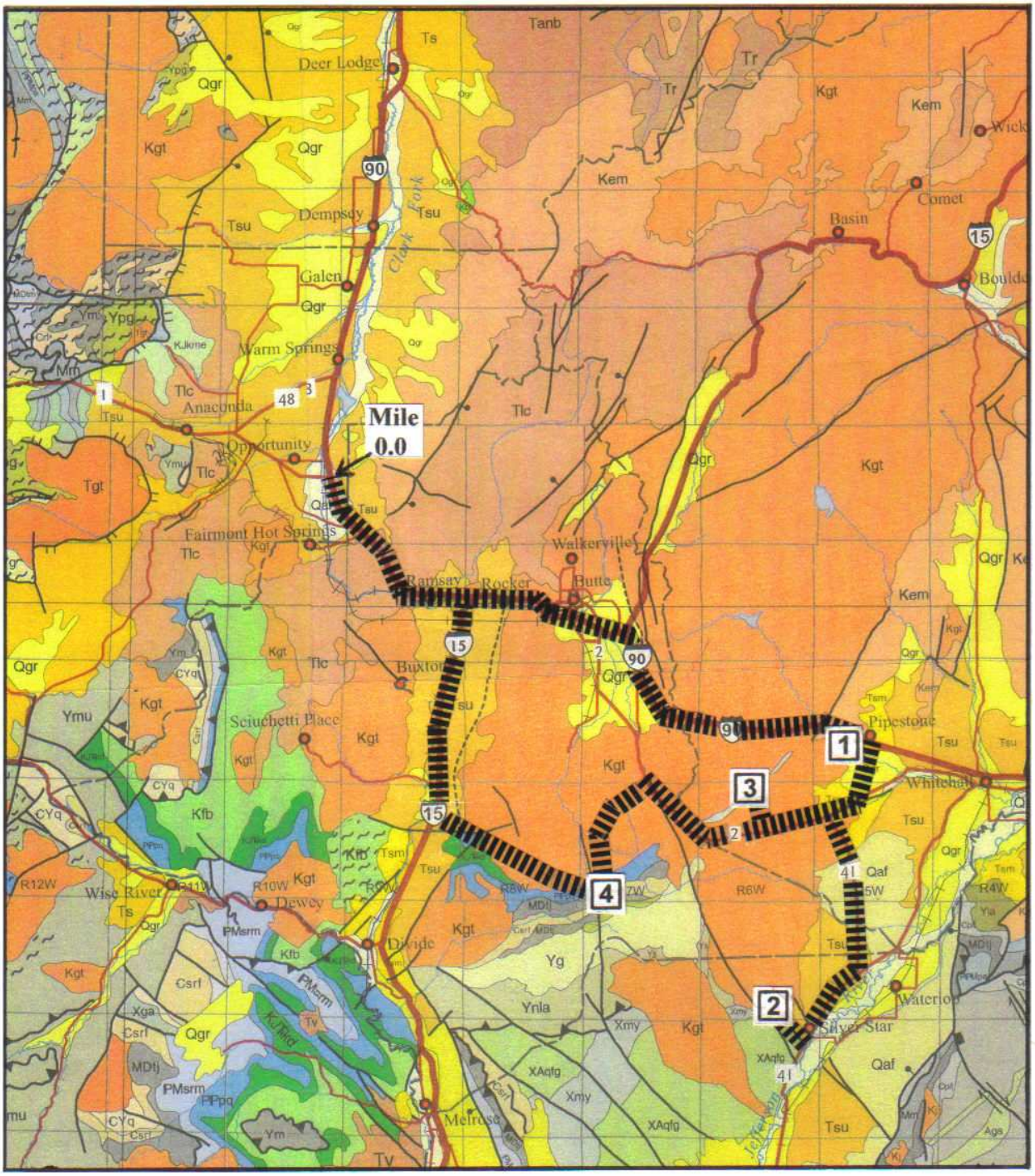

Figure 1. Northern Highland Mountains field trip route and Stops. Map shown is modified from part of the Geologic Map of Montana (2007).

Return to the vehicles, drive back to I-90 (Pipestone Exit 241).

Reset odometer to 0.0 Stay on the frontage road (Bluebird Lane-Pipestone Road) eastbound.

0.8 Hot Springs Road. Turn right (south). Cross Pipestone Creek; passing old buildings of the Pipestone Hot Springs resort. Traveling over Quaternary pediment gravels for next 3 miles.

3.9 Junction - Highway 2. Turn west.

5.0 Cactus Junction - Highway 41. Turn south. The highway climbs through Tertiary sediments and then across another Quaternary alluvial fan. Note local accumulations of large alluvial boulders.

13.5 Junction - Highway 287. Turn right southwest.

17.2 Entering Silver Star.

17.4 Cemetary Road. Turn right and follow gravel road uphill.

19.0 Enter Madison Gold property.

19.1 Broadway Mill on right. Mine office on left - park here.

STOP 2 **Stop 2. Madison Gold deposit**. This stop will examine the economic geology of the active Madison Gold skarn deposit (see Gammons et al., 2010). All of the sites described here are on private mine property accessed via a locked gate, and visitors must secure permission from the owners, Coronado Resources. The most convenient place to park in the area is near the mine office or the waste rock and ore stockpiles. The Madison Gold portal is at the bottom of a steep gulch (Tom Benton Gulch). Mine trucks using the loop road usually drive in a counter-clockwise direction, as shown by the arrows in Figure 3.

The Madison Gold property is located a short distance to the north of the historic Broadway Mine (Fig. 3), the largest gold producer in the Silver Star district. The Madison Gold and Broadway mines are localized along a mineralized skarn deposit near the contact between Mississippian limestone of the Madison Group and granodiorite of the Cretaceous Rader Creek pluton. The active Madison Gold operation is being developed by an elliptical decline to explore the down-dip extension of copper and gold mineralization that crops out at the surface as a series of three small open pits (the Black, Victoria, and American Pits). The main access portal is located immediately south of the American Pit, which has been partially back-filled.

Stop 2A Black Pit. The Black Pit is so-named due to conspicuous outcrops of hedenbergite skarn along the south rim of the pit. The hedenbergite forms radiating clusters of prismatic crystals up to 5 cm long, with a dark green to black color. The contact between hedenbergite skarn and recrystallized limestone is steeply dipping and knife-sharp. On the north wall of the Black Pit is a body of white, brecciated marble that, according to Price (2005), carries higher gold grades than the adjacent hedenbergite skarn. The breccia is clast-supported, has a loose, sandy matrix, and includes several boulders and cobbles of hedenbergite skarn. It is possible that the breccia represents colluvium that filled a solution-collapse structure within the Madison. If so, the elevated gold grades could be detrital in origin, washed into the cracks from mineralized skarn outcrops further uphill (see discussion in Price, 2005).

Stop 2B Jasperoid Waste Rock. At the

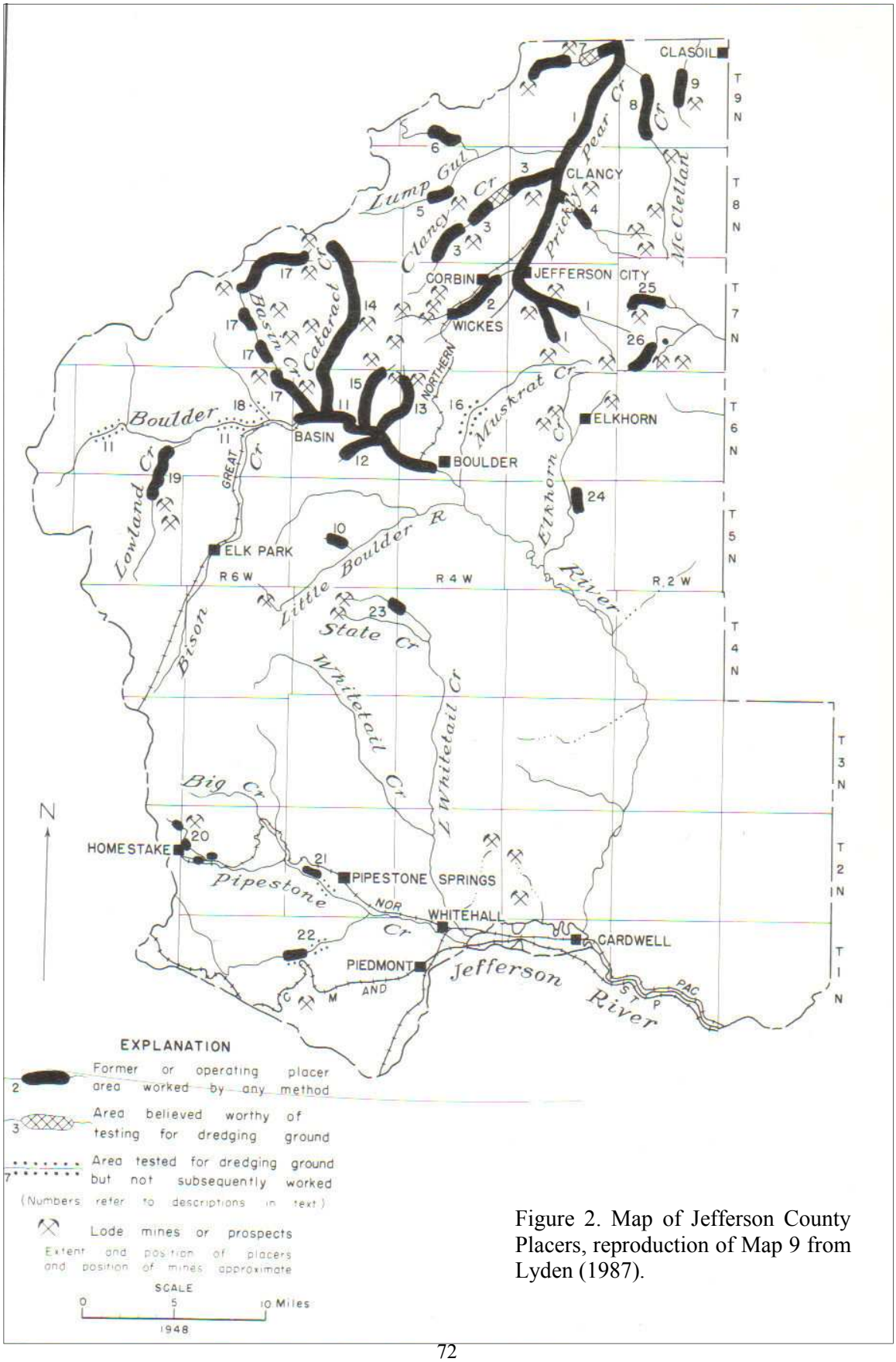

Figure 2. Map of Jefferson County Placers, reproduction of Map 9 from Lyden (1987).

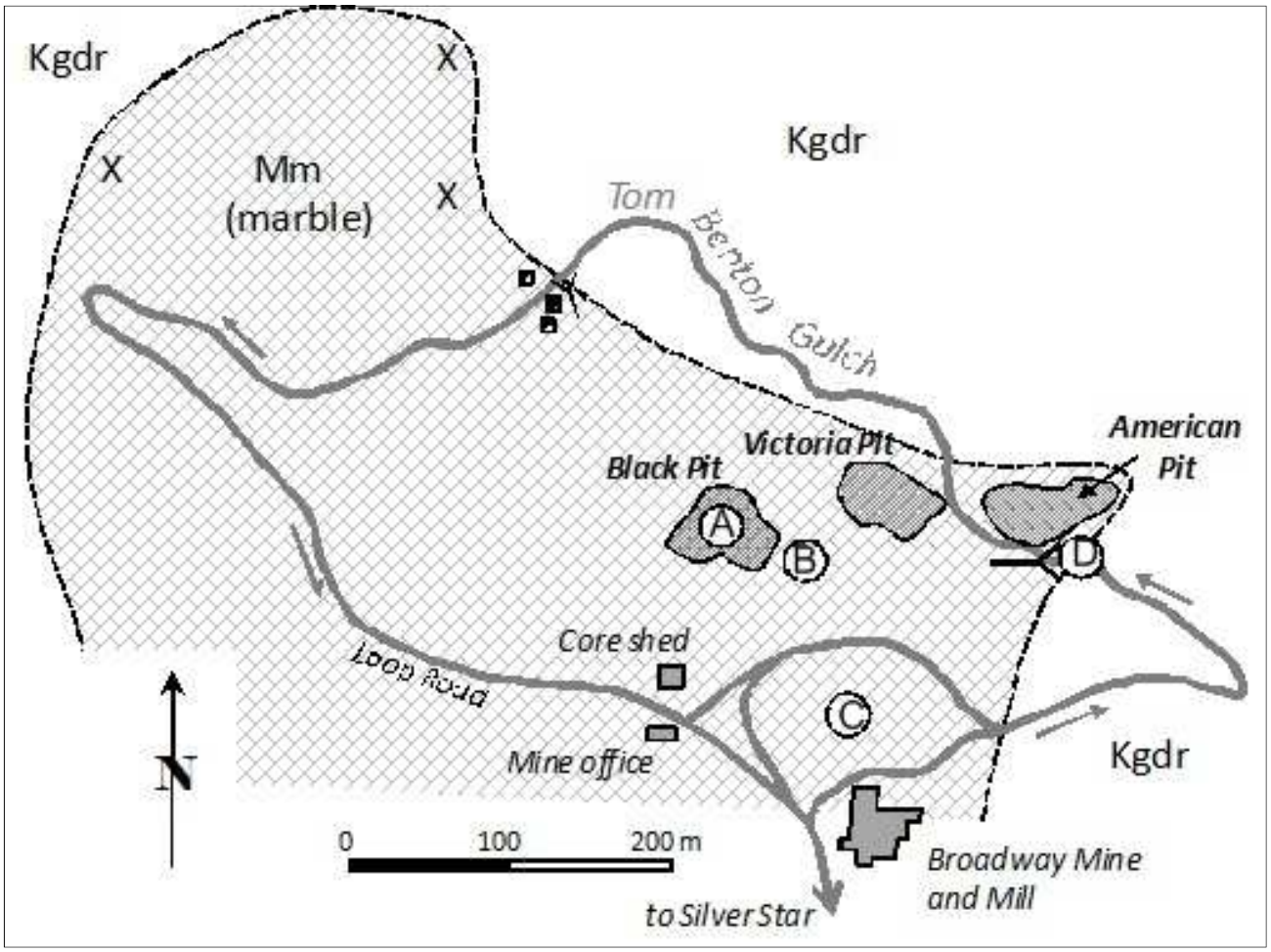

Figure 3. Map of mine workings and simplified geology near the Broadway and Madison Gold mines, Silver Star district, Montana. A through D refer to stops described in the text. Kgdr = Rader Creek granodiorite; Mm = Madison Group limestone.

time of this writing, a large dump of barren jasperoid from the underground workings of the Madison Gold deposit forms the east wall of the Black Pit. Excellent examples of jasperoid can be collected here. As mentioned in the companion paper (Gammons et al., 2010), the jasperoid at Silver Star is very Fe-rich, explaining its deep brown-orange-red coloration. It is also locally elevated in gold, and was an important ore for the historic Broadway Mine, as well as the active mine. Gold-bearing jasperoid cannot be distinguished visually from barren jasperoid, and therefore every bucket load must be assayed. Some of the jasperoid is cut by irregular veins of white calcite. The origin of the jasperoid and calcite veins is discussed in the companion paper.

Stop 2C Ore Stockpiles. Depending on what the miners are finding underground, the ore stockpiles may contain gold-bearing jasperoid, gold- and copper-rich primary sulfide ore, or black, secondary chalcocite ore. With some effort, it should be possible to find good examples of all three ore types. The gold-bearing jasperoid resembles the waste jasperoid in every aspect except gold concentration. A number of different ore minerals can be found in the primary sulfide ore, including pyrite, pyrrhotite, and chalcopyrite, with lesser amounts of bornite and magnetite. These sulfides were introduced, along with trace amounts of gold, during the waning stages of the primary skarn event. The primary sulfide minerals are surrounded by hedenbergite or garnet-diopside skarn that

has locally been retrograde-metamorphosed to chlorite and other hydrous minerals. The chalcocite ore consists of rock that is rich in black chalcocite (Cu_2S) which has replaced pre-existing sulfides, mainly pyrite. In places the chalcocite is dense and compact, and is hard when struck with a hammer. More commonly, especially in piles that have been exposed to weathering for a period of time, the chalcocite is crumbly and sooty, and easily falls apart when picked up. The grade of copper in the chalcocite ore is very high, averaging between 25 to 50% Cu.

Stop 2D Madison Gold portal. Walking or driving down the loop road to Tom Benton Gulch, one will find the main portal of the Madison Gold decline. Roadcuts to the immediate east (opposite the trailer near the portal entrance) include some good examples of epidote-rich endoskarn developed in the Rader Creek granodiorite. Unaltered granodiorite crops out further east and up the hill. Facing the portal, the north (right-hand) rib of rock near the entrance is a good example of garnet-diopside skarn. The diopside (medium green) is fine-grained: individual crystals are hard to make out, even with a hand lens. The garnet is a pale brown color and locally forms crystals up to 1 or 2 cm in diameter. The garnet-diopside skarn is developed closest to the contact with the granodiorite, and grades westwards (away from the pluton) to hedenbergite skarn. These relationships are obscured by a later, lower-temperature hydrothermal event that formed steeply-dipping jasperoid bodies. A cut near the east end of the Victoria Pit (presently used for mine ventilation) exposes an interesting outcrop of jasperoid next to hedenbergite that has been altered to a yellow clay mineral, tentatively identified as nontronite (i.e., Fe(III)-rich smectite). Nontronite is known to form by alteration of hedenbergite (Eggleton, 1975). Further work is in progress.

Madison Gold decline. Access to the decline is only possible with a mine employee and full mine gear (hard hat, lamp, self-rescuer, steel-toed boots). The decline is 1500 feet long at present and drops 265' in elevation at a 15% grade. The general layout of the underground workings with respect to the open pits at the surface is shown in Figure 4. Good exposures of most of the aforementioned rock types are found along the walls of the Madison Gold decline. The geology is complex, but essentially consists of garnet-diopside skarn near the portal grading to hedenbergite skarn further to the west, both containing localized veins or bands of primary sulfide minerals (mainly pyrite, pyrrhotite, and chalcopyrite). A steeply-dipping body of jasperoid cut by calcite veins is well-exposed along the decline. Most of the high-grade chalcocite bodies have been mined out, but examples of secondary chalcocite and native copper can be found with some effort.

Return to vehicles and retrace our route through Silver Star on Hwy 287 to Hwy 41 to Cactus Junction.

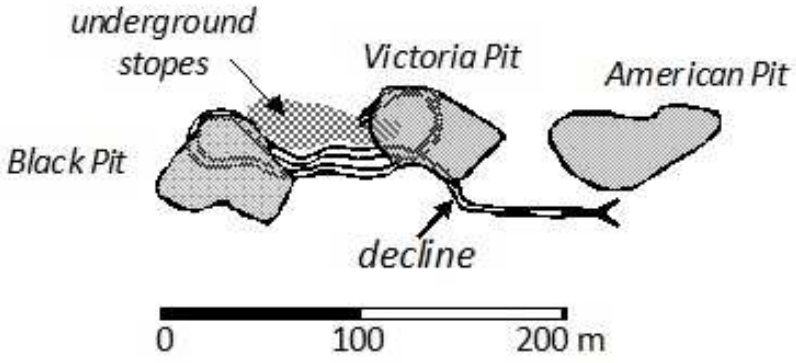

Figure 4. Location of the Madison Gold decline with respect to surface mine workings. Most of the production from the underground mine has come from the cross-hatched area.

Reset odometer to 0.0 at Cactus Junction (Hwy 41 jct w/ Hwy 2). Turn west toward Pipestone Pass and Butte. Note highwalls and tailings of ground sluice placer operations on both sides of highway for the next 1/2 mile.

4.8 Toll Mtn. Road (to Toll Mtn. Campground). Turn north; Figure 5 shows the geology along the route to Stop 3. Road passes low, rounded outcrops of Rader Creek granodiorite.

7.6 "Y" intersection with Upper Rader Creek Road. Bear left toward campground.

8.0 "Y" intersection with Road 9319. Bear right - do not follow signs to the campground.

8.3 Cross cattle guard.

8.35 Road to Trail 88 and Moose Creek on right. Stay straight on 9319, cross Elkhorn Spring Creek.

8.4 Park in the grassy area between the forks of the creek.

STOP 3 **Stop 3. Toll Mountain screen/pendant.** This stop is a 1/4 mile-long walking traverse that gains 150 ft elevation. From the parking area, a clockwise traverse across the west-facing hillslope takes us from Cretaceous Butte quartz monzonite through a near-vertical or overturned (and relatively thin?) lower Cambrian section of Flathead Sandstone, Wolsey Shale, Meagher Limestone +/- Park Shale. An aplitic phase of the Rader Creek granodiorite has intruded much of the southeast flank of the screen/pendant. Metasomatism near the intrusive contacts has produced locally massive garnet +/- diopside skarn especially in the Wolsey and Meagher carbonate strata. Reconnaissance-scale mapping suggests the alteration and weak sulfide mineralization exposed in the adit and pit workings may be controlled by north and northwest-trending faults.

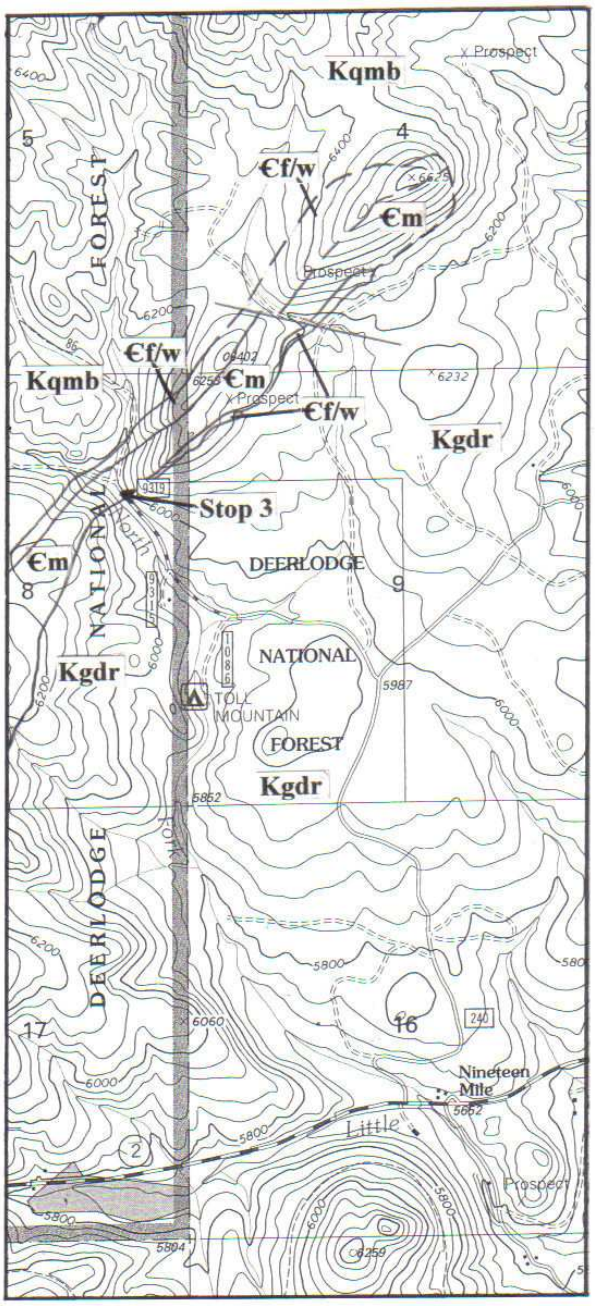

Figure 5. Toll Mountain screen/pendant. Kqmb = Butte Quartz monzonite, Kgdr = Rader Creek granodiorite, Cm = Meagher Limestone, Cf/w = Flathead Sandstone + Wolsey Shale. Geology summarized from mapping of Cox (1989). Map shown is part of the Grace, MT 7.5 Minute USGS topographic quadrangle, 1996.

Screen / Pendant Geology

The Toll Mountain structural zone is called a "screen" or "screen/pendant" for simplicity in this writing. Much of the following discussion is taken from a private report on regional mineral exploration (Cox, 1989). The Toll Mountain screen/pendant is a curvilinear, NE-trending regional-scale fault zone which can be traced southwest along the northwestern flank of the Highland mountains toward Highland City (Stop 4, this road log) and possibly as far northeast as the Elkhorn mining district near Boulder (see Figure 1). The screen parallels much of the eastern boundary of the Boulder batholith and may have been structurally active from the late Cretaceous through Tertiary.

In the Toll Mountain area, the metamorphosed Paleozoic strata dip 30-80 degrees NW or more, and are overturned. Two or more discrete structural slices within the screen are indicated by abrupt changes in the dip and thickness of stratigraphic packages; there may also be some repeated stratigraphy. Strata are weakly to moderately folded except along the east flank of Toll Mountain which contains a tight NE-plunging syncline in the Meagher Limestone and metamorphosed Belt sediments.

The question of whether the metamorphic strata represent a roof pendant or structural screen has not been resolved. One structural aspect that is clear is the distinct fault/ fracture grain within the metamorphic rocks that parallels the NE-trending fault system. Another prominent structural grain is represented by closely spaced NW and NNW-trending faults which cut the screen/pendant on the east and west flanks of Toll Mountain. These faults produced a complex surface lithologic pattern and appear to have been the principal conduits for mineralizing fluids.

Return to the vehicles, retrace our route back to Highway 2.

Reset odometer to 0.0 at Highway 2. Turn west (right) toward Pipestone Pass and Butte.

3.0 Z Bar T road on the right.

3.2 Highway 2 crosses through the trace of the Toll Mountain screen which is occupied here entirely by granitic rocks.

5.0 Pipestone Pass. Continental Divide. For the next 1.6 miles, roadcuts in the switchbacks show locally strong argillic alteration, especially along high-angle shears and veins. Is this the upper level expression of a concealed porphyry system?

7.3 US Forest Service Road 84. Turn south (sharply left) and follow Rd. 84 toward the Highland mine.

8.2 Road goes under trestle.

10.0 "Y" intersection. Take the left fork toward Moose Creek.

13.0 Roadcuts expose veining and FeOx alteration in Kqmb.

15.2 Cattle gaurd. **15.3** US Forest service gate.

15.8 Highland Junction - Road 84 / Continental Divide Trail and Road 8520. Turn left (southeast) on road 8520.

16.1 Butte Highlands Gold Project. Turn left through the gate and proceed uphill to the mine office.

STOP 4 Stop 4 Butte Highlands Gold Project

Highlands District Geology and Resources

Butte Highlands is located within a favorable geologic domain that has hosted several multi-million ounce gold deposits including Butte, Golden Sunlight, Montana Tunnels, and Virginia City. The property was extensively drilled by Placer Dome, Battle Mountain, ASARCO, and Orvana Minerals in the 1980s and 1990s, and contains historic mineralization outlined by Orvana (not compliant with NI 43-101 or SEC Guide 7) exceeding 500,000 ounces of gold at a grade of nearly 0.30 ounces of gold per ton (oz/t). Past drilling highlights include gold intercepts of 50 feet of 0.65 oz/t, 31 feet of 1.06 oz/t, and 11.50 feet of 1.99 oz/t. Current estimates exceed 750,000 ounces of gold at 0.27 ounces of gold per ton (oz/t) with an approximate mine life of 10 years.

The project area is underlain by a series of middle to late Cambrian sedimentary strata which overlie the Proterozoic Belt Supergroup. Tight asymmetric folds are reported to occur in the Cambrian rocks. The sedimentary rocks have been intruded by the Cretaceous Boulder batholith which locally includes quartz monzonite of the Burton Park stock as well as satellite sills and dikes of diorite and gabbro. A prominent northeast trending (Trans-Challis) lineament bisects the district. A parallel feature appears to also control the southeast edge of the Burton Park stock. Numerous smaller scale faults range in orientation from east-west to slightly northwest, and north to northeast. Many of these appear to have provided channels for mineralization.

Gold mineralization is hosted primarily by skarn in the Wolsey formation originally comprised of interlayered shale and dolomitic mudstone with some silts and thicker carbonates. Average thickness of the Wolsey is ~220 feet although thicker in some drill holes. Higher grade mineralization occurs within the sediments proximal to diorite sills and dikes. Between 1988 and 1996, prior operators Placer Dome, Battle Mountain, ASARCO, and Orvana Minerals demonstrated the presence of a wide and continuous mineralized zone by drilling 46 core holes (36,835 feet) and 132 reverse-circulation holes (61,338 feet) within the district. The vast majority of this drilling was conducted in the Nevin Hill area which is included in the original Timberline property.

Project Economics and Management

An economic analysis considered a 1,000 ton-per-day operation averaging 0.287 ounces of gold per ton, yielding annual gold production of approximately 85,000 ounces per year over a 10-year mine-life. It forecast a 2-year development time, primarily to drive an exploration decline (which may also serve as a production ramp) at an estimated cost of $15-million to $18-million. Although there are suitable sites for an on-site mill and tailings pond on the property, they are not currently envisioned since custom milling capacity is available at existing nearby facilities. The resulting reduction in development lead-time, as well as in permitting and construction costs, will have a substantial positive impact on project economics.

Timberline Resources has a 50% carried to production ownership interest in its Butte Highlands Joint Venture Gold Project. In July 2009, Timberline Resources Corporation and Ron Guill formed a joint venture operating company, Butte Highlands JV, LLC ("BHJV"), for the further exploration, development, and mining at this site. Timberline also finalized the Operating Agreement for the joint venture with Highland Mining, LLC ("Highland"), an affiliate of Small Mine Development, LLC ("SMD"), both of which are

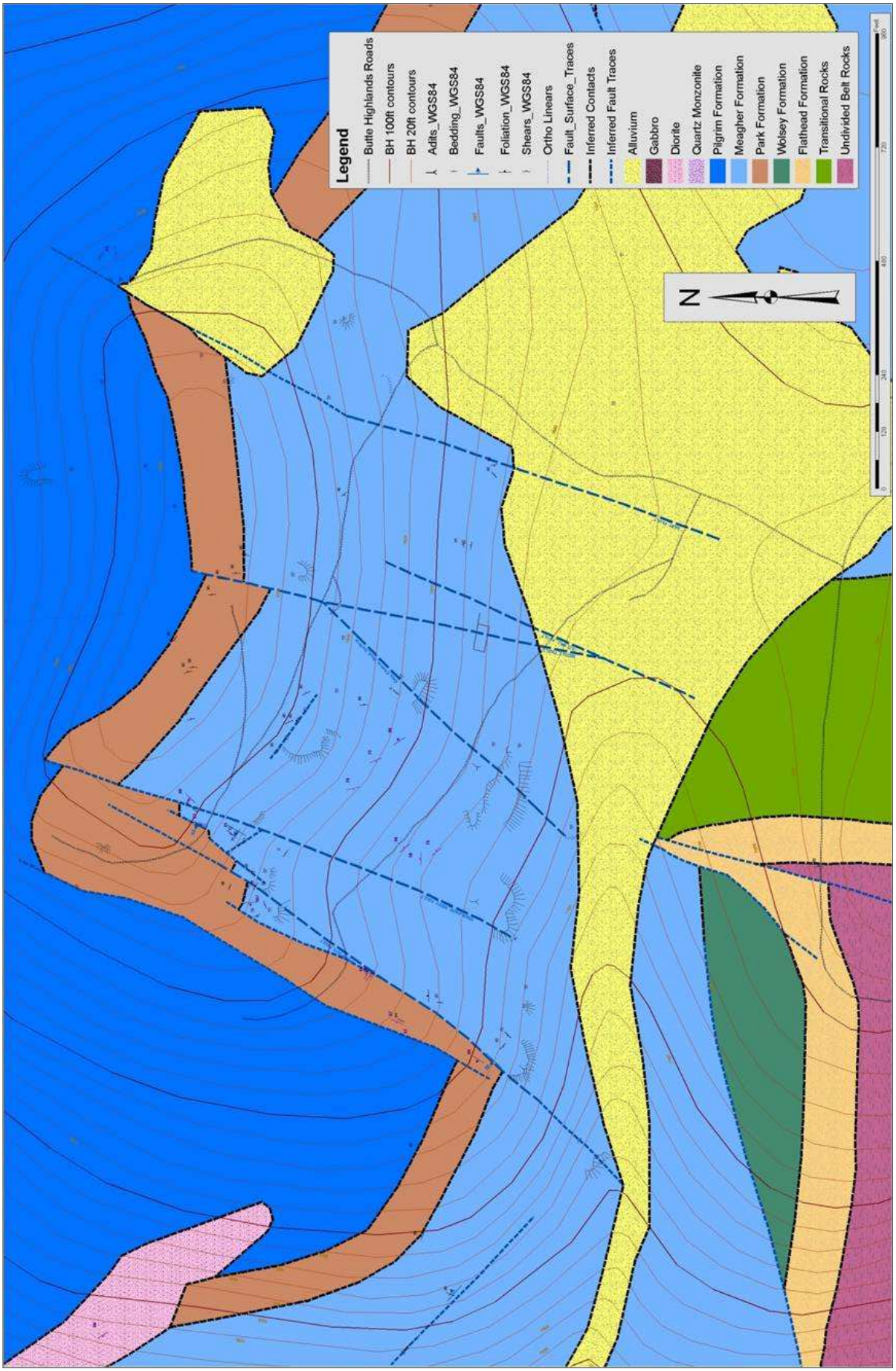

Figure 6. Geologic Map of the Nevin Hill area, Butte Highlands Gold Project.

controlled by Mr. Guill, a Timberline Director. Timberline and Highland agreed that Highland will fund the development of the underground gold mine at Butte Highlands, and that SMD will perform all development activities to advance the project to production. Under terms of the agreement, Timberline will be carried to production by Highland, and both Timberline's and Highland's 50-percent share of costs will be paid out of proceeds from future mine production.

On August 18, 2009, Timberline received its Amended Exploration Permit from the Montana Department of Environmental Quality (DEQ). This permit authorizes the company to proceed with its Butte Highlands underground development and exploration activities as a precursor to production.

Timberline and its 50% joint venture partner are now authorized to construct exploration drifts, perform surface and underground drilling, and extract a bulk sample. The DEQ permit allows a total surface disturbance of approximately 50 acres, including 20 acres for surface facilities. The exploration plan involves construction of drifts approximately 14 feet wide by 16 feet high and 6,700 feet in length. A drill program to further define and expand the resource anticipates 120 drill holes from 10-15 drill stations located throughout the drifts. The drill holes will average 500 feet in length for a total of approximately 60,000 feet of core drilling. The plan also anticipates collecting a 10,000 ton bulk sample. Underground development, exploration drilling and bulk sampling is anticipated to take approximately one year.

Site developments will include a ventilation raise area, a facilities area (shop, on-site power generation, fuel storage, and explosives storage), sediment and recycle water ponds, and waste rock storage. Improvements associated with the exploration project will include all facilities necessary for this development and future production, and will be confined to private lands owned by Timberline and the joint venture operating company.

This concludes the field trip. From Highland Junction, you can retrace our route back to Highway 2 and then north to Butte and Anaconda or you can follow the equally well-maintained US Forest Service Road 84 toward the Feeley Exit on I-15; this route follows the Moose Creek drainage for about 3 miles and then turns northwest toward Feeley.

Acknowledgements

The authors thank John and Karen Brower for the invitation to visit their property. Our visit to the Madison Gold project, especially the underground tour, was made possible by Dan Everett and Coronado Resources. Zane Smith of Timberline Resources provided background text on the Butte Highlands project and made arrangements for our visit. We also thank Ted Antonioli and Larry Johnson for their encouragement and keeping the dry run mileage on track.

Figure 7. View down the exploration decline, Butte Highlands Gold Project.

References cited

Cox, B.E., 1989, Report of 1989 Exploration - Toll Mountain Project, Jefferson County, Montana: Intracompany report for Golden Sunlight Mines, Inc., 8 p.

Czehura, S., and Zeihen, G., 2000, The Continental Orebody - Montana Resources: Guidebook of the 25th Annual Tobacco Root Geological Society Field Conference, p. 63-65.

Eggleton, R.A., 1975, Nontronite topotaxial after hedenbergite: American Mineralogist, v. 60, p. 1063-1068.

Gammons, C.H., Sotendahl, J., and Everett, D., 2010, Secondary enrichment of copper at the Madison Gold skarn deposit, Silver Star District, Montana: Northwest Geology, this volume.

Lyden, C.J, 1948, Gold Placers of Montana, Revised 1987: Montana Bureau of Mines and Geology, Reprint 6, 120 p.

Price, B.J., 2005, Madison Gold Property, Silver Star area, Madison Co., Montana, USA: Technical Report prepared for Minera Capital Corp., 118 p.

Vuke, S.M., et al., 2007, Geologic Map of Montana: Montana Bureau of Mines and Geology, Geologic Map 62.

A WALKING TOUR OF THE EOCENE ANACONDA DETACHMENT FAULT ON STUCKY RIDGE NEAR ANACONDA, MONTANA

Jeff Lonn and Colleen Elliott
Montana Bureau of Mines and Geology, Montana Tech, 1300 W. Park Street, Butte, MT 59701
jlonn@mtech.edu, celliott@mtech.edu

Introduction

This 5-mile off-trail hike is short on miles, but long on effort, and includes approximately 2000 feet of elevation gain and a steep scramble up a rocky bluff. We will walk along the Anaconda detachment fault, a mylonitic, low-angle normal fault zone that bounds the metamorphic core of the Anaconda metamorphic core complex, and examine lithologies and structures on both sides of the fault system.

Geologic Setting

The sinuous, aptly named Anaconda detachment fault is the major structural feature of the recently recognized Anaconda metamorphic core complex (O'Neill and others, 2002, 2004; Kalakay and others, 2003), and has been traced for over 60 miles along strike from the northeastern corner of the Flint Creek Range to the southeast flank of the Anaconda Range in the Big Hole Valley (Fig. 1). It dips gently east-to- southeast, separating amphibolite facies metasedimentary rocks intruded by granitic plutons on the west from lower grade sedimentary rocks to the east. Mineral lineations plunge east-southeast (102°-108°) and shear-sense indicators consistently show top-to-the-east-southeast transport. It was active from at least 53 to 47 Ma, and probably until 38 Ma (Grice and others, 2005; Grice, 2006). The timing and transport direction are identical to that of the parallel Bitterroot detachment fault 60 miles to the west, and the two are thought to be coeval "nested" core complexes (Foster and others, 2007).

The geology of the amphibolite-grade footwall rocks is extremely complex. Peak metamorphism of exposed rocks occurred at depths up to 12-18 km (Grice, 2006) during a period of Cretaceous crustal thickening produced by thrusting and intrusion prior to 75 Ma (Stuart, 1966; Kalakay and others, 2003; Grice and others, 2004, 2005; Grice, 2006; Haney, 2008). Near the end of peak metamorphism (about 79 Ma; Grice, 2006), the >40,000-foot-thick Mesoproterozoic through Mesozoic section was tectoni-

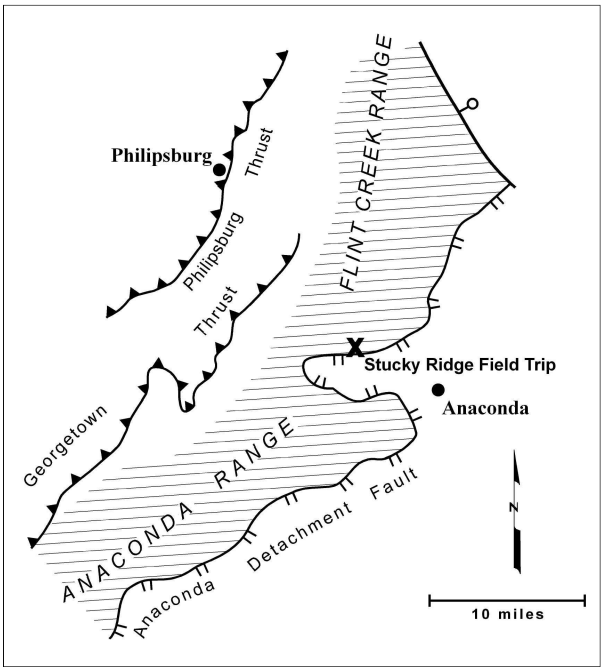

Fig. 1. Location of the field trip area with respect to major tectonic features of the Anaconda area. Cross-hatched area contains amphibolite-facies metamorphic rocks. Tick symbol on hanging wall of faults.

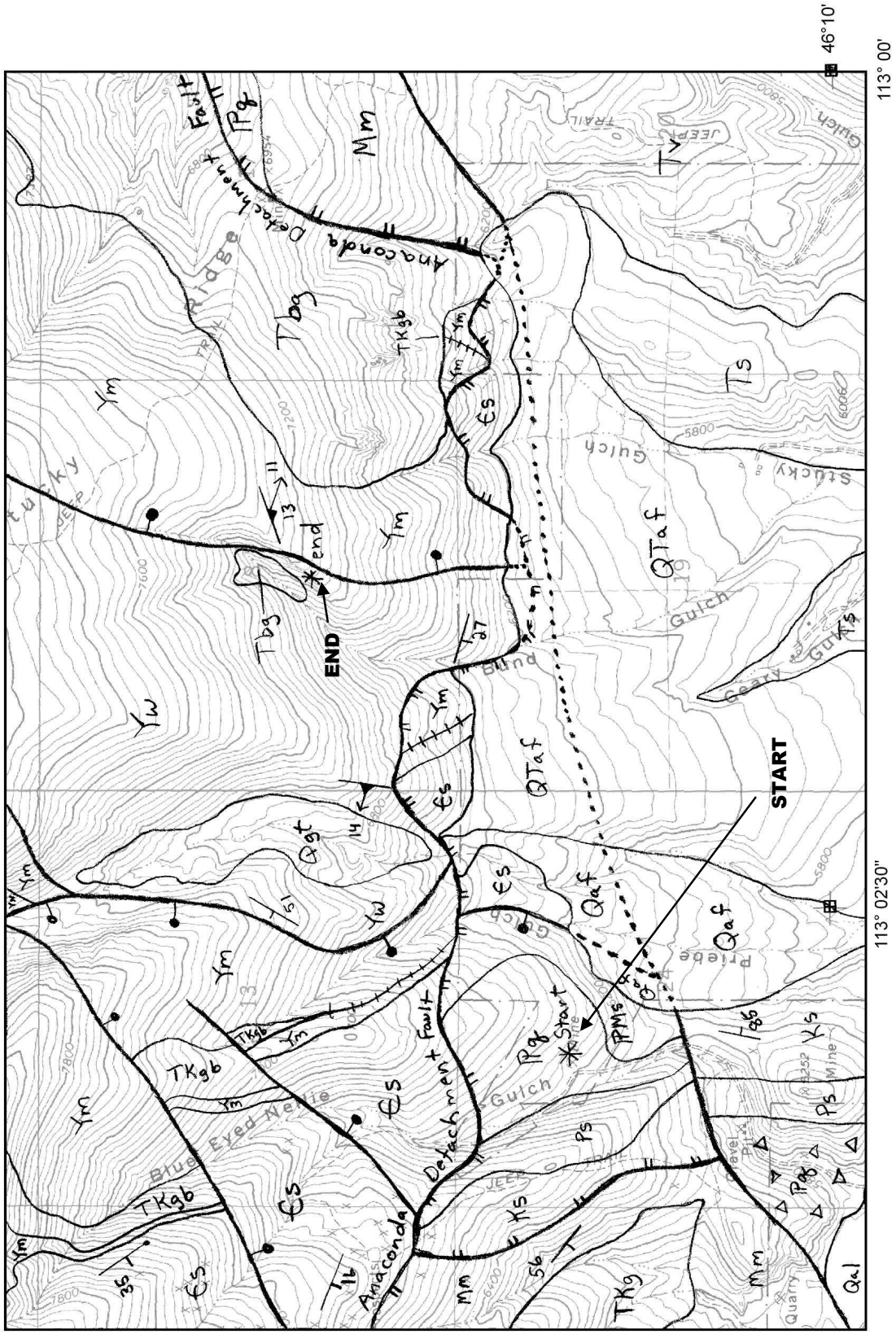

Fig. 2. Geologic map of the field trip area. Hiking route begins at the asterisk marked "start" and travels NE along Anaconda detachment to asterisk marked "end". Units from oldest to youngest: Yw—Wallace Fm; Ym—Missoula Gp; Ꞓs—Flathead, Silver Hill, and Hasmark Fms; Mm—Madison Gp; lPMs—Amsden Fm and Madison Gp; lPq—Quadrant Fm; Ps—sedimentary rocks; Ks—Kootenai Fm and Colorado Gp; TKgb—gabbro and diorite; TKg—granite; Tbg—Lost Creek granite; Tv—Lowland Creek volcanic; Ts—Anaconda beds; QTaf—alluvial fan deposits; Qgt—glacial till; Qaf—alluvial fan deposits; Qal—alluvium. Compiled from Emmons and Calkins, 1913; Csejtey, 1962; Lonn and others, 2003; Berger and Elliott, 2006. Map represents Lonn's interpretation. Topographic base from West Valley 7.5' quadrangle; contour interval 40 ft.

cally thinned by an array of bedding parallel structures that include: concordant mylonitic shear zones that cut out stratigraphic section, zones of vertical shortening that flatten the units through plastic flow, and brittle bedding-parallel faults that place younger units over older units. These structures are attributed to a period of late Cretaceous synorogenic extension in the Sevier hinterland (Lonn and McDonald, 2004a,b; Lonn and Lewis, 2009). Subsequent tectonism deformed the rocks into tight, NNE-striking, *west*-verging folds, many of which are overturned or recumbent. In addition, another period of thrust faulting occurred (Lonn and McDonald, 2004a; Berger and Elliott, 2006) that may be related to these folds. Voluminous plutonism also occurred between 80 and 50 Ma. The Eocene Anaconda detachment system cuts across all of these structures, although some intrusions, such as the Lost Creek granite (unit *Tbg* on Fig. 2), were intruded synchronously with, and probably facilitated, movement along the detachment. A retrograde hydration event also occurred during unroofing of the metamorphic core, and replaced most of the porphyroblasts with muscovite (Berger and Elliott, 2006). More folding and brittle faulting followed, modifying the trace of the Anaconda detachment.

Proterozoic through Mesozoic sedimentary rocks of the hanging wall exhibit brittle, ductile, and metamorphic fabrics inherited from the Cretaceous events, as well as extreme brecciation resulting from transport along the Anaconda detachment. Eocene Lowland Creek volcanic rocks that interfinger with coarse clastic and landslide deposits derived from unroofing of the Anaconda core complex unconformably overlie these rocks in fault bounded basins (O'Neill and others, 2004; O'Neill, 2005).

The complex structural history of this area might be summarized as follows (modified from Lonn and others, 2003; Berger and Elliott, 2006):

D_1: Horizontal shortening driven by convergent tectonism produced crustal thickening accompanied by intrusion (middle to late Cretaceous).

D_2: Amphibolite-grade metamorphism and formation of bedding-parallel foliation (S_2), shear zones, and faults that tectonically thinned the strata; accompanied by intrusion (late Cretaceous).

D_3: Thrust and reverse faulting, west-vergent folding, and creation of related foliation (S_3), accompanied by intrusion (late Cretaceous).

D_4: Exhumation of the Anaconda core complex beneath the top-east Anaconda detachment; formation of associated mylonite (S_4), accompanied by intrusion and extrusion (Eocene).

D_5: NE-SW-directed folding (F_5) that lacks axial plane foliation.

D_6: Brittle normal and strike-slip faulting and formation of N-S vertical fracture cleavage (S_6) (Oligocene-Holocene?).

On this field trip we will walk along the mylonitic lower strand of the Anaconda detachment fault and be able to compare and contrast lithologies and structures in its hanging wall and footwall.

To the trailhead
Mileage

0.0 Main street, downtown Anaconda. Drive west on State Highway 1.

1.0 Safeway. On your left is the Anaconda (Pintler) Range; the smooth slope that drops towards us is developed on the resistant Anaconda mylonite. To the right is a timbered plateau that slopes south, the opposite direction; this is Stucky Ridge and is our destination. It is also developed on the Anaconda mylonite. You are driving up the West Valley corrugation, a broad gentle syncline whose axis is parallel to the direction of transport on the Anaconda detachment. The West Valley corrugation separates the Anaconda and Flint Creek Ranges topographically, but geologically these mountains are one and the same. Watch your speed for the next few miles through the Anaconda speed trap!

5.2 Turn right on Philips Road.

5.3 Turn left on North Cable Road at the "T" intersection.

5.6 Turn right on unmarked dirt road just past a small quarry that exposes steeply dipping sedimentary rocks, and drive north towards Blue-Eyed Nellie Gulch.

5.7 Forest service gate that is open during the summer months. High-clearance vehicles only beyond this point; all others should park here. Road proceeds up Blue-Eyed Nellie Gulch through brecciated upper Paleozoic and Mesozoic sedimentary rocks in the Anaconda detachment fault hanging wall.

6.2 Steep roads fork in both directions; stay on track in valley bottom.

6.7 Park at the quarry where there is ample space.

The Hike

You are now at the asterisk marked "start" on Fig. 2, and will work your way northeast, following the trace of the Anaconda detachment to the asterisk labeled "end".

The quarry is developed in brecciated Quadrant Formation (*lPq*) that is just above the lower strand of the Anaconda detachment. The detachment can be seen just up-valley (north) as a line of white outcrops that are composed of mylonitic Cambrian Hasmark Formation (*€s*). In most places the hanging wall of this fault is a chaotic jumble of various formations. In fact, O'Neill and Lageson (2003) termed this particular area the "West Valley chaos". In some places, a distinct upper strand exists that parallels the lower strand (Fig. 3a), but in this area the structure is less ordered. However, the open knob immediately to the south is underlain by Cretaceous sedimentary rocks on the other side of at least one fault.

Traverse upward along the right (south) side of the quarry and climb to the crest of the ridge above the quarry. From the ridge top, our destination is visible to the east. The timbered plateau is Stucky Ridge and is capped by the fault plane of the Anaconda detachment fault (Fig. 3b). The fault plane also defines the smooth southward slope of Stucky Ridge; there the detachment dips south into the West Valley corrugation. The rounded orange outcrops that protrude from this slope in the distance are Lost Creek granite (*Tbg*), which appears to have been emplaced while the detachment was active. Our route contours eastward near the base of this slope, crossing the first canyon, Prieble Gulch, near

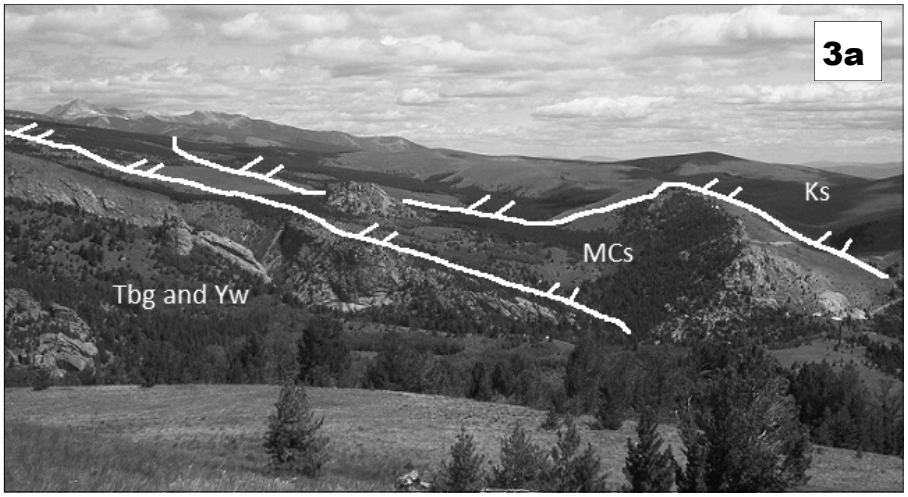

Fig 3. a) View of the two parallel strands of Anaconda detachment system looking north from Stucky Ridge. Tick marks on hanging wall. Units: Tbg and Yw—Lost Creek granite and Wallace Fm; M€s—sedimentary rocks; Ks—sedimentary rocks.

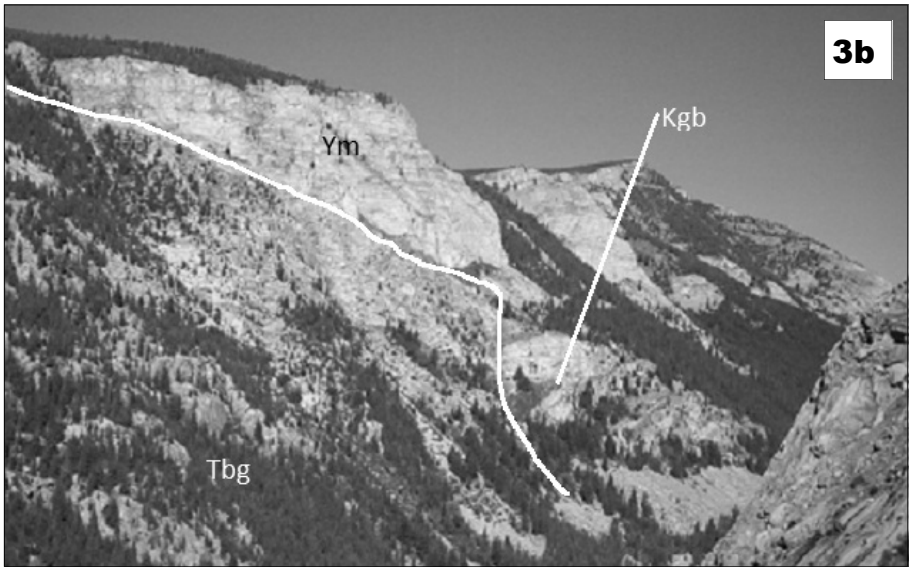

b) South wall of Lost Creek Canyon showing relationships between units: Yw—Wallace Fm; Kgb—gabbro and diorite sills; Tbg—Lost Creek granite. Plateau is capped by the Anaconda mylonite.

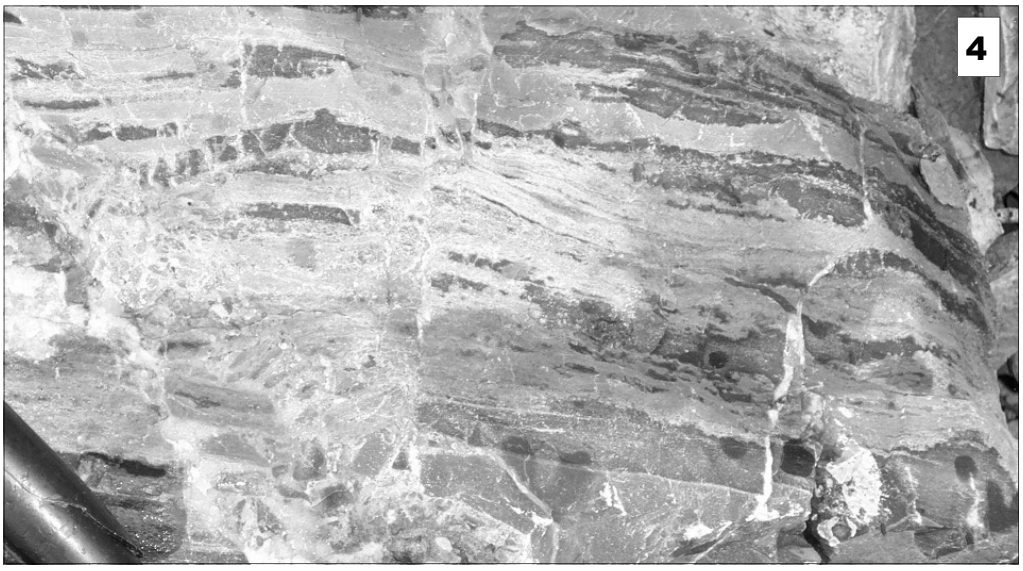

Fig. 4. Deformed Madison Group limestone in the hanging wall of the detachment near the start of the hike. Black bands are chert. Foliation is thought to be Cretaceous and not related to the Eocene mylonite.

its mouth, and ascending the second canyon, Bund Gulch, to the cliffs visible on its east rim. Essentially, we will be walking along the Anaconda detachment fault all day.

Descend towards the mouth of the first drainage, aiming for the fenced knob on the other side. Along the way, the rocks underfoot change from Quadrant quartzite (*lPq*) to Madison limestone (*Mm*), still in the hanging wall of the Anaconda detachment. However, note the prominent mylonitic-appearing foliation in the Madison (Fig. 4). Did the foliation form through shear along the Eocene Anaconda detachment, or is it inherited from an earlier event? We interpret this foliation to be S_2, having formed parallel to the beds during the Cretaceous extensional event. Obviously there are metamorphic rocks in the hanging wall of the Anaconda detachment, which is uncharacteristic of a classic core complex. Perhaps this is in part due to the fact that the Anaconda core complex exhibits less exhumation than many others such as the Bitterroot core complex (Foster and others, 2007).

Ascend the knob with the fence; it is composed of dolomite breccia (Cambrian Hasmark Formation, *€s*?). The adjacent small saddle marks the Anaconda detachment, with schistose Mesoproterozoic Missoula Group rocks (*Ym*) on the north side. No mylonite was found here; perhaps a late brittle fault cut it out. Looking back to the northwest into the footwall, the Cambrian Flathead Formation (*€s*) forms a rib at the top of the ridge on the other side of the drainage. The Missoula Group is quite thin here as a result of a bedding-parallel fault (see Fig. 2) attributed to the Cretaceous extensional event.

Cross the next drainage, filled with glacial till, and ascend along the fenceline through gray and white dolomite of the Hasmark Formation, quartzite of the Flathead Formation, schistose Missoula Group, and into a diorite sill within the uppermost Missoula Group. This sequence is interpreted to be in the hanging wall of the Anaconda detachment: higher on this slope a bench marks the trace of the fault, with mylonitic Wallace Formation (*Yw*) on the other side. Lineations in the mylonitic Wallace trend ESE-WNW. The west-dipping hanging wall sequence exposed here, including the diorite sill near the top of the Missoula Group, is repeated at the hill with the quartzite rib that we viewed from the knob, but the rib is in the footwall of the Anaconda detachment. Restoration of the hanging wall rocks along a WNW bearing to the rib (see Fig. 2) suggests displacement along this strand of the Anaconda detachment is only 3500 feet! But we have already seen that Cretaceous rocks are in close proximity; clearly other fault strands were active in the exhumation of the footwall rocks.

Gabbro and diorite sills of at least two ages occur in the area. The earlier intrusions are thought to be Cretaceous because some have developed a foliation that is parallel to the bedding-parallel S_2 fabric in the country rocks. One of these deformed diorite sills in the eastern Anaconda Range yielded a U-Pb crystallization date of 75 Ma (Grice, 2006). There are also younger mafic intrusions that appear to be an early phase of the Eocene Lost Creek granite. These are deformed only along the Anaconda detachment, and we will examine them in Bund Gulch. The sill here is tentatively assigned to the older Cretaceous unit.

Continue contouring through schistose and gneissic Missoula Group rocks and cross the covered lower strand of the Anaconda detachment into pale green and white, calc-silicate-rich metasedimentary rocks assigned to the Mesoproterozoic Wallace Formation. Contour into Bund Gulch. The opposite canyon wall displays gently south-dipping layers in the Wallace Formation. Do these lay-

ers represent bedding, transposed bedding, or mylonite developed along the Anaconda detachment, which here forms a dip slope? We will be able to examine them closely as we ascend the cliff up-canyon.

Walk up the canyon floor. The raspberry brush and talus make for tough traveling, although maybe the raspberries will be ripe in August. You will have ample time to view boulders that contain pinch-and-swell beds and limestone, verifying that this is indeed Wallace Formation. At least some of the layers must represent bedding . Eventually you will reach an open area with rusty-weathering granite outcrops visible ahead and a large cliff to your right. We will ascend the talus slope here, but first pause to examine some of the granite float.

The granite is coarse-grained biotite granite that is part of the Lost Creek stock (*Tbg*). The stock is intruded discordantly into Belt rocks along the Anaconda detachment (Fig 3b). Here the granite is massive and non-foliated, but mylonite and breccia are inconsistently developed in it where the Anaconda detachment forms its roof near the mouth of Lost Creek Canyon. It probably intruded the Anaconda detachment syntectonically like many of the intrusions in the eastern Anaconda Range (Foster and others, 2007), and its age is estimated at 53 Ma. Prospects and mines explore the margins of the granite.

Before reaching the large rusty-weathering granite outcrops, ascend the talus towards the base of the cliffs to the right. The cliffs expose many interesting relationships between rock types (Fig. 5a). The layers do appear to be sedimentary beds, although some of them appear to be sheared parallel to the beds. The associated foliation is interpreted to be S_2 that formed in the Cretaceous extensional event, but in this area the Anaconda mylonite is also parallel to these layers. Note that a cross-cutting cleavage (S_3) also occurs; it is thought to have formed in association with later Cretaceous folding and /or thrusting (Berger and Elliott, 2006). Undeformed granitic sills and dikes that are probably related to the Eocene Lost Creek granite are common, and probably emplaced synkinematically with the Anaconda detachment. Some granitic sills are rimmed by deformed mafic material (Fig. 5b) as if the mafic rock represents an early phase of the granite. Either the mafic rock was more easily deformed than the granite, or it crystallized early enough to be deformed by ductile shear along the Anaconda detachment, while the granite did not.

Continue up through a cleft on climber's right; exit to the rim is aided (or perhaps made more dangerous) by wooden ladders that must have been placed for access to the mines below. When were these mines active? It has probably been long enough to be untrusting of the rungs, but we can easily scramble up using natural steps in the rocks. Note that as you ascend the final 30 feet, the bedded and layered character of the rock fades: it is replaced by intervals of foliated limestone containing silty or sandy porphyroclasts, alternating with layers of dark-colored, hard, flinty mylonite. Lenses of breccia also occur. These uppermost rocks represent the Anaconda detachment fault itself. Here the Eocene mylonite (S_4) has developed parallel to the Cretaceous bedding-parallel foliation (S_2), so it is hard to distinguish the two. This area underscores the difficulties of deciphering the structural history of the Anaconda region. As many as six generations of deformational structures are evident (Berger and Elliott, 2006), with at least two generations of mylonitic fabric, at least three fold generations, and at least three generations of brittle faults.

Turn left and walk north along the rim formed by the resistant mylonite. The hang-

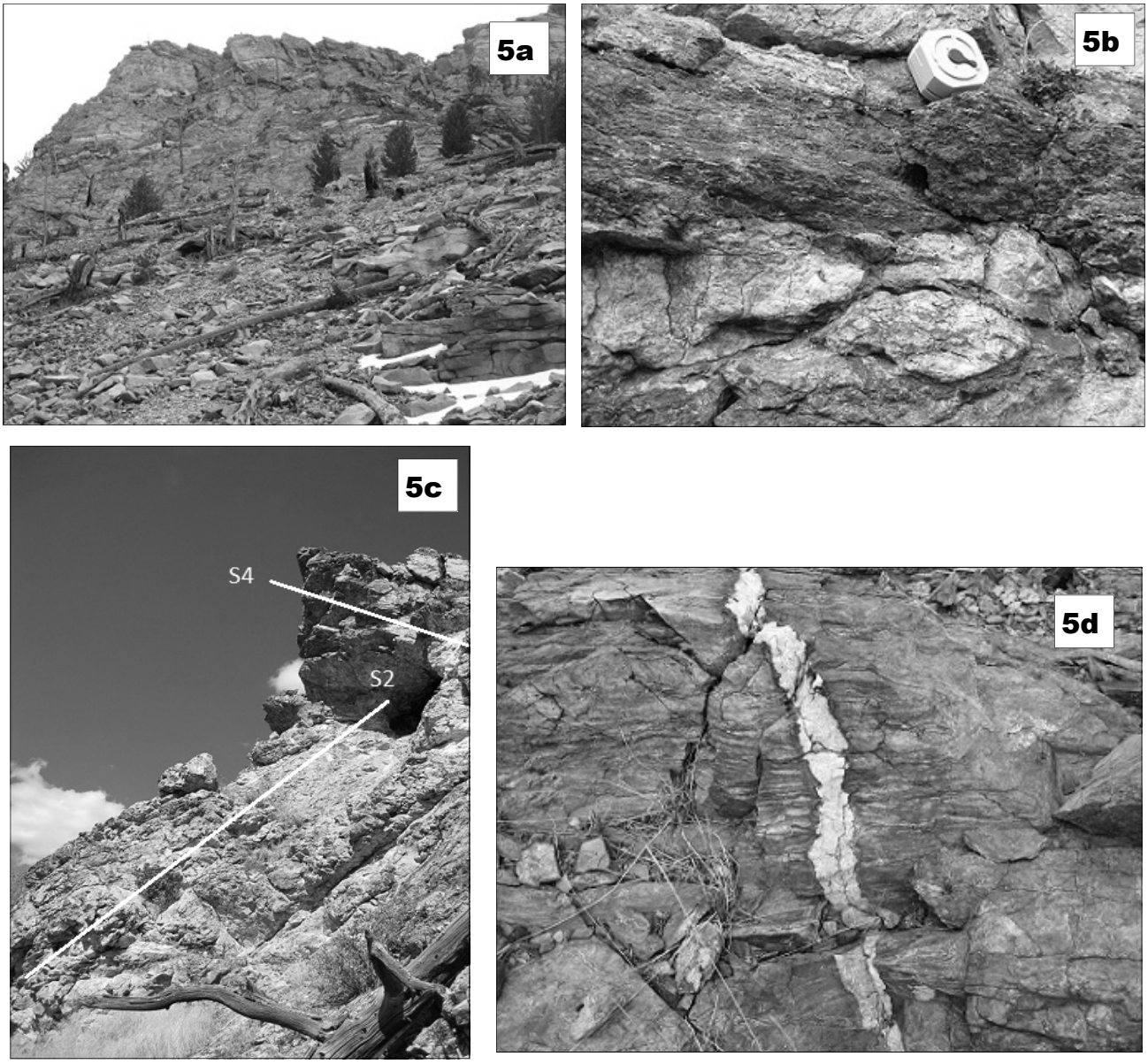

Fig. 5. a) View of the cliffs of Bund Gulch showing light colored granitic sills in horizontally layered Wallace Fm. b) Close-up of a granite sill that is rimmed with deformed mafic rock. Deformation is the result of shear along the Eocene Anaconda detachment. c) Eocene Anaconda mylonite (S_4) cutting the Cretaceous foliation and layering (S_2) north of Lost Creek. In the field trip area, the two foliations are parallel. d) Aplite dikelet cutting Eocene mylonite.

ing wall rocks have been eroded away. Mylonitic lineations are difficult to locate, but they bear ESE-WNW. If we find some, we will look for shear-sense indicators to verify the top-east movement of the Anaconda detachment (Fig. 6). A few aplite dikelets cut the mylonite (Fig. 5c), again illustrating the syntectonic character of the igneous rocks here. Note also the float of unfoliated mafic igneous rock that could be either Eocene or Cretaceous.

About 100 yards northward along the rim, the rock turns much darker. We have crossed a N-S-trending fault that must be older than the Anaconda detachment because the mylonite is now is developed in the Missoula Group. You can see that mylonite developed in these metasediments is not as obvious as mylonite developed in igneous rocks, and perhaps explains why this core complex went so long unrecognized.

END OF TRIP. Return to the cars by walking down the mylonitic surface forming the east rim of Bund Gulch until crossing becomes easier, and then retrace your steps to the cars.

References Cited

Berger, A., and Elliott, C., 2006, Detailed structural geology of the central part of the West Valley 7.5'quadrangle, southwest Montana: Montana Bureau of Mines and Geology Open File Report 560, 10 p., map scale 1:24,000.

Csejtey, Bela, 1962, Geology of the southeast flank of the Flint Creek Range, western Montana: Princeton, NJ, Princeton University, Ph.D. dissertation, 175 p., map scale 1:62,500.

Emmons, W.C., and Calkins, F.C., 1913, Geology and ore deposits of the Philipsburg quadrangle, Montana: U.S. Geological Survey Professional Paper 78, 271 p.

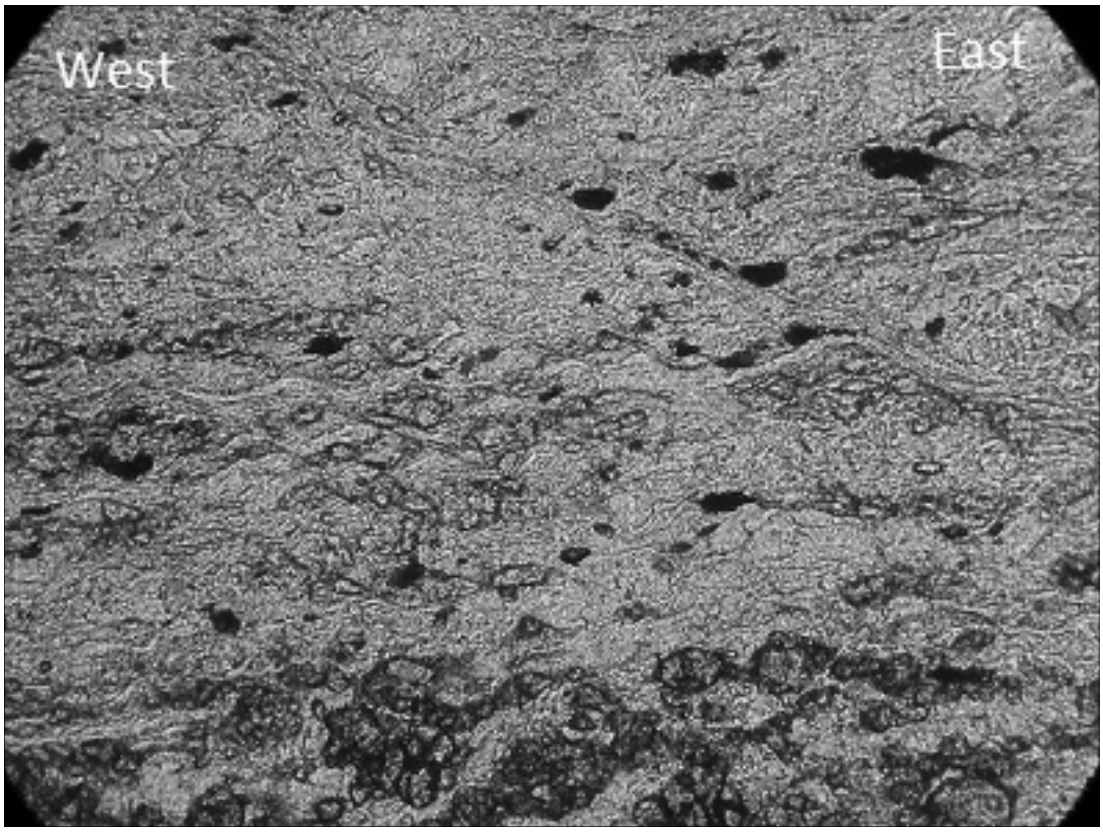

Fig. 6. Photomicrograph of Anaconda mylonite sample collected near Lost Creek with extensional shear bands that show top-east shear sense. Mylonite is developed in meta-Wallace Fm; dark porphyroclasts are clinozoisite.

Foster, D.A., Doughty, P.T., Kalakay, T.J., Fanning, C.M., Coyner, S., Grice, W.C., and Vogl, J., 2007, Kinematics and timing of exhumation of metamorphic core complexes along the Lewis and Clark fault zone, northern Rocky Mountains, USA: Geological Society of America Special Paper 434, p. 207-232.

Grice, W.C., Jr., 2006, Exhumation and cooling history of the middle Eocene Anaconda metamorphic core complex, western Montana: Gainesville, University of Florida, M.S. thesis, 260 p., map scale 1:100,000.

Grice, W.C., Jr., Foster, D.A., Kalakay, T.J., Bleick, H.A., and Hodge, K., 2004, Style and timing of crustal attenuation in the Anaconda metamorphic core complex, western Montana: Geological Society of America Abstracts with Programs, v. 36, no. 5, p. 546.

Grice, W.C., Jr., Foster, D.A., and Kalakay, T.J., 2005, Quantifying exhumation and cooling of the Eocene Anaconda metamorphic core complex, western Montana: Geological Society of America Abstracts with Programs, v. 37, no. 7, p. 230.

Haney, E.M., 2008, Pressure-temperature evolution of metapelites within the Anaconda metamorphic core complex, southwestern Montana: Missoula, University of Montana, M.S. thesis, 110 p.

Kalakay, T.J., Foster, D.A., and Thomas, R.C., 2003, Geometry and timing of deformation in the Anaconda extensional terrane, west-central Montana: Northwest Geology, v. 32, p. 124-133.

Lonn, J.D., and McDonald, C., 2004a, Geologic map of the Kelly Lake 7.5' quadrangle, western Montana: Montana Bureau of Mines and Geology Open File Report MBMG 500, 15 p., scale 1:24,000.

Lonn, J.D., and McDonald, C., 2004b, Cretaceous(?) syncontractional extension in the Sevier orogen, southwestern Montana: Geological Society of America Abstracts with Programs, v. 36, n. 4, p. 36.

Lonn, J., and Lewis, R., 2009, Late Cretaceous extension and its relation to the thin stratigraphic section in the Philipsburg area: A field trip to Carpp Ridge: Northwest Geology, v. 38, p. 141-152.

Lonn, J.D., McDonald, C., Lewis, R.S., Kalakay, T.J., O'Neill, J.M., Berg, R.B., and Hargrave, P., 2003, Preliminary geologic map of the Philipsburg 30' x 60' quadrangle, western Montana: Montana Bureau of Mines and Geology Open File Report MBMG 483, 29 p., scale 1:100,000.

O'Neill, J.M., 2005, Syntectonic Anaconda Conglomerate (new name)—A stratigraphic record of early Tertiary brittle-ductile extension and uplift in southwestern Montana: U.S. Geological Survey Professional Paper 1700, Chapter A, p. 1-15.

O'Neill, J.M., and Lageson, D.R., 2003, West to east geologic road log: Paleogene Anaconda metamorphic core complex: Georgetown Lake Dam-Anaconda-Big Hole Valley: Northwest Geology, v. 32, p. 29-46.

O'Neill, J.M., Lonn, J.D., and Kalakay, T., 2002, Early Tertiary Anaconda Metamorphic Core Complex, southwestern Montana: Geological Society of America Abstracts with Programs, v. 34, no. 4, p. A10.

O'Neill, J.M., Lonn, J.D., Lageson, D.R., and Kunk, M.J., 2004, Early Tertiary Anaconda metamorphic core complex, southwestern Montana: Canadian Journal of Earth Sciences, v. 41, p. 63-72.

Stuart, C.J., 1966, Metamorphism in the central Flint Creek Range, Montana: Missoula, University of Montana, M.S. thesis, 103 p., map scale 1:6,000.

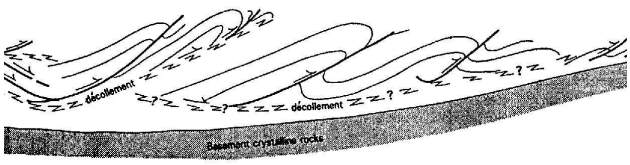

CABLE MOUNTAIN MINING DISTRICT, MONTANA: A ROAD LOG FOR UPPER WARM SPRINGS CREEK, HIDDEN LAKE AND CABLE MOUNTAIN

Skip Yates[1], Henry Follman[2], and Ted Antonioli[3]
[1]Lolo, Montana; [2]Lovelock, Nevada; [3]Missoula, Montana

Introduction

Cable Mountain is a NNE-trending ridge between the North Fork of Flint Creek and upper Warm Springs Creek that stretches over 6 miles from Georgetown to Fred Burr Pass (Figure 1). The larger historic gold mines in this district include Southern Cross, Cable, Hidden Lake and Red Lion; smaller mines and gold mineralization occur throughout the mountain's entire length. Cable Mountain lies east of and below the Georgetown thrust fault and just south of the Philipsburg batholith. Complexly faulted and folded strata range from Precambrian upper Wallace formation hornfels to Mississippian Madison limestone.

A major fault, variously called the Twin Peaks or Hidden Lake fault, places Precambrian Belt Supergroup strata on the west against Paleozoic strata (mostly Madison formation) on the east. The dip of this fault changes along strike from easterly in upper Warm Springs Creek to westerly at the Hidden Lake mine, as shown by extensive drilling during gold exploration. Large intrusive granodiorite bodies include the Philipsburg batholith to the north and the Cable stock on the south. Smaller intrusive bodies, some possibly as young as Eocene, range in composition from alaskite to diorite.

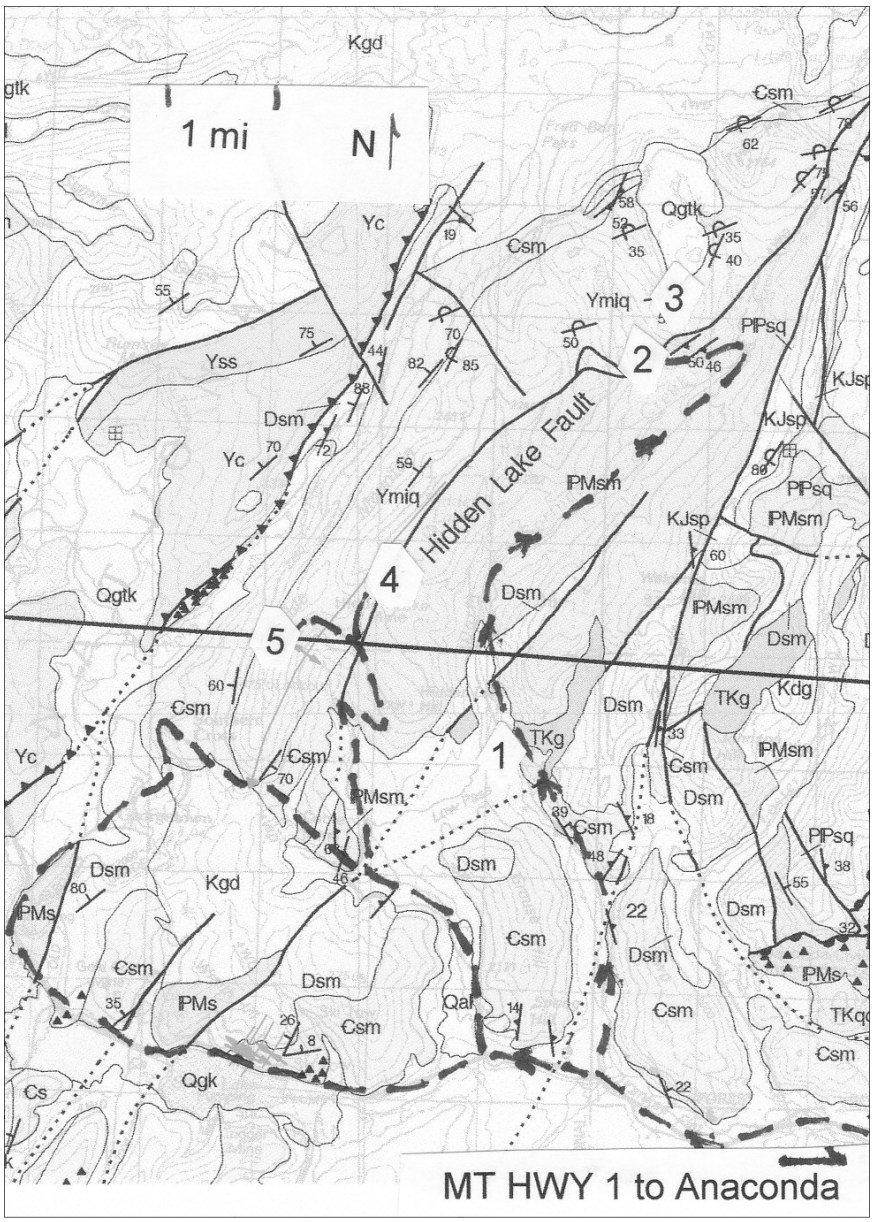

Figure 1. Index map to Cable Mountain/upper Warm Springs field trip road log. Base map is the geologic map in Lonn, et al, 2003.

This field trip will attempt to shed light on some of the complex structural relationships and will examine several key gold and silver deposits on Cable Mountain. Skip Yates is the primary author for stops in upper Warm Springs Creek, Henry Follman for the Hidden Lake mine, and Ted Antonioli for the Cable Mountain and Cable mine areas.

Road Log

0.0 Anaconda High School. Head north on Main Street to Commercial Avenue (MT Hwy 1). Turn left on Commercial and head west towards Georgetown Lake and Philipsburg.

10.5 Turn right on Warm Springs Creek Road. Signs for Lower Warm Springs Campground.

12.8 Lower Warm Springs Campground. Valley floor is glacial till. Mostly Cambrian Hasmark dolomite on hillsides. Just beyond the campground on the right we will go upsection through Cambrian Red Lion, Silurian Maywood, Devonian Jefferson and Mississippian Madison formations.

STOP 1 13.9 STOP 1. Large pull-off on right side of road. Talus on hillside is from a small altered granitic intrusive, labeled "Granite Porphyry of Upper Warms Spring Creek" by Emmons and Calkins (1913). Quartz and potassic feldspar phenocrysts in fine grained siliceous groundmass with abundant pyrite and sericite with rare disseminated chalcopyrite. This intrusive does not form bold outcrops; in fact it underlies Clay Charlie Basin just to the east of this stop. There is also a small exposure on the west side of Warm Springs Creek. Contact with Madison appears concordant in places.

14.8 Very rough road to Hidden Lake mine on left.

19.2 Cross thrust(?) fault from Madison limestone onto upper Wallace (?) calc-silicate hornfels.

19.5 Small exposure of two different intrusives approximately 150 ft above road.

19.8 Cross the West Fork of Warm Springs Creek.

From here proceed west up rough jeep trail approximately 0.5 mile to

STOP 2 STOP 2. Silver Queen Mine. There is a small klippe (detachment) of Hasmark dolomite on top of upper Wallace (or Shepard?) hornfels. Quartz-tetrahedrite ore was mined for silver from a shallow shaft and two drifts. Copper oxides are common in the waste rocks on the dump. Select samples were reported to assay over 200 oz/ton Ag. The contact between the Hasmark and Precambrian strata is a limonite-rich tactite zone that ranges up to several feet in thickness.

From the creek crossing, proceed north on jeep road slowly climbing up ridge to the east.

At 0.8 mile, road switchbacks in an old clearcut. Continue south on level road approximately 0.5 miles to

STOP 3 STOP 3. Nineteen Hundred and St. Thomas high-grade gold mines. Both mines worked thin sheeted vein zones that cut across bedding. At the St. Thomas, which is approximately 400 feet north of the Nineteen Hundred, the vein contains tourmaline and specimens containing visible gold can be found on the dump. Ap-

proximately 600 feet south of the Nineteen Hundred, there is a unique outcrop of white quartzite breccia with large fragments.

General discussion, West Fork of Upper Warm Springs.

Richard Sherry and Skip Yates mapped the West Fork as part of a minerals evaluation for gold ore in the late 1980s. Richard Sherry, who passed away in 2008, did the lion's share of the mapping. A simplified version of the mapping is shown in Figure 2. The West Fork is a complex stratigraphic and structural area with several unresolved questions, especially in the vicinity of the Nineteen Hundred Mine.

Imbricate thrusting is suggested by numerous northeast-trending veins and faults that crosscut bedding at low angles. The strata are almost all overturned: the few upright bedding orientations appear to be due to small scale folding. Younger northwest-trending faults offset the northeast structures. Subtle east-west structures appear to be a contributing factor in localizing mineral deposits.

One travels down-section descending southeast from the top of Cable Mountain into the West Fork. Overturned Cambrian Red Lion, Hasmark, Silver Hill and Flathead formations cap Cable Mountain. The Cambrian is noticeably thinned, especially near the contact of the Philipsburg batholith. Unconformably (?) below the Flathead is thick sequence of Missoula group quartzite composed of at least three members: 1) up to 1000 feet of light gray to gray, fine-grained, cross-bedded quartzite, 2) up to 2000 feet of white, medium-grained, massive to cross-bedded quartzite, and 3) up to 1000 feet of gray, fine-grained, cross-bedded quartzite. It is likely that at least some of this quartzite correlates with the Mount Shields formation. In the Nineteen Hundred mine vicinity, this lower gray quartzite is structurally underlain by gray phyllite, medium to coarse-grained white quartzite and gray phyllitic non-cross-bedded quartzite. Elsewhere, the lower gray quartzite is in structural (thrust?) contact with upper Wallace (or Shepard?) actinolite-biotite-diopside hornfels.

Return to MT Hwy 1 by the same route. Reset odometer. Turn west toward Georgetown Lake.

0.9 Miles. Turn right on Cable Creek Road.

Proceed approximately two miles to junction with Cable mine road to left. Keep straight.

Proceed approximately three additional miles to junction with Cable Lookout road. Keep right. In approximately one additional mile the road passes through the site of the Hidden Lake mine.

STOP 4. Hidden Lake mine

STOP 4

Background

The Hidden Lake Mine property consists of four contiguous patented claims (Gold Bug No. 1 and 2 and the Cecelia May No. 1 and 2, US Mineral Survey Number 9593, 80 acres private property) surrounded by U.S. Forest Service lands, all lying in sections 34, and 35, T6N, R13W Granite County, Montana. The nearest town is Anaconda, some 15 miles to the east. The area is forested at 7300 to 7700 feet elevation on the east flank of Cable Mountain. There is snow in the winter and access can be difficult from January through May. There is a small lake (Hidden Lake) approximately one-half mile to the northeast. The property is owned by Coastal Mines, a Texas Corporation. Figure 3 shows the claim boundaries and location.

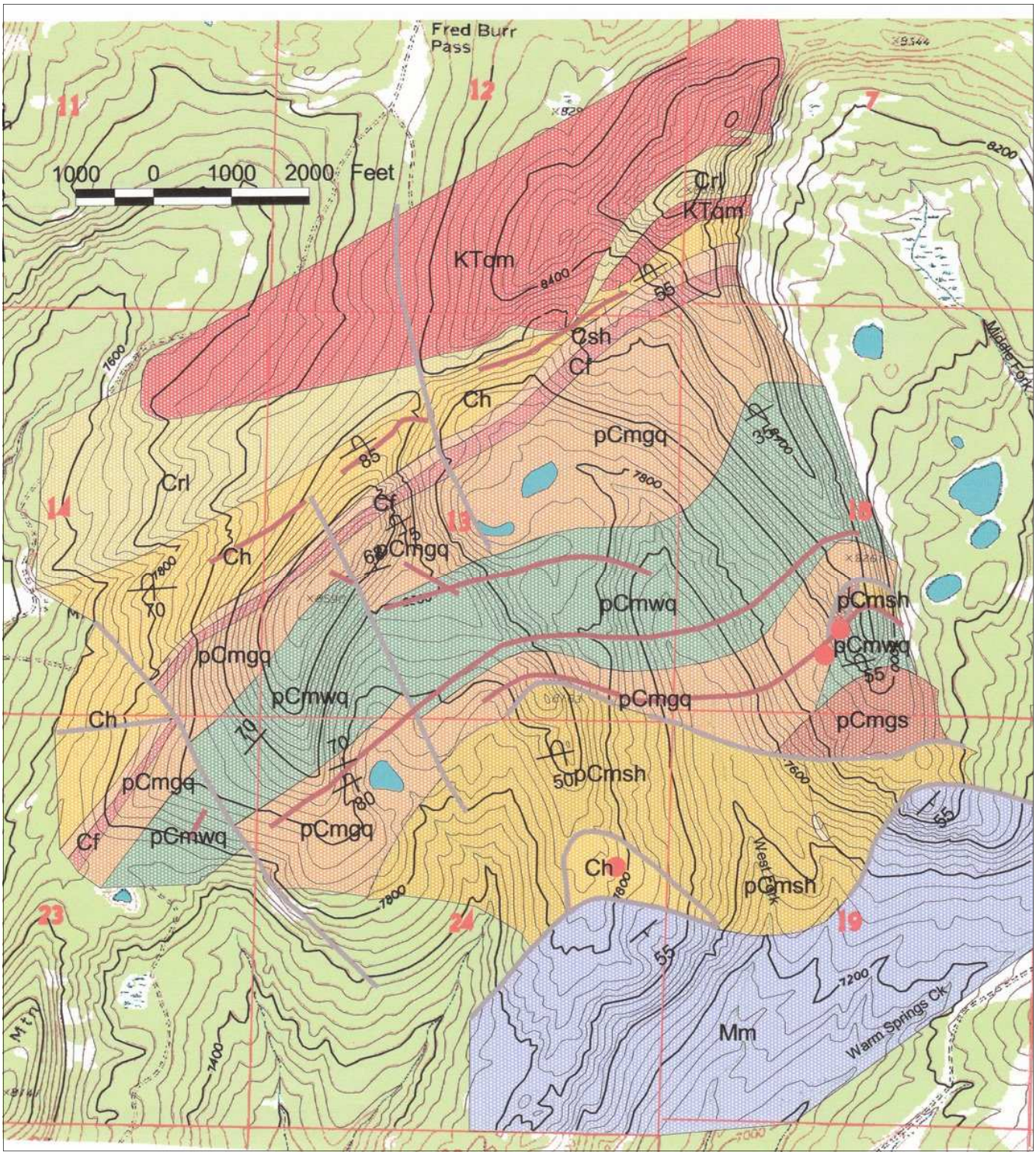

Figure 2. Geologic map of upper Warm Springs Creek, by Richard Sherry and Skip Yates, 1990. KTqm = Cretaceous or Tertiary quartz monzonite intrusive. Mm = Mississippian Madison limestone. Crl = Cambrian Red Lion. Ch = Hasmark. Csh = Silver Hill. Cf = Flathead. pCmgs = Missoula Group gray siltite. pCmgq = Missoula Group gray cross-bedded quartzite. pCmwq = Missoula Group white quartzite. pCmsh = upper Wallace (or possibly Missoula Group Shepard?) calc-silicate actinolite-biotite hornfels. Red lines=mineralized faults. Gray lines = unmineralized faults. Fault lines solid where exposed, dashed where covered. Red dots = mines discussed in text.

Historically, the property forms a mining sub-district (Hidden Lake District) within the greater Cable Mountain Mining District (sometimes listed under the Georgetown District), and there are several other nearby sub-districts with significant historic gold production. Earll (1972) provides information on all the significant mines and prospects.

The Southern Cross mine, approximately two miles to the southwest, has documented production of approximately 250,000 gold ounces, with some reports stating as high as 400,000 gold ounces. The Cable mine, 2.5 miles to the south, produced on the order of 180,000 gold ounces. The Red Lion mine, 2.5 miles to the north, produced as much as 10,000 ounces. Directly to the west a half-mile is the Golden Eagle mine, which reportedly produced a few thousand ounces. There is considerable data available on these mining districts and brief historical commentaries of the various mines and districts can be viewed at http://www.deq.state.mt.us/abandonedmines/linkdocs/66tech.mcpx

With the exception of Hidden Lake and the nearby Golden Eagle, all the important deposits in the district were found in limestone near granodiorite intrusives, particularly at the Cable mine where extremely high-grade gold ores were found.

The Hidden Lake mine produced some 24,132 ounces of gold from approximately 98,000 tons of ore during 1934 through 1939 (most of the production during 1935-38) using a 75-ton-per-day Cyanide / Merill-Crowe milling plant.

The mine was originally developed by a 200' shaft, with crosscuts and a winze down to the 450' level. Stope were in many places as wide as 40-60 feet for 200-400 feet along strike. The ore occurred in shattered quartzite and argillite within a highly faulted zone known regionally as the Hidden Lake fault.

It is unclear why the mine eventually shut down, but it is likely that new development work did not keep up with the pace of the rapid mining of the largest stopes and insufficient new development capital was available once the big stopes were depleted. The mine sat idle until 1986 when Coastal purchased the property.

During 1987 and 1988, Coastal mined 10,000 tons (mostly dump material with a minor amount of freshly mined material from surface) of ore grading 0.134 oz/t Au and transported it to a plant site 37 miles west, outside of Philipsburg, MT. There the ore was crushed to minus 3/4" and heap leached. From this exercise, slightly more than 1,000 ounces were recovered with an approximate gold recovery of 75%.

From 1986 through 1993 exploration options were taken on the property in succession by Meridian Minerals, Western Gold Exploration (West Gold), and finally by Pegasus Gold. The total work consisted of 96 drill holes representing 36,540 feet of drilling, surface and road-cut sampling, and geophysics.

The primary exploration objective was to determine the feasibility for large-scale open-pit mining. Although the drilling was generally viewed as successful, the deposit was viewed as too small by those companies and the property was subsequently returned to Coastal. Per the option agreements, Coastal was entitled to all non-interpretive data from the exploration and currently has possession of all raw data, drill logs, maps, assays, etc.

Figures 3-6 of this report are by Henry Follman of Coastal Mines.

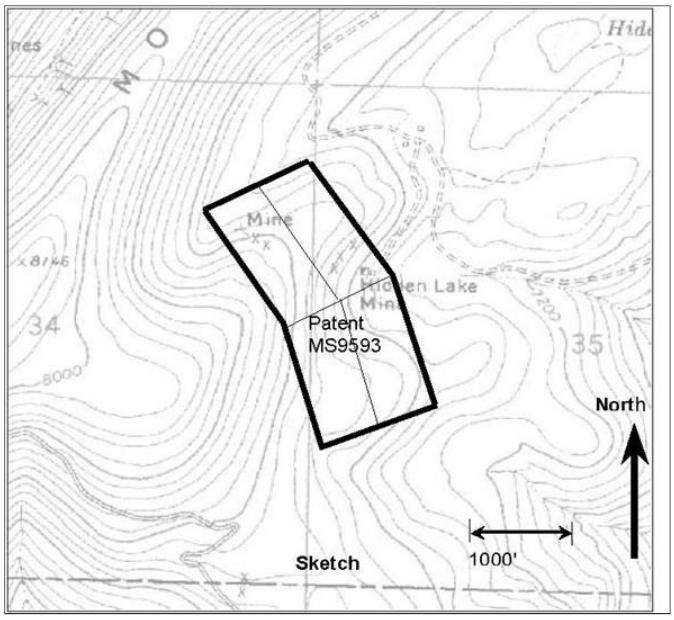

Figure 3. Location map of Hidden Lake mine showing patented ground.

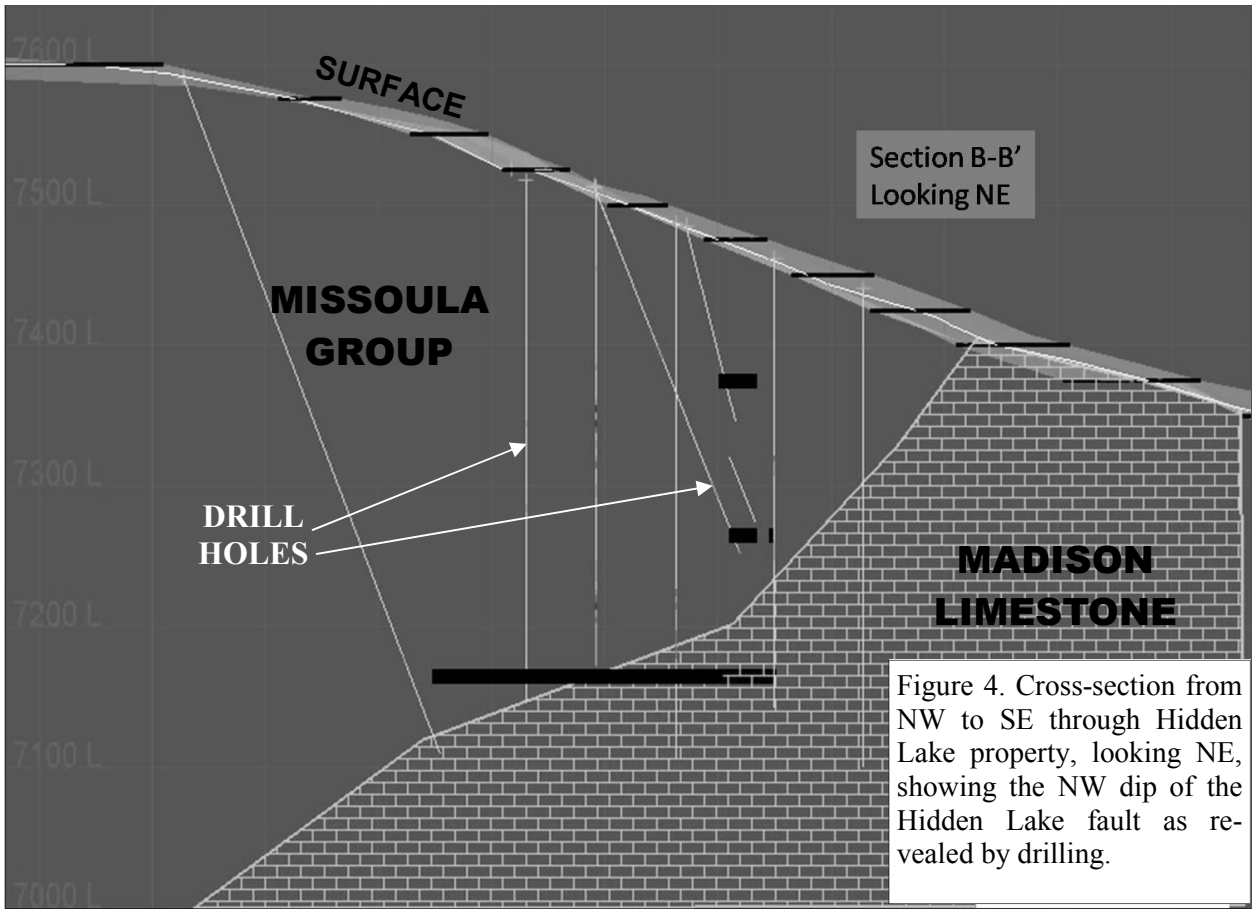

Figure 4. Cross-section from NW to SE through Hidden Lake property, looking NE, showing the NW dip of the Hidden Lake fault as revealed by drilling.

Geologic Description

The Hidden Lake mine is situated on the northeast trending Hidden Lake fault (called the Twin Peaks fault by Emmons and Calkins, 1913), a regional structure extending some 25 miles. To the northeast along strike, in the vicinity of Twin Peaks, this fault is well exposed and dips southeast. Emmons and Calkins (1913) and others have interpreted the Twin Peaks/Hidden Lake fault to be a normal fault juxtaposing Belt quartzite against Paleozoic (mostly Madison) limestone. However, in the mine area, drill hole data suggest that the Hidden Lake fault dips westerly (Figure 4), and is cut by an ENE-striking, steeply east-dipping normal fault that drops the quartzite-limestone contact (footwall) down to the south (Figures 5 and 6). Virtually all of the mineralization occurs in a wide zone of severely shattered and broken quartzite in the hanging wall of the Hidden Lake fault.

The quartzite has been mapped in previous work as various units within the Precambrian Belt Supergroup, but Cambrian Flathead quartzite may be present as well. The limestone has generally been regionally mapped as Mississippian Madison limestone, but drill data from the mine area indicate the limestone may, in part, be one or all of the Cambrian limestones (Silver Hill, Hasmark, or Red Lion formation), or the Devonian Maywood or Jefferson formation. Given the complexity of faulting in the area, there may be several of the above-named limestone units present on the property. Black or green siltstone and shale were encountered in many of the drill holes; these are not known to be Madison strata, though just east of the mine the limestone is clearly Madison. Emmons and Calkins' map (1913) shows a faulted wedge of lower Paleozoic rocks between the Belt quartzite and the Madison.

In many of the drill holes the black siltstones were logged as hornfels, and some of the limestones were logged as marble, indicating a nearby igneous intrusive although no igneous rocks were encountered in any of the drill holes, and there are no igneous outcrops in the immediate area.

The mineralized zone is generally interpreted to be a huge weakly mineralized (0.01-0.04 oz/t Au) fault gouge that contains numerous lenticular and rod-shaped pods of high grade ore (0.1- 2.0 oz/t Au), ranging in thickness from 5 to 50 feet, striking either northwest or northeast at various dips and plunges, ranging from nearly flat to vertical, the overall trend being northeast. The majority of the mineralized drill intercepts occur between depths of 200 to 400 feet. However, there are a few important exceptions to this generalization evidenced by the drilling. There have been six intercepts of significant high-grade material between 55’ and 95’ below surface. There are also significant gold-mineralized exposures in some of the road cuts. It appears that mineralization is thickest and most intense where northwest or east-west structures intersect the main northeast structure. The ore at Hidden Lake occurs as iron oxides (limonite, hematite, and goethite) after pyrite, with small amounts of residual pyrite particularly at the deeper levels. Visible free gold can be observed occasionally at the surface, and was observed once while drilling. Silver content is negligible and no base metals or other impurities are associated with the ore.

Retrace route back toward Cable. Turn right on Cable Mountain road for approximately one mile to a turn-around on Cable Mountain.

STOP 5 STOP 5. Cable Mountain area. Coarse Missoula Group feldspathic quartzite and conglomerate dip moderately to the west and northwest, in contrast to the Missoula

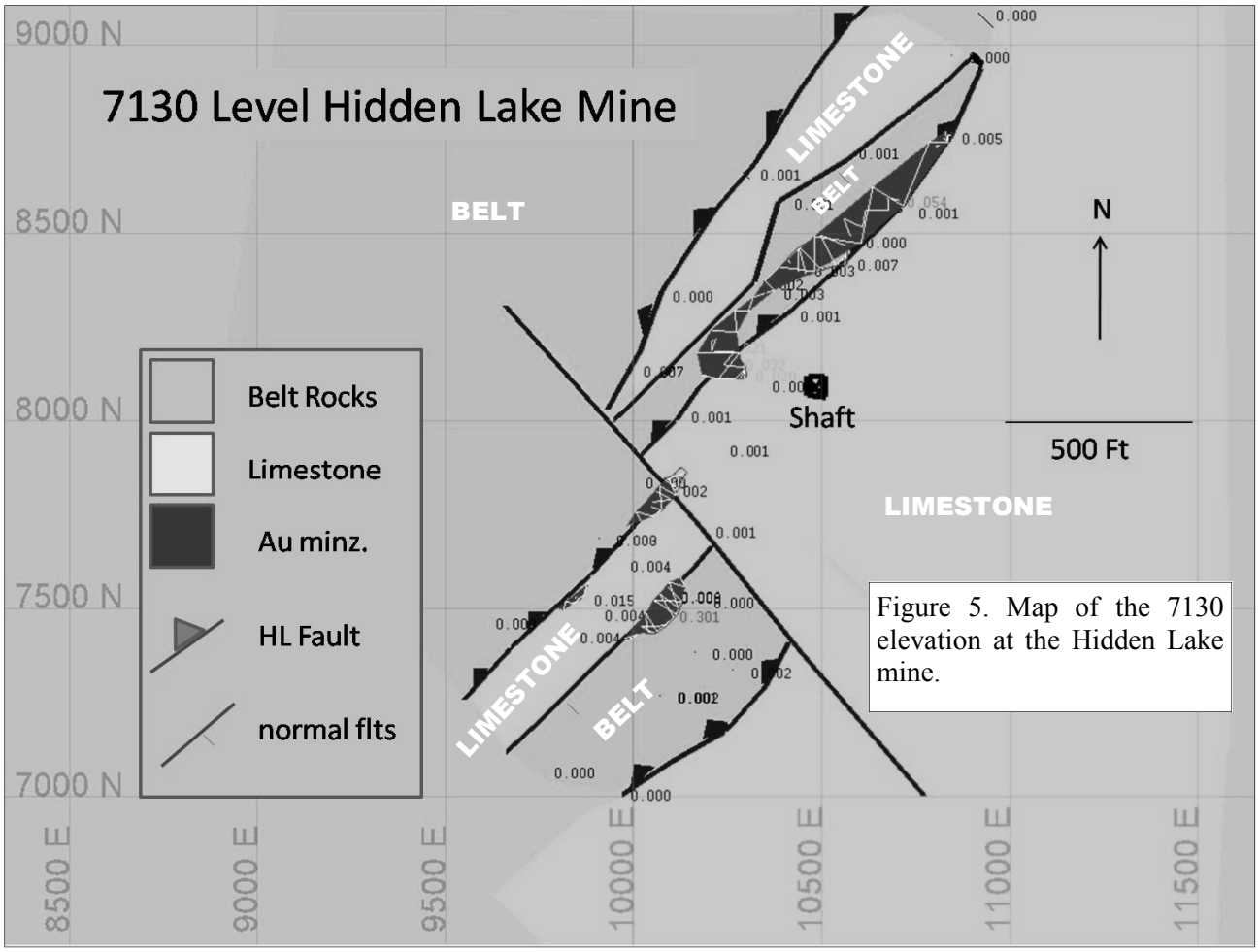

Figure 5. Map of the 7130 elevation at the Hidden Lake mine.

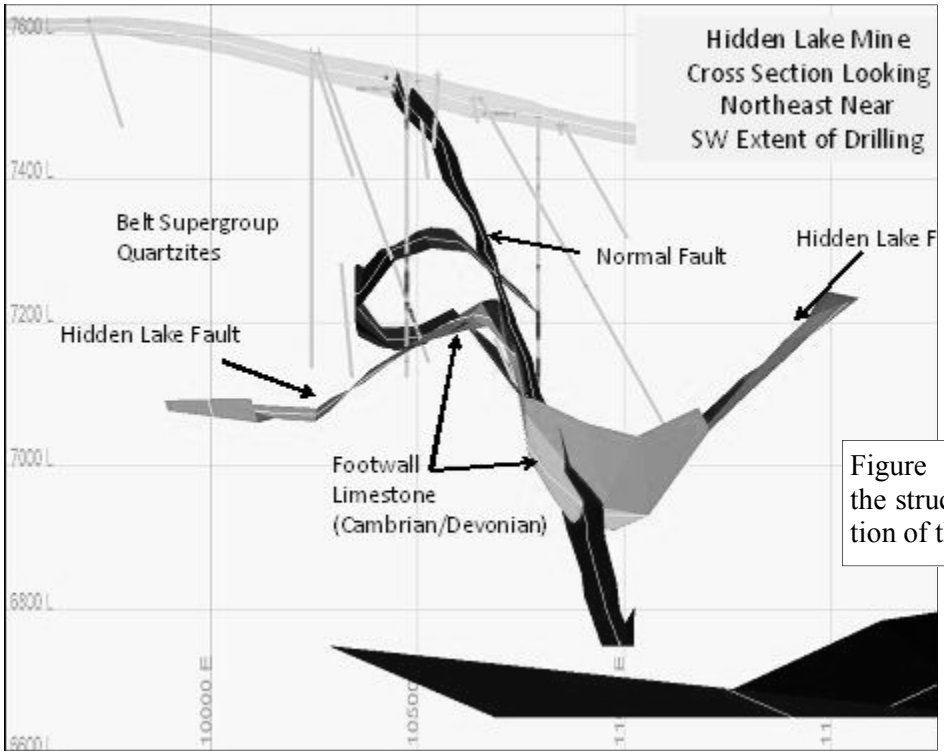

Figure 6. Cross-section through the structurally complex SW portion of the Hidden Lake property.

Group strata in upper Warm Springs Creek, which are overturned and dip to the southeast. Apparently, the strata and the Hidden Lake fault are in normal sequence here with upright bedding and a major fault placing the Missoula Group quartzite over Paleozoic rocks. The simplest interpretation is that the Missoula Group strata have been thrust from the west over the Paleozoic rocks, similar to the structural sequence along the great Georgetown overthrust, the next major fault to the west. Toward the northeast along Cable Mountain, the entire package becomes more steeply dipping and eventually even overturned in upper Warm Springs Creek.

There is no Missoula Group conglomerate exposed on Flint Creek hill (Georgetown thrust plate) that is as coarse as the conglomerate here on Cable Mountain. The Bonner formation conglomerate may be correlative but there are also conglomerate lenses in some exposures of the Mount Shields 2 formation.

Retrace route to Cable Creek. Turn right and proceed up hill on county road toward Southern Cross through the Cable mine area. The county road crosses the upper portion of surface workings at the Cable mine. Below these workings are the uppermost reaches of the Cable placer. Some of the lode ore mined here was very high grade, with coarse gold occurring as replacements in the Hasmark dolomite near the contact with the Cable stock. In the deeper workings of the Cable mine, low grade copper-gold ore predominated (Emmons and Calkins, 1913).

Continue on county road through the Southern Cross District to Georgetown Lake, turning east at the lake on Montana Highway 1 for the trip back to Anaconda.

References

Earll, F. N., 1972, Mines and Mineral Deposits of the Southern Flint Creek Range, Montana: Montana Bureau of Mines and Geology Bulletin 84.

Emmons, William H. and Calkins, Frank C., 1913, Geology and Ore Deposits of the Philipsburg Quadrangle, Montana: U. S. Geological Survey Professional Paper 78.

Lonn, J.D., McDonald, C., Lewis, R.S., Kalakay, T.J., O'Neill, J.M., Berg, R.B., and Hargrave, P., 2003, Preliminary geologic map of the Philipsburg 30' x 60'quadrangle, western Montana: Montana Bureau of Mines and Geology Open-File Report MBMG 483, 29 p., scale 1:100,000.

FIELD GUIDE TO TERTIARY OUTCROPS OF THE BIG HOLE VALLEY – ANACONDA TO BIG HOLE PASS

Warren Roe
Department of Geosciences, University of Montana, Missoula, MT 59812
warren.roe@umontana.edu

Introduction

In southwestern Montana and eastern Idaho, Tertiary sediments have long been studied as recording post-Sevier extensional tectonism. Several models have been proposed for extension. Janecke (1994) documents a narrow north-south trending zone of Eocene-Oligocene extensional supradetachment basins and metamorphic core complexes located roughly along the Idaho-Montana state line. She hypothesizes that the Big Hole basin formed in this zone, implying it was hemmed in by rift shoulders of the Pioneer and Anaconda mountain ranges. Thomas (1995) offers an alternate configuration of a basin open to the east with only the Anaconda Range being topographically high on the western edge of the basin, implying that the Pioneer Mountains were uplifted later.

Zircon is a heavy, stable mineral whose crystal lattice at the time of crystallization retains radioactive isotopes of uranium (namely 235 and 238) while generally excluding lead (Pb), giving an almost ideal chronometer. U-Pb dating of numerous individual detrital zircons creates a "signature" that can be matched to potential source rock areas. In southwestern Montana, the presence or absence of certain populations can indicate the presence or absence of fault-related paleotopography and/or sediment dispersal patterns.

Another technique used to evaluate paleodrainages and topography in southwestern Montana is the distribution of "2-mica" sands (containing both muscovite and biotite) in Tertiary sediments. Muscovite is common in the Chief Joseph pluton of the Anaconda Range; few other major sources of muscovite are known in the region (Figure 4). Detrital zircon geochronology is another technique increasingly used in provenance analysis. Stroup (2008) analyzed detrital zircons in modern 2-mica sands eroding off of the Anaconda Range and noted a peak at 75 Ma (Figure 4).

Roughly speaking, two major sedimentary units are described in southwestern Montana: the ~50-20 Ma Renova Formation and the 17-4 Ma Sixmile Creek Formation (Figure 1). They are separated by a regionally-recognized Middle Miocene angular unconformity.

This field guide covers recent sedimentology, stratigraphy, U-Pb dating, and detrital zircon work performed on the few outcrops in the Big Hole valley. Figures 2 and 3 show the location of the Big Hole and general locations of the outcrops. Because of difficult access, poor footing, and standing-room limitations, some of the stops in this guide describe them from a distance. Additionally, laboratory work is ongoing at the time of writing and the following observations and conclusions are still somewhat tentative.

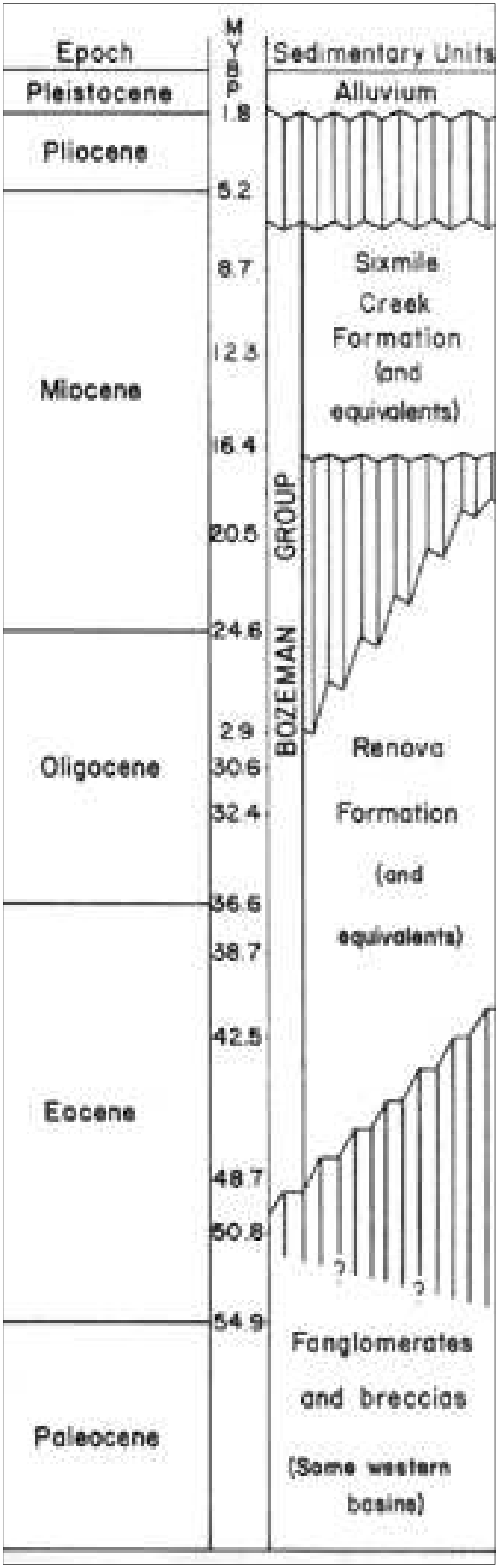

Figure 1. Generalized stratigraphy of Tertiary Renova Formation and Sixmile Creek Formation in southwestern Montana. Various authors have different definitions for the base of the Renova Formation. Figure modified from Fields et al. (1985).

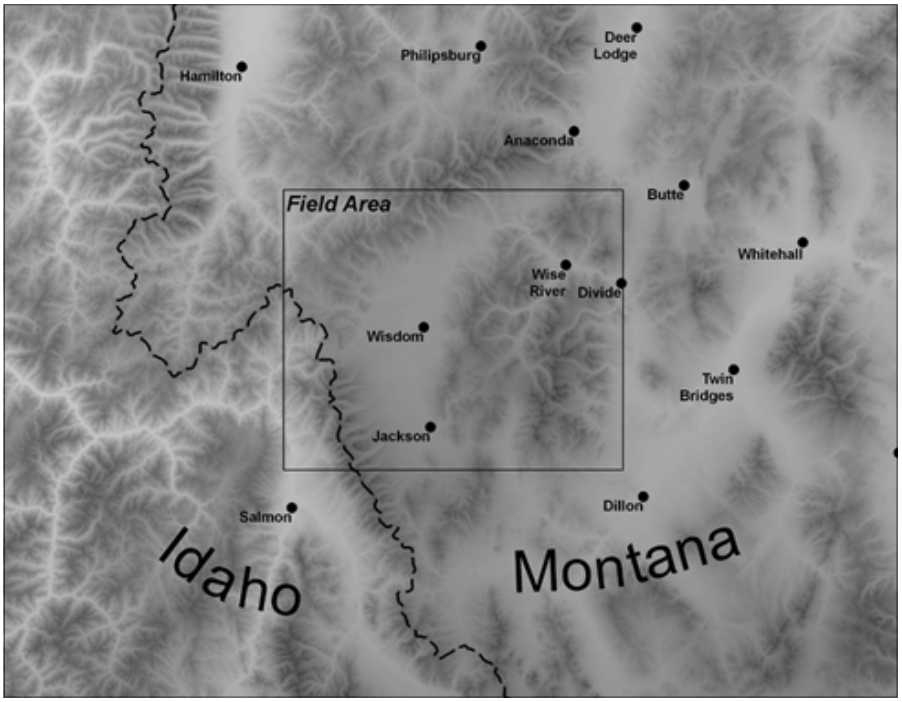

Figure 2. Overview of the location of the study area. Width of figure is 155 miles (250 km).

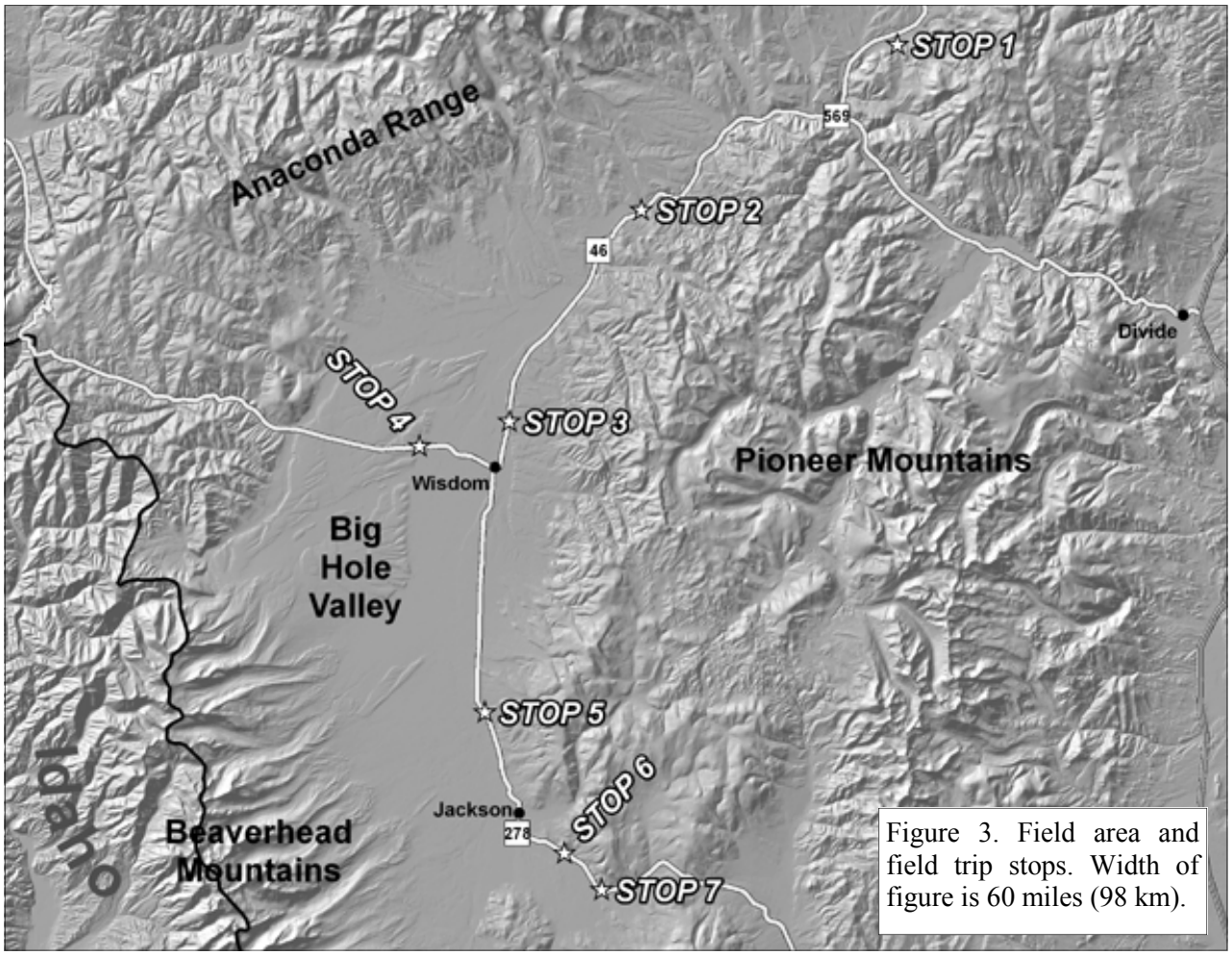

Figure 3. Field area and field trip stops. Width of figure is 60 miles (98 km).

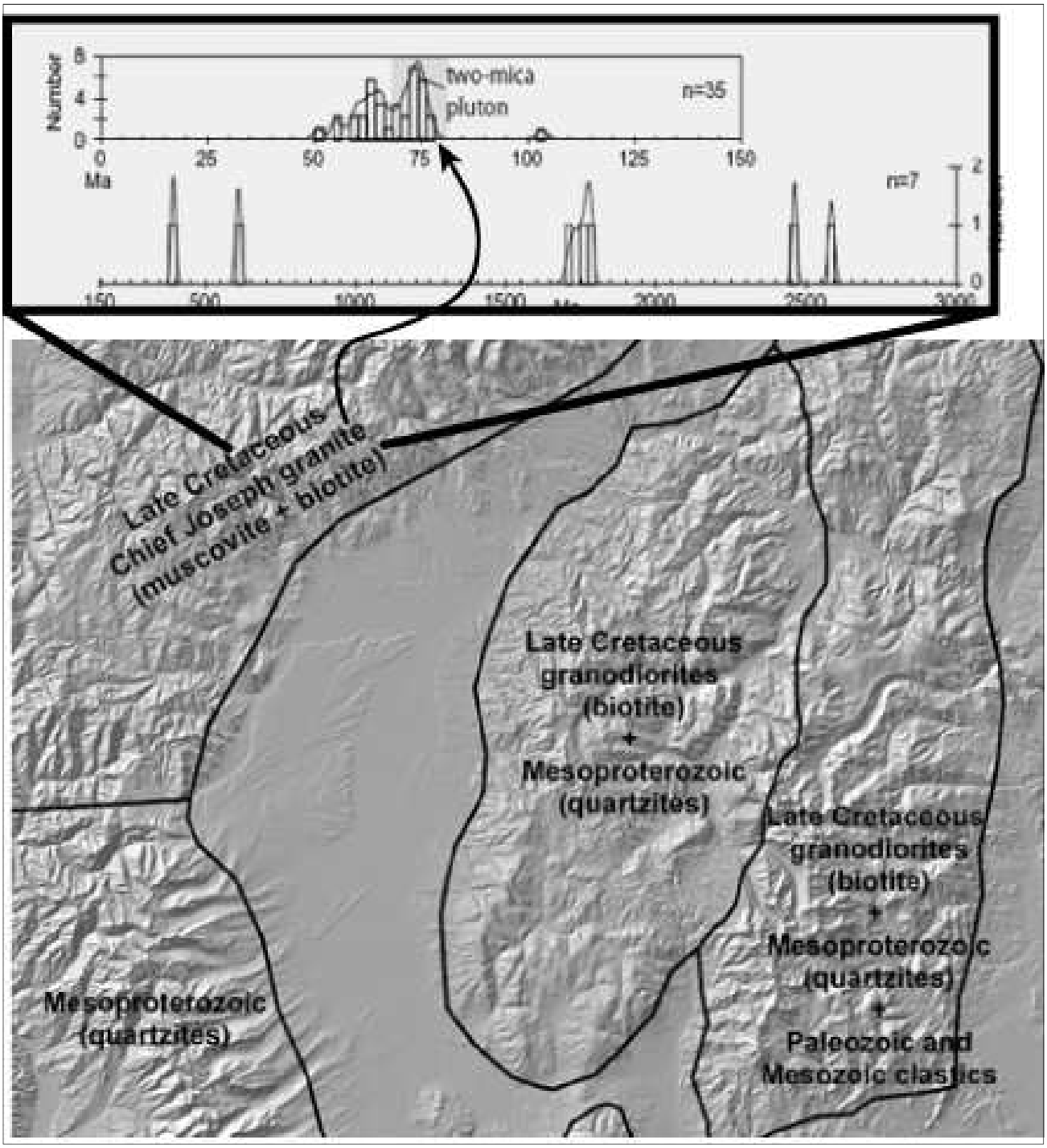

Figure 4. Cartoon of source rock areas. Note the 2-mica granite in the Anaconda Range (upper left) versus 1-mica (biotite) sources in the Pioneer Mountains (right side). The zircon ages shown at top were taken from modern sands weathering off the Chief Joseph pluton at Mussigbrod Creek by Stroup (2008). Given the data here, the Chief Joseph pluton's "signature" in sands should be reflected by the presence of muscovite and a detrital zircon peak at 75 Ma. The zircon age distribution figure is modified from Stroup (2008).

Road Log

From downtown Anaconda, follow Route 1 east out of town. As you pass the large smelter smoke stack, turn right on to Route 569 (Mill Creek Road). One mile on, reset your odometer as you cross the train tracks.

Mile 0 – Train track crossing on Mill Creek Rd.

STOP 1 Mile 15.8 – STOP 1 – view of French Creek outcrop

To the west, a meander of French Creek has exposed over 30 meters of flat-lying tuffaceous Tertiary beds. The outcrop consists of laterally discontinuous white and tan clay, silt, tuff, and coarse sand. Carbonaceous woody material is evident in some layers along with yellow and orange nodules and staining. Clay layers have distinctive blocky fracture. All of these are probably all pedogenic features, though no clear paleosol horizons are visible. Several silty layers are massively bedded with occasional matrix-supported pebbles, cobbles, and sticks. Locally, a slight fining-upward texture is noted in these beds. These are interpreted as fine-grained debris-flow (mudflow) deposits. Thin (<0.5 m thick) sand bodies are texturally immature, poorly sorted, and sometimes contain distinct "books" of biotite. Sand bodies are generally channelized, though no bed forms are visible. Muscovite is present but very uncommon.

Volcanic zircons from a tuff at the base of the outcrop were analyzed at Boise State University via chemical abrasion-thermal ionization mass spectrometry (CA-TIMS), giving an Oligocene date of 29.602 ± 0.009 Ma. Three other grains produced dates of 29.99 ± 0.03 Ma, 73.40 ± 0.02 Ma, and 76.46 ± 0.13 Ma, indicating the tuff was reworked. A sand above the tuff produces detrital zircons clustered around 28.9 Ma (Figure 5). While only 40 grains were analyzed in total (three giving Proterozoic ages), some generalizations may be made from the available data.

French Creek zircons form a peak at 72.0 Ma, slightly younger than the 74.5-75.0 Ma peak expected from 2-mica sources in the Anaconda Range. Also, the complete absence of 48-53 Ma grains suggests the Lowland Creek volcanics outcropping two miles away to the northeast and southeast were not feeding sediment in to the French Creek outcrop. This puzzling absence suggests that sediments were being transported from the west or south, and the northern Pioneers were not contributing sediment to this outcrop at 29.6 Ma.

Mile 21.1 (5.3 miles from previous) – At the stop sign, turn right on to Route 43.

Mile 33.4 – Turn right on to Lower North Fork Rd and drive approximately 0.1 miles to the top of the slight hill.

STOP 2 Mile 33.5 (12.4 miles from previous stop) – STOP 2 – Chalk Bluff overlook

Visible in a landslide scarp to the south are the west-dipping beds of Chalk Bluff. This area contains the best-studied Tertiary units of the Big Hole valley. Ralph Nichols' former ranch is located 1.5 miles north. He described a single tooth fragment from Chalk Bluff as tentatively Oligocene in age (Hanneman and Nichols, 1981; R. Nichols, pers. comm.). Debra Hanneman (1987a, b) mapped two USGS quadrangles here and Fritz et al. (2007) briefly describe a small volcanic flow (basanite; 21.9 ± 0.3 Ma) two miles northwest of Chalk Bluff.

Chalk Bluff is approximately 85 meters tall and consists of massive tuffaceous light tan clay and mud with occasional sand float.

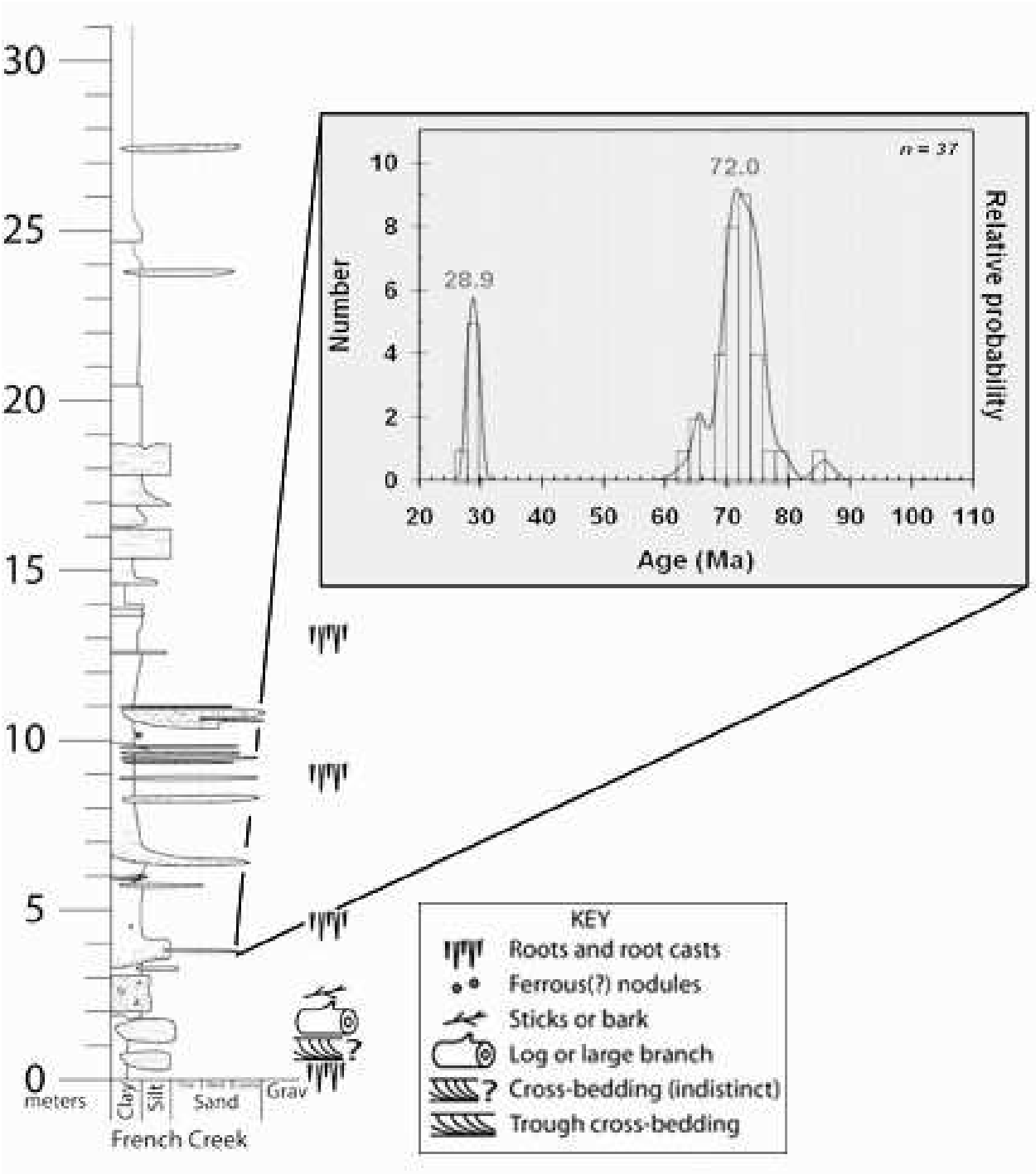

Figure 5. Stratigraphy of STOP 1 at the French Creek outcrop.

Bedding is very faint and most obvious from a distance. Small reddish nodules are present as are large concretions (0.5 m diameter). The almost complete lack of sedimentary structures makes assigning a depositional environment difficult, but the occasional presence of sand grains and lack of grading in otherwise featureless clay-silt matrix suggests debris flow sedimentation.

Immediately east of Chalk Bluff, foliated biotite-rich granodiorite and gneiss outcrop in road cuts and in scattered small outcrops. A zone of deep red clay separates these units from Chalk Bluff. The very fine grain size, presence of slicks, and deep red color suggest this clay could be a paleosol developed atop the gneiss and granodiorite, with the Chalk Bluff beds resting on top. However, the clay is dissimilar to other paleosols observed in the Big Hole, lacks any sedimentary structures (bedding, root casts, etc), shows no gradation in to a regolith, and contains no biotite found in rocks below. Combined with the extremely fine grain sizes in Chalk Bluff and the hypothesized debris-flow depositional mechanism (which would likely entrain rip-ups of any paleosol), I suggest the red clays are instead fault gouge of a down-to-the-west normal fault post-dating the Chalk Bluff beds.

The shallow west dip at Chalk Bluff, tentative Oligocene date, and firm Miocene date

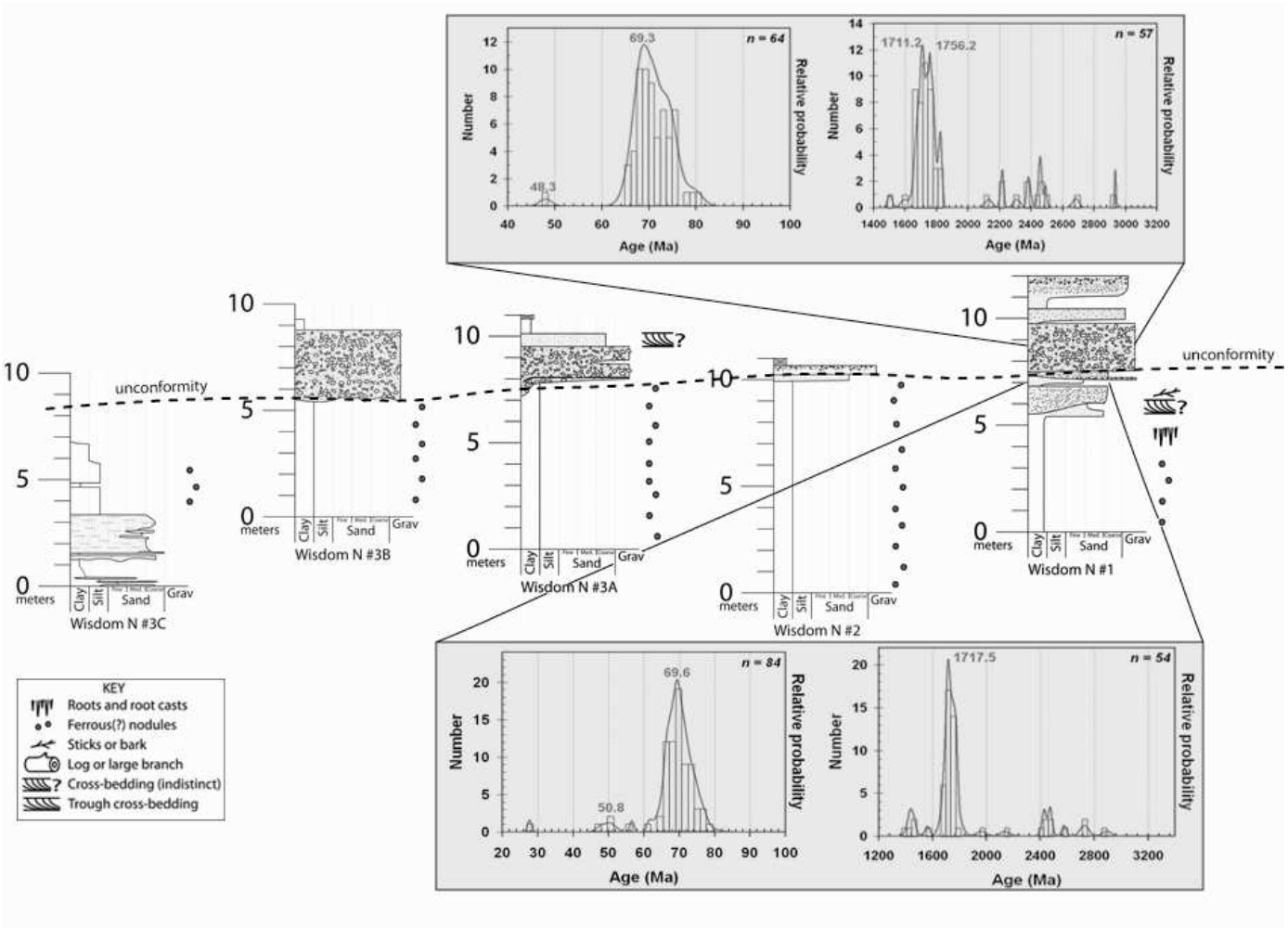

Figure 6. Stratigraphy of STOP 3 at the Wisdom North outcrops. The stratigraphic sections have been hung from the gravel-capped unconformity. Muscovite is present above and below the unconformity. Note the similarity between the detrital zircon populations.

further west (at an almost identical elevation) suggest a pervasive westerly dip across the valley in this area. If the interpretation here of a fault on the east side of the valley is correct, I hypothesize early normal faulting on the west side of the valley (top to the east) tilted valley fill toward the west and was followed by later normal faulting on the east side of the valley (top to the west).

STOP 3 Mile 47.0 (13.5 miles from previous) – STOP 3 – Wisdom North

Pull in to the large turnout on the right (west) side of the road. This stop is a series of five outcrops. Four are along the road and numbered 1 through 4 from south to north (right to left). The fifth is behind the Wisdom Cemetery on the wooded bluff visible about a half mile north. Fossil fragments of the Barstovian (13.6-16.3 Ma) and Arikareean (20.8-30.6 Ma) North American stages have tentatively been identified here (R. Nichols, pers. comm.).

The outcrops consist of laterally discontinuous clay, sand, and gravel. Muscovite is common throughout. Quartzite gravel caps the tops of all outcrops here and has eroded into units below, which appear to dipping slightly to the south (best visible in outcrop 3). This erosional contact is tentatively identified as an angular unconformity. Units below the unconformity are generally fine-grained and have pedogenic features in the form of distinct reddish nodules, blocky fracture, yellowish horizons, occasional small vugs, and orange, yellow, and brown mottling. The sand is coarse-to-pebbly, 2-mica, sometimes cemented with white silica, and commonly contains petrified wood. Above the unconformity, gravels are largely quartzite (with very minor weathered 2-mica granite) and have basal mud-ball rip-ups and distinctive white-cemented clasts of sandstone clearly derived from units below. At the time of writing, a white tuffaceous debris flow at the base of the cemetery bluff (below the unconformity) and a thin, irregular, dirty tuff at the base of the gravel (resting on the unconformity) are undergoing CA-TIMS at BSU.

The angular unconformity recognized in outcrop combined with fossil evidence suggest this unconformity could be the regionally-recognized Middle Miocene angular unconformity. If it is, detrital zircons across the unconformity exhibit strikingly similar age distributions: the largest peaks are at 69.3 Ma and 1717.5 Ma above the unconformity, while below the peaks are 69.6 Ma, 1711.2 Ma, and 1757.6 Ma (Figure 6). A single zircon below the unconformity produces a robust 27.7 ± 0.6 Ma date, providing a possible maximum age to this unit.

The presence of muscovite suggests input from the 2-mica Chief Joseph pluton in the Anaconda Range, but the detrital zircon data once again show a Late Cretaceous peak younger than expected of the Chief Joseph pluton. Either the Chief Joseph pluton has a more complex emplacement history than suggested in the data of Stroup (2008), or the muscovite has been derived from some other unknown source.

STOP 4 Mile 52.2 (6.1 miles from previous) – STOP 4 – Wisdom West

Overall this outcrop is similar to those at Wisdom North: laterally discontinuous channelized 2-mica sand and clay capped by quartzite gravel. No fossil fragments have been found here and no tuff have been identified. However, a basal sand produced five zircons which gave detrital zircon dates clustered around 11.6 Ma (Figure 7). This is striking because lithostratigraphically this outcrop appears to be a fine-grained Renova equivalent (i.e., >20 Ma). A large population of Eocene grains clustered around 50.9 Ma

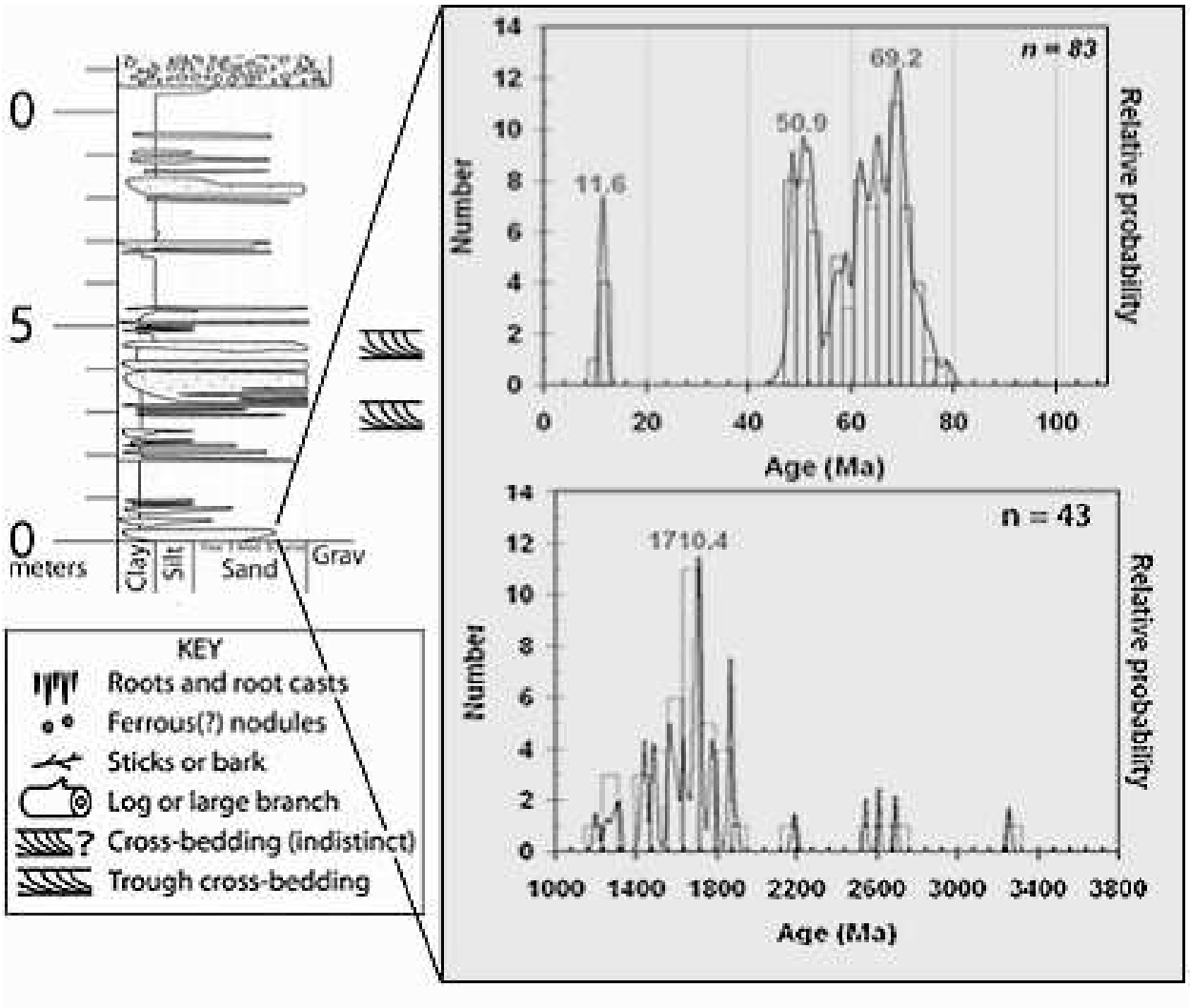

Figure 7. Stratigraphy of STOP 4 at the Wisdom West road cut. Note the peak of young zircons clustered around 11.6 Ma.

also differentiate this from previous outcrops, suggesting sediment input from the Challis or Lowland Creek volcanic centers (or possibly similar young grains from the Chief Joseph pluton: c.f. Stroup, 2008). Again, pervasive muscovite and a 69.2 Ma zircon population peak provide conflicting evidence for sediment derivation from the Chief Joseph pluton.

Mile 56.0 (3.8 miles from previous) – Turn right (south) on to Route 278 toward Jackson Hot Springs.

STOP 5 Mile 68.5 (12.5 miles from previous) – STOP 5 – Jackson North

This unusual white outcrop is extremely tuffaceous and has plentiful small red nodules. A small amount of gravel may cap the top. Bedding, bed forms, and other sedimentary structures are not visible, possibly due to bulldozing of the outcrop. However this outcrop has produced a good zircon population (J. Crowley, pers. comm.) that is undergoing CA-TIMS dating at BSU at the time of writing. This is tentatively identified as strati-

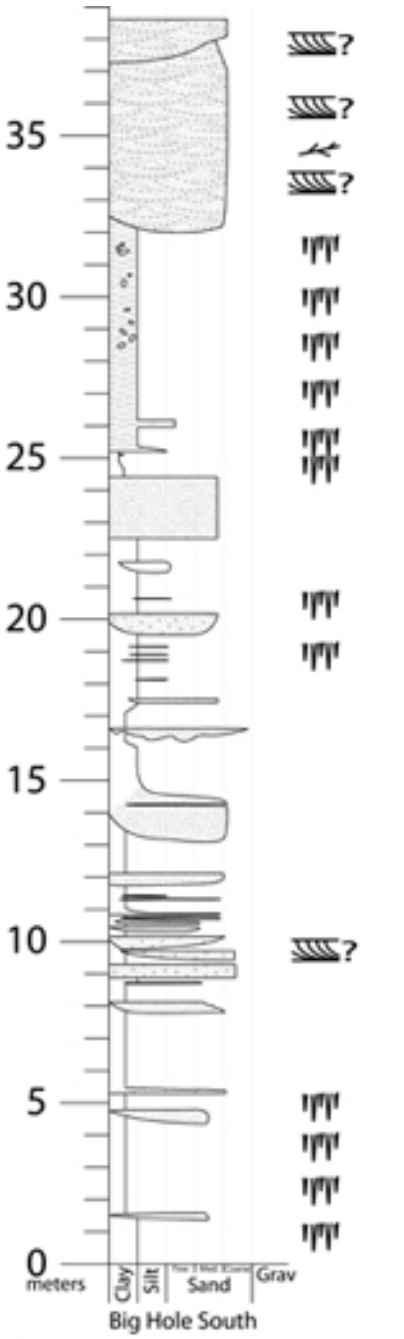

Figure 8. Stratigraphy of STOP 6 at the Big Hole South road cut. Note the channelized sand and numerous root casts. This outcrop is rich in detrital biotite but no muscovite is present.

graphically lower than units found at the next two stops to the south.

STOP 6 Mile 77.3 (8.8 miles from previous) – STOP 6 – Big Hole South

This tall road cut consists of interlayered clay and sands (Figure 8). The clay shows pedogenic features in the form of greenish silicified (?) root casts and occasional orange or yellow mottling. Some clays contain poorly sorted matrix-supported coarse sand or pebbles, suggesting a mudflow or debris flow deposit. Sands tend to be coarse and channelized, with some small lateral accretion surfaces and clay cut-banks clearly preserved in outcrop. These features were difficult to measure due to 2D outcrop faces, but they qualitatively tend to show paleoflow directions perpendicular to the outcrop face (i.e. in to or out of the outcrop). Gravelly sand at the top are very well cemented and have indistinct cross-bedding, also difficult to measure. No muscovite is found anywhere in the outcrop but all units tend to be rich in biotite. No detrital zircons or tuffs were sampled here. Biotite-rich granodiorite directly to the north is the likeliest source for this sand and mud, suggesting paleoflow from the flanks of the West Pioneers.

STOP 7 Mile 79.9 (2.6 miles from previous) – STOP 7 – Rob's Outcrop

This final outcrop features thick, coarse, trough cross-bedded 2-mica sand dipping toward the southeast. The sand contains abundant fossilized wood. Dip-corrected trough cross-beds show southeasterly flow as do trend and plunge readings from two fossilized logs preserved in outcrop (Figure 9).

Southeasterly paleoflow readings disagree somewhat with more east-oriented paleoflow

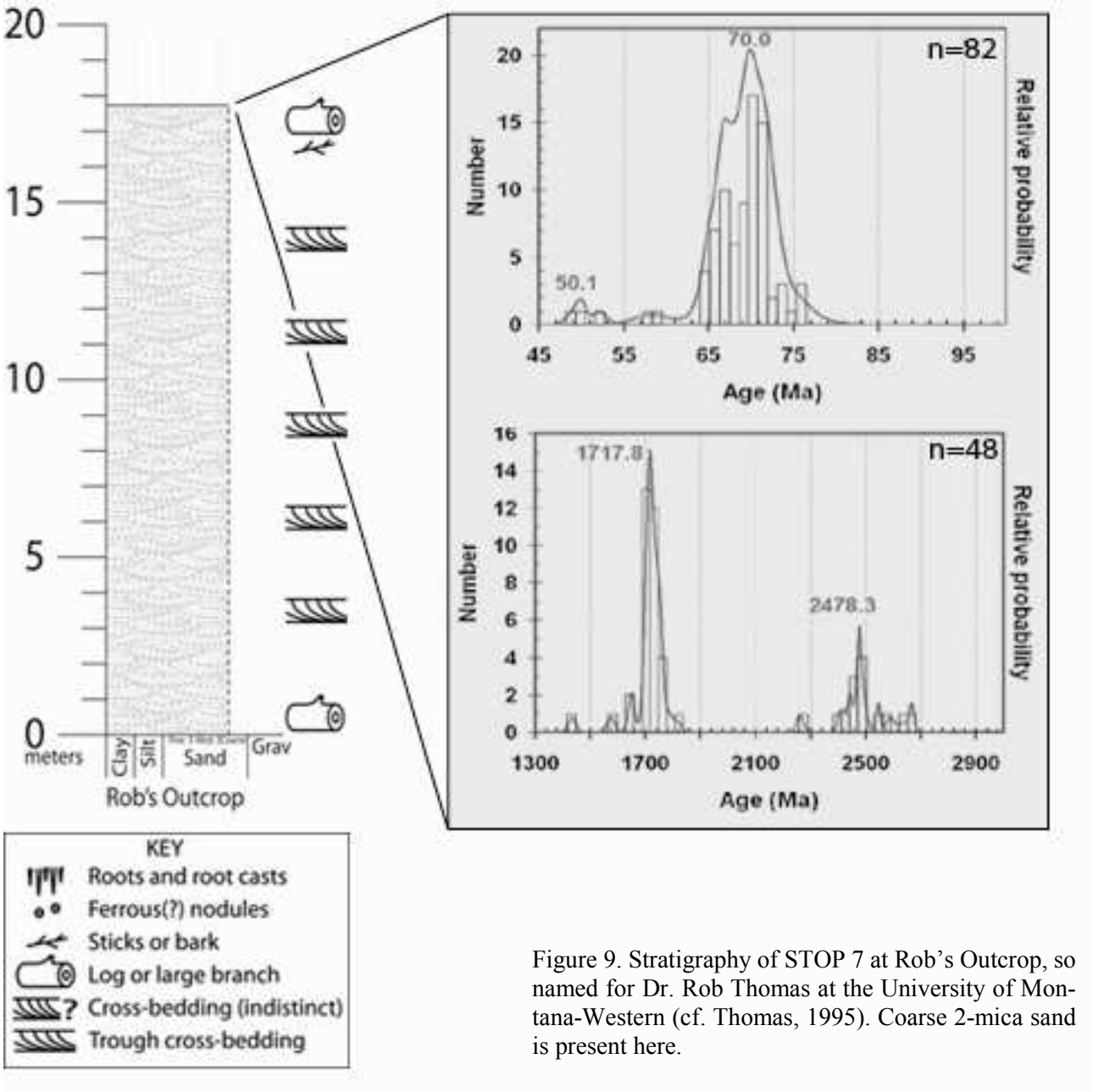

Figure 9. Stratigraphy of STOP 7 at Rob's Outcrop, so named for Dr. Rob Thomas at the University of Montana-Western (cf. Thomas, 1995). Coarse 2-mica sand is present here.

indicators from Thomas (1995) at this same outcrop, but the overall point is the same: all paleoflow indicators point almost exactly 180° to the modern drainage direction and suggest the high topography south of the Big Hole pass was not an impediment to this drainage carrying 2-mica sand probably derived from the west.

Acknowledgements

Detrital zircon U-Pb dating was performed using LA-ICP-MS at Washington State University under the auspices of Dr. Jeff Vervoort. Charles Knaack and Rich Gaschnig provided vital help collecting and interpreting the data. Dr. Julie Baldwin helped with detrital zircon separation, preparation, and interpretation. At Boise State University, Drs. Mark Schmitz and Jim Crowley performed

the U-Pb TIMS dating of tuffs. This research was made possible by grants from the American Association of Petroleum Geologists, the Geological Society of America, the Colorado Scientific Society, the Wyoming Geological Association, as well as scholarships from the Tobacco Root Geological Society, Billings Geophysical Society and the University of Montana Patrick J. McDonough fund.

References

Fields, R.W., Tabrum, A.R., Rasmussen, D.L., and Nichols, R., 1985, Cenozoic rocks of the intermontane basins of western Montana and eastern Idaho: *in* Flores, R.M., and Kaplan, S.S., eds., Cenozoic Paleogeography of the West Central U.S., Rocky Mountain Section, Society of Economic Paleontologists and Mineralogists, p. 9-36.

Fritz, W.J., Sears, J.W., McDowell, R.J., and Wampler, J.M., 2007, Cenozoic volcanic rocks of southwestern Montana: Northwest Geology, vol. 36, p. 91-110.

Hanneman, D.L., 1987a, Geologic map of the Pine Hill quadrangle, Beaverhead and Deer Lodge Counties, Montana: U.S. Geological Survey Miscellaneous Field Studies Map MF-1930, scale 1:24:000.

Hanneman, D.L., 1987b, Geologic map of the Pintler Lake quadrangle, Beaverhead and Deer Lodge Counties, Montana: U.S. Geological Survey Miscellaneous Field Studies Map MF-1931, scale 1:24:000.

Hanneman, D.L., and Nichols, R., 1981, Late Tertiary sedimentary rocks of the Big Hole Basin, Southwest Montana: Abstracts with Programs, Geological Society of America, vol. 13, no.4, p. 199.

Janecke, S.U., 1994, Sedimentation and paleogeography of an Eocene to Oligocene rift zone, Idaho and Montana: Geological Society of America Bulletin, vol. 106, p. 1083–1095.

Stroup, C.N., 2008, Provenance of Cenozoic continental sandstones in Southwest Montana: evidence from detrital zircons: Unpublished Master's thesis, Idaho State University, 117 p.

Thomas, R.C., 1995, Tectonic significance of Paleogene sandstone deposits in southwestern Montana: Northwest Geology, vol. 24, p. 237–244.

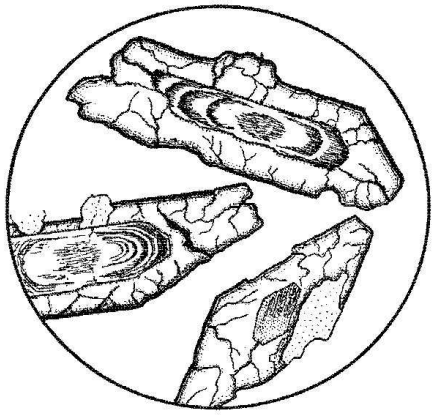

LOST LAKES AND RE-ARRANGED RIVERS: NEOTECTONIC DISRUPTION OF THE MIDDLE MIOCENE BIG HOLE RIVER BASIN, SW MONTANA

James W. Sears
University of Montana, Missoula

Introduction

This field trip investigates neotectonic re-arrangement of Middle Miocene drainages in the Anaconda - Twin Bridges region of southwestern Montana. I propose that a Middle Miocene river basin linked deep rift-valley lakes in the Big Hole and Jefferson grabens (Fig. 1). The spillway of 'Miocene Lake Big Hole' eroded Big Hole Canyon between Wisdom and Divide, and material eroded from the canyon prograded an enormous fan into a second lake in the Jefferson graben, 'Miocene Lake Twin Bridges'. The grabens opened during a period of intense crustal disturbance associated with initiation of Basin-and-Range faulting during outbreak of the Yellowstone hotspot in eastern Oregon. The Miocene valleys were later disturbed and deflected by neotectonic faulting coincident with passage of the hotspot northeastward along the eastern Snake River Plain. The Big Hole River abandoned its Miocene course and cut Maiden Rock Canyon between Divide and Melrose, circled the south side of McCarty Mountain and then cross-cut its own gravel fan across the Biltmore Hills near Twin Bridges.

Middle Miocene tectonics

A short burst of intense Middle Miocene tectonism punctuated late Cenozoic south-

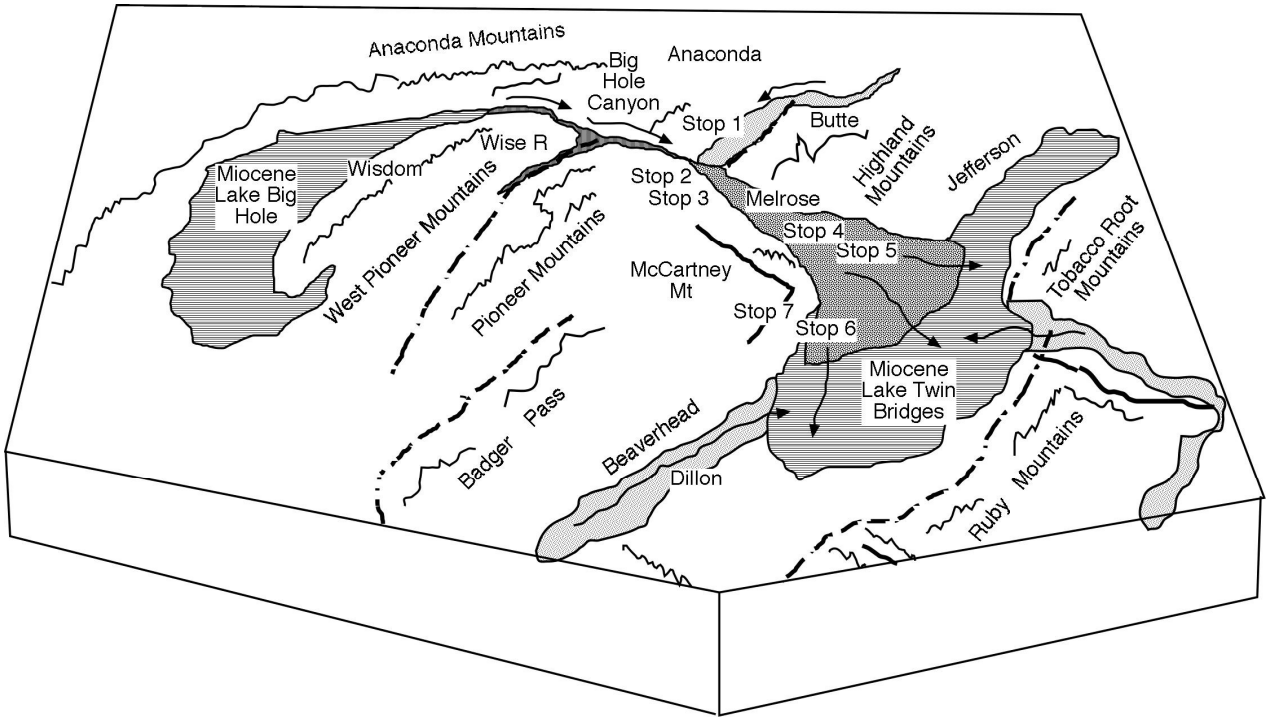

Figure 1. Miocene Lake Big Hole drains through Big Hole Canyon to feed giant fan into Miocene Lake Twin Bridges. Field trip stops are marked.

western Montana. The crust split along several graben valleys that fan outward from the initial outbreak point of the Yellowstone hotspot in southeastern Oregon (Sears et al., 2009). They correlate with events that led up to the outbreak, from 20 to 17 Ma. Sears (1995) proposed that the grabens record crustal extension across the northeast segment of a large dome that rose in conjunction with the birth of the hotspot.

The Middle Miocene grabens re-routed drainage patterns in southwestern Montana. Broad river valleys followed the graben axes, and where grabens were offset in en echelon arrays, the rivers ponded into deep lakes that spilled through canyons. By 17 Ma, the region established through-going, integrated drainages, the progenitors of today's upper Clark Fork, Missouri, and Yellowstone drainage basins. The lakes filled with sediment while the canyons eroded downward to base level, establishing run-of-the-river valleys with equilibrium profiles.

The Sixmile Creek Formation filled the valleys with hundreds to thousands of feet of debris flows, fluvial gravels, overbank sediments, lake beds, tephra, and basalt. Fritz and Sears (1993) divided the Sixmile Creek Formation into three interlayered lithologic members – the Sweetwater Creek debris flows, Big Hole River fluvial gravels, and Anderson Ranch tephras.

The base of the Sixmile Creek Formation rests on a profound angular unconformity that maps the Middle Miocene disturbance (Fields et al., 1985). It overlies deeply eroded bedrock in the upper reaches of the valleys, cutting across fold-and-thrust structures and intrusives of the Rocky Mountains. In the direction of plunge of the grabens, the Sixmile Creek Formation progressively onlaps thick Eocene Dillon volcanics (Fritz et al., 2007) and late Eocene-to-Early Miocene Renova Formation mudstones and sandstones. In many grabens the unconformity spans 20-17 Ma, but locally, younger Renova beds are preserved, shrinking the hiatus to less than 1 million years (Barnosky et al., 2007). In the deepest parts of the grabens, the Renova is overlain by lake beds that may correspond in age to the Middle Miocene unconformity in up-reach regions (McLeod, 1987). The lake beds largely comprise recycled Renova muds and bouldery debris flows in which recycled Renova mud and granite grus are the matrix.

Many of the grabens broaden into triangular valleys at their northeast ends. These reaches contain the youngest parts of the Renova Formation, and possible early Sixmile Creek Formation lake beds. They represent places where the floors of the grabens sank below the base level of erosion and runoff ponded into lakes. The lakes rapidly aggraded sediment from the easily erodable Renova Formation of the uplifted regions. Much of the early sediment slurried into the lakes in debris flows. Massive boulders 'floated' into mud or granite grus matrix from the underlying bedrock soil zones (Sears et al., 2009). The stratigraphy is classically inverted, with bouldery debris flows at the base, representing the Renova and underlying soil zones, and stream-washed gravel higher up, representing contributions from the sub-Renova bedrock. Cobble provenance shows that the rivers flowed into the depressions from different directions along the grabens and their flanks.

Miocene Big Hole River basin

This field trip focuses on one particular Miocene drainage basin, that of the Big Hole River. It builds upon the basic interpretation of Sears et al. (1995, 2009).

I suggest that a major tributary of the Miocene Big Hole River flowed out of a deep lake ('Miocene Lake Big Hole') in the Big Hole Valley along a canyon that cut across a structural sag in the Pioneer Range. Miocene Lake Big Hole occupied a long, narrow, north-trending graben between the Pioneer and Beaverhead Mountains. Exploration seismology and drilling revealed that the graben contains at least 10,000 feet of Miocene lake beds on top of 6,000 feet of Renova Formation and Eocene volcanics. The seismic reflection profiles show flat-lying lake beds concordant with the Renova Formation, indicating that Lake Big Hole achieved its depth rapidly, and its floor plunged well below sea level. I suggest that the Miocene Big Hole River was joined by a tributary river that drained the Pioneer Mountains at Wise River, then cut across the east Pioneers. A river flowing from a lake will only carry clasts with a provenance downstream from the outlet; upstream clasts will prograde into lake deltas. We will see cobbles from the Pioneers in the Sixmile Creek Formation at Stop 3.

I propose that a major tributary joined the Miocene Big Hole River from the north at Divide. This northern stream had headwaters in the Boulder batholith north of Butte. A remnant of the upper part of the valley forms the Elk Meadows valley along I-15. This valley crossed the future site of Butte, and proceeded down the broad graben occupied by I-15 from Rocker to Divide. The graben plunged to the south, as shown by the successive southward onlap of the Sixmile Creek Formation over the Boulder batholith, Eocene volcanics, and Renova Formation. Vuke (2004) mapped the graben.

The drainage was beheaded by Silver Bow Creek and captured by the Clark Fork basin. The decapitation was enabled by normal faulting along the Continental fault at Butte. Today, headward erosion has shifted the Continental Divide southward along the course of the Miocene Valley, as we will see on our field trip near Stop 1.

Downstream from the confluence of the Big Hole and its northern tributary, the Miocene river flowed through a broad valley between McCartney Mountain and the Highland Mountains. Evidence for the former flow of the valley comes from clast compositions in Sixmile Creek Formation gravel in remnants of valley fill, as we will see at Stop 4. These include cobbles and boulders of granite, spotted hornfels, Archean gneiss, and Flathead sandstone and conglomerate that were derived from the Highland Mountains on the east flank of the graben that contained the river.

The Miocene Big Hole River spread out into a broad fan as it passed into the Twin Bridges area of the Ruby graben. The fan is miles wide and thousands of feet thick as it plunges into a deep depression at the Jefferson graben. Hanneman and Wideman (1991) showed that the Jefferson basin is very deep and filled with Tertiary sediments. The fan becomes finer grained as it broadens downward into the depression. The base is bouldery diamictite and the upper part is stream gravel, silt and sand. I suggest it passes into lake beds near Twin Bridges.

The Twin Bridges depression also received a river flowing down the Beaverhead graben from the southeast. That river had headwaters in central Idaho, as shown by clast provenance.

Neotectonic breakup of the Miocene Big Hole River basin

The present-day Yellowstone volcanic field has an associated thermal bulge that is some 400 km wide and 500 m high (Smith et al., 2009). Extension of the dome appears to

have generated numerous active normal faults that have raised mountainous fault blocks, dropped grabens and broken up drainages in southwest Montana. Some of these neotectonic faults disrupted the Miocene Big Horn River basin.

The northernmost disruption is near Butte, where the Continental fault crossed the northern tributary of the Miocene Big Hole River and allowed the headwaters of the Clark Fork basin to capture the headwaters of the Big Hole basin. That shifted the Continental Divide southward.

Faults along the edges of the Divide graben diverted the Big Hole River into a new channel where it cut a deep canyon between Divide and Melrose. The abandoned stretch has hundreds of feet of Miocene Big Hole River stream gravel preserved, as we will see at Stop 3. The abandoned gravel is tilted and faulted due to the neotectonics that also diverted the river.

The Big Hole River then flows around the south side of McCarty Mountain where it cuts across two faults that disturb the Sixmile Creek Formation, and cuts a deep notch through a Quadrant Quartzite ridge called the Hogback. McCarty Mountain and the Hogback both actively rise on normal faults so that the river and its tributaries incise the bedrock of the famous Block Mountain field area, mapped by innumerable geology field camp students.

The Big Hole River then cuts across its own gravel fan, providing outcrops through an 800-foot deep valley. Other faults cut and tilt the gravel fan near Twin Bridges, so that hundreds of feet of strata are exposed. Many of the faults reactivated older faults that formed during the Middle Miocene.

ROAD LOG

The first part of the road log uses roadside mile markers for reference locations. The second part uses odometer mileage because mile markers are not present on the county roads.

START: Interstate on-ramp #211, I-90 E (Intersection of Montana 441 and I-90 E). Go east on Interstate 90, toward Butte.

Eocene Lowland Creek volcanic rocks in outcrops, both sides of interstate. Dark basalt overlies light rhyolite ash. This is a common relationship for the basal Eocene volcanics from near Bearmouth to near Dillon. It may represent evacuation of a magma chamber.

MP 219: Red soil is probably Eocene laterite developed on Cretaceous Boulder batholith – Butte quartz monzonite.

TAKE EXIT 219 TO I-15 S, toward Dillon.

MP 119 to 120: Deep soils on Boulder batholith overlain by bouldery diamictite of basal Sixmile Creek Formation. Boulders are orange-weathering granite derived from the batholith, in a matrix of granite grus. Diamictite represents debris flows that entered broad Middle Miocene paleovalley that I-15 S follows for next 20 miles. This is the northern tributary of the Miocene Big Hole River basin.

MP 112: Cross Continental Divide. This is the approximate edge of the Yellowstone Volcanic Plateau geoid bulge as mapped by Smith et al., 2009. The divide marks where headward erosion of the Clark Fork and Big Hole basins compete within the Middle Miocene paleovalley.

STOP 1 STOP 1: REST AREA at MP 109: View to north of well-preserved cross-section of broad Miocene paleovalley, exactly at Continental Divide. The paleovalley followed a Middle Miocene graben that has a master fault on the east and tilted the Renova Formation. The Sixmile Creek Formation lies with angular unconformity on the Renova along the length of the paleovalley.

I suggest that the Miocene paleovalley originally drained south, from the Boulder batholith into the Missouri basin, joining the Big Hole River near Divide. The Continental fault cross-cut the paleodrainage near Butte and allowed the Clark Fork basin to capture the upper reaches of the Miocene paleovalley.

The large ornamental boulders at the rest area are typical of boulders in the basal Sixmile Creek Formation.

CONTINUE SOUTH ON I-15. The Miocene paleovalley is disrupted by active normal faults associate with the Yellowstone bulge. Neotectonics reactivated Middle Miocene faults.

TAKE EXIT 102 toward Divide and Wisdom. Turn right and head west on Montana 43. East-tilted Renova Formation with unconformable cap of Sixmile Creek Formation in cut on right.

TURN LEFT at first intersection, about 1/2 mile from I-15. Head south on frontage road. Pleistocene flood plain eroded into low hills that are underlain by tilted Renova Formation and capped by Sixmile Creek Formation.

STOP 2 STOP 2. About 1 mile south on frontage road, beside irrigation pump/pivot. Farm house on left. There may be a bunch of black cattle standing around.

Here we see the Big Hole River emerging from its canyon through the Pioneer Mountains, passing into the Miocene paleovalley, and then turning abruptly to enter the deep Maiden Rock Canyon cut into the shoulder of the east Pioneer Mountains. That deep canyon meanders through the most resistant formation in the region – the Pennsylvanian Quadrant Quartzite, and then the river re-emerges into the broad paleovalley, near Melrose, only to turn south and curve around McCarty Mountain.

Meanwhile, the thick Sixmile Creek Formation gravel fill of the Big Hole paleovalley continues unabated to the east of the Maiden Rock canyon. I suggest that faulting in the Yellowstone Hotspot geoid bulge diverted the river from its Miocene course.

In the near ground to the east, the base of the hills expose east-tilted, well-cemented, coarse conglomeratic sandstones of the Renova Formation. These are granitic sandstones that Thomas (1995) showed were derived from the Chief Joseph batholith prior to uplift of the Pioneer Mountains in the Middle Miocene. They display east-flowing paleochannels, and resemble well-cemented sandstones in the Big Hole Valley on the west side of the Pioneer Mountains. The sandstones are probably Oligocene in age. They were tilted in Middle Miocene, when the graben formed and captured the broad drainage. Initial graben formation is related to stretching on a broad dome associated with the outbreak of the hotspot about 17 Ma; disruption of the drainage is related to ongoing deformation within the smaller modern Yellowstone hotspot bulge.

PROCEED along frontage road to the south, around sharp turn and up the steep grade.

MP 8. Gravel quarry in Sixmile Creek Formation.

STOP 3 STOP 3. Pull over on right shoulder of road at about MP 7.5 (not marked). Long road cut on left side reveals sedimentary structure of Sixmile Creek Formation filling of Middle Miocene paleovalley. The beds are tilted and faulted – several normal faults are exposed in the road cut. Some pebbles are pitted and fractured due to tectonic stress. The gravel contains far-travelled clasts of red feldspathic Belt sandstones – probably Bonner Formation from the west Pioneer Mountains, and much brown-weathering Quadrant Quartzite. There is a granite grus matrix, probably derived from Pioneers or Boulder batholith. Channels are present.

CONTINUE SOUTH on frontage road to Melrose. Sixmile Creek formation gravel continues in road cuts and hills for next 7 miles. The east-tilted Renova formation can be seen in ravines beneath the stream-rounded gravel of the Sixmile Creek Formation on the east side of the road. The fault on the east side of the graben forms faceted spurs against the Highland Mountain block. This fault was active in Middle Miocene to form the main graben that formed the paleovalley and has been reactivated to disrupt the drainage. Good views of the broad Miocene paleovalley to the south on the east side of McCartney Mountain, the prominent peak in the foreground.

CONTINUE THROUGH MELROSE TO INTERSECTION OF 'HIGH ROAD' TO TWIN BRIDGES, ABOUT 0.5 MILES.

0.0 TURN LEFT ON HIGH ROAD AND RESET ODOMETER. High Road is graded gravel county road that passes under I-15 and leads east to Twin Bridges. It passes the prominent pyramidal rock. That rock is Quadrant Quartzite dipping west off the Highland Mountains. It formed a buried hill within the Miocene paleovalley, exhumed by Pleistocene erosion. The road traverses a Pleistocene fan that is partly made up of recycled Sixmile Creek Formation gravel. As the road passes the pyramid it proceeds down to the Miocene bedrock surface cut on limestones of the Madison and Snowcrest Groups exhumed from beneath the Sixmile Creek gravel.

Pass Quadrant Quartzite pyramid.

3.8 Cross gully

5.4 Cattle guard at State/Fed land boundary.

7.1 As road proceeds over the low pass, rounded, brown gravel hills of Sixmile Creek gravel come into view to the south. In the distance is the Ruby Range, an active fault block.

STOP 4 7.7 STOP 4. Park on right side of road opposite stream cut in bouldery debris flows of Sixmile Creek Formation. Hike a short distance down through sagebrush to the stream cut. This is a typical example of the bouldery diamictite facies of the basal Sixmile Creek Formation (Sweetwater Creek Member). Here we see meter-scale boulders and stream rounded cobbles floating in a granite grus matrix. Clasts include Flathead conglomerate, Archean granitoid gneiss, spotted hornfels, and granite. I suggest this is a debris flow that entered the paleovalley from the northeast, sourcing the Boulder batholith and Highland Mountains. The basal debris flows of the Sixmile Creek Formation record a period of tectonic instability, when Eocene paleovalleys channeled debris flows into new Middle Miocene grabens. This relates to outbreak of the Yellowstone hotspot in eastern Oregon at about 17 Ma.

STOP 5 8.7 STOP 5. About 1 mile past Stop 4, park on right side of road at top of hill just past a long road cut of stream-rounded gravel. Walk back down along the gravel road cut.

This is typical of the clast-supported, stream-gravel facies of the Sixmile Creek Formation (Big Hole River Member). This facies interfingers with the Sweetwater Creek diamictite facies. The gravels include far-travelled lithologies, including Belt Supergroup (Bonner) probably from the west Pioneer Mountains. I suggest it is the downstream continuation of the gravel that we saw at Stop 3. This is part of an immense gravel fan that spreads into the Jefferson Valley near Twin Bridges, ahead to the east. As we continue to the east, we will be going down the depositional dip of the fan. The rounded brown hills are typical of the Sixmile Creek Formation gravel. Here it is thousands of feet thick. I suggest this gravel was partly derived from the excavation of the canyon of the Big Hole River west of Divide (Stop 2) where the Big Hole River flowed out of a rift lake basin in the Big Hole Valley. The fan was joined by gravel coming from the north, near Butte. The fan has now been broken up by active normal faults along the flank of the Highland Mountains to the east.

CONTINUE TO SOUTHEAST ON HIGH ROAD TOWARD TWIN BRIDGES. Road proceeds through miles of Sixmile Creek Formation gravel, with occasional buried hills and fault blocks of Archean basement complex. Bouldery facies of Sixmile Creek Formation locally seen near basal contact with Archean. Ruby Range is to south and Tobacco Root Range is to east. Ruby Valley is an active graben.

Town of Twin Bridges is to east. East of Twin Bridges is the prominent Cedar Creek Fan, a Pliestocene fan that recycles Miocene gravel.

17.5 Descend the Sixmile Creek Formation fan and enter Pleistocene floodplain of Beaverhead River Valley. Note grain size has decreased as we traversed down the fan.

18.5 TURN RIGHT ON MT 41, toward Dillon, and proceed to Biltmore Road (#211). Beaverhead Rock is to the south. It comprises Paleozoic rock buried by Sixmile Creek Formation, exhumed by Pleistocene erosion.

25.5 TURN RIGHT ON BILTMORE ROAD. Cross Pleistocene valley floor and approach Sixmile Creek Formation of distal fan. As road winds through Biltmore hills, note interlayered gravel, sand, silt, and clay in bluffs and road cuts. I suggest that this is where the fan spread into Miocene Lake Twin Bridges.

STOP 6 28.0 STOP 6. TOP OF HILL. Good view of massive gravel fan of Sixmile Creek Formation, burying bedrock hills, and spreading out from west to east. It dips to southeast, and is thousands of feet thick. Note Archean bedrock hills where active fault cuts gravel fan and lifts basement. Stream-rounded gravel beside road is smaller than at Stop 5, but has similar composition.

CONTINUE NORTH ON ROAD.

30.1 Sign for Talon Ranch. Cross cattle guard. Hills ahead are all Sixmile Creek Formation gravel – Big Hole River Member.

31.9 Gravel cliffs on left.

32.6 Cattle Guard, STOP at top of hill on terrace.

STOP 7 32.7 STOP 7. View across river of Sixmile Creek Formation overlying unconformity on tilted Eocene Dillon volcanics. Note columnar jointing in Block Mountain basalt. Basal Sixmile Creek Formation has very large (10 m) blocks of granite in basal Sweetwater Creek Member across river. To west, Big Hole River flows through notch cut in Quadrant Quartzite. Ridgeline of Hogback is exhumed Eocene erosional surface, notched in Pleistocene. Here the Big Hole River crosses its own fan, having been diverted back at Melrose to flow around McCartney Mountain to the south. An active normal fault is on the west side of the Hogback and lifts the Hogback and intersects another normal fault that trends northwest and lifts McCartney Mountain. Uplift of these faults responsible for tilting the Sixmile Creek Formation gravels and causing incision of the notch.

CONTINUE WEST ON ROAD.

34.5 TURN SOUTH (LEFT) AT INTERSECTION.

38.4 Traverse along valley of Upper Cretaceous Colorado Group shales and sandstones in footwall of Sandy Hollow thrust, which brings up Quadrant Quartzite and Snowcrest Group. Low outcrops near road are nearshore marine sandstones of Flood Member of Blackleaf Formation.

39.4 Metal tank on right near hilltop. Here Eocene volcanics with petrified wood at base overlie erosion surface and are overlain by Sixmile Creek Formation gravel derived from Pioneer Mountains as a large fan.

40.8 END ROAD LOG AT INTERSECTION OF MT 91. TURN LEFT TO GO SOUTH TO DILLON, OR RIGHT TO GO NORTH TO INTERSECT I-15 N.

References cited

Barnosky, A.D., Bibi, F., Hopkins, S.S.B., Nicols, R., 2007, Biostratigraphy and magnetostratigraphy of the mid-Miocene Railroad Canyon sequence, Montana and Idaho, and age of the mid-Tertiary unconformity west of the Continental Divide: Journal of Vertebrate Paleontology, 27: 204-224.

Fields, R.W., Rasmussen, D.L., Nichols, R., Tabrum, A.R., 1985. Cenozoic rocks of the intermontane basins of western Montana and eastern Idaho: *in* Flores, R.M., and Kaplan, S.S., eds., Cenozoic paleogeography of the west-central United States: Rocky Mountain Section of the Society of Economic Paleontologists and Mineralogists, p. 9-36.

Fritz, W.J., and Sears, J.W., 1993, Tectonics of the Yellowstone hotspot wake in southwestern Montana: Geology, 21: 427-430.

Fritz, W.J., Sears, J.W., McDowell, R.J., and Wampler, J.M., 2007, Cenozoic volcanic rocks of SW Montana: Northwest Geology, 36.

Hanneman, D.L., and Wideman, C.J., 1991, Sequence stratigraphy of Cenozoic continental rocks, southwestern Montana: Geological Society of America Bulletin, 103:1335-1345.

Landon, S.C., and Thomas, R.C., 1999, Provenance of gravel deposits in the mid-Miocene Ruby Graben, southwest Montana: Geological Society of America Abstracts with Programs, v. 37, no. 7, p. 292.

McLeod, P.J., 1987, The depositional history of the Deer Lodge basin, western Montana: M.S. thesis. University of Montana, Missoula, 61 p.

Pierce, K.L., and Morgan, L.A., 1992, The track of the Yellowstone hot spot: Volcanism, faulting, and uplift: Geological Society of America Memoir, 172: 1-54.

Sears, J.W., 1995, Middle Miocene rift system in SW Montana: Implications for the initial outbreak of the Yellowstone hotspot: Northwest Geology, 25: 43-46.

Sears, J.W., Hurlow, H.A., Fritz, W.J., and Thomas, R.C., 1995, Late Cenozoic disruption of Miocene grabens on the shoulder of the Yellowstone hotspot track in southwest Montana: Field guide from Lima to Alder, Montana: Northwest Geology, 24: 201-219.

Sears, J.W., and Thomas, R.C., 2007, Extraordinary Middle Miocene crustal disturbance in southwestern Montana: Birth of the Yellowstone hot spot?: Northwest Geology, 36.

Sears, James W., Hendrix, Marc S., Thomas, Robert C., and Fritz, William J., 2009, Stratigraphic record of the Yellowstone hotspot track, Neogene Sixmile Creek Formation grabens, Southwest Montana: Journal of Volcanology and Geothermal Research, vol. 188.

Smith, Robert B., Jordan, Michael, Steinberger, Bernhard, Puskas, Christine M., Farrell, Jamie, Waite, Gregory P., Husen, Stephan, Chang, Wu-Lung, and O'Connell, Richard, 2009, Geodynamics of the Yellowstone hotspot and mantle plume: Seismic and GPS imaging, kinematics, and mantle flow: Journal of Volcanology and Geothermal Research, v. 188, p. 26-56.

Thomas, R.C., 1995, Tectonic significance of Paleogene granitic sandstone in the Renova Formation, southwestern Montana: Northwest Geology, v. 24, p. 237-244.

Vuke, S.M., 2004, Geologic map of the Divide area, southwestern Montana: Montana Bureau of Mines and Geology, Open File Report MBMG 502, scale 1:50,000.

Whitchurch, A., and Gupta, S., 2007, Reconfiguration of Miocene rivers by passage of the Yellowstone hotspot: Geophysical Research Abstracts, 9:A-11516.